San Vicente Port

Development plan for a multipurpose terminal

Koen Gribnau,
Igor Koevoets,
Mart-Jan Hemel,
Menno Onrust

Cover: Container vessel at the San Vicente Port (Own photo, 12 September 2018)

San Vicente Port

Development plan for a multipurpose terminal

by

Koen Gribnau,
Igor Koevoets,
Mart-Jan Hemel,
Menno Onrust

Project group logo

Date:	7 November 2018	
Project duration:	September 2018 – November 2018	
Supervisors:	Prof. dr. ir. Mark van Koningsveld,	TU Delft
	Dr. ir. drs. René Braam,	TU Delft
	Dr. ir. Rafaél Aranguiz	UCSC, daily supervisor

TU Delft

Redactions were made to the full version of this report to protect confidential corporate information.

Preface

This is the development plan for the San Vicente Port.

This report is the final report of our multidisciplinary project. The multidisciplinary project (CIE4061) is a course in the master program of Civil Engineering at the Delft University of Technology. This means that the main purpose of this report is associated to educational ends. The project was realised from September 2018 to November 2018.

The project is carried out at the Universidad Católica de la Santísima Concepción (UCSC) in collaboration with the Delft University of Technology. Empresa Portuaria Talcahuano San Vicente (the port authority of San Vicente Port) is the client in the project.

We would like to thank our supervisor Rafaél Aranguiz for finding the project, providing sufficient background and helping us when we got stuck. Special thanks to Mary Hayes from the international office of the UCSC, for the warm welcome and the help with finding an accommodation. We would like to thank the Seminario Internacional de Ingeniería y Operación Portuaria (SIOP) organisation for giving us the opportunity to present our findings during the seminar. Also, we would like to thank Omar Salgado Oportus and Guacolda Vargas Cruz for receiving us at the port authority and providing sufficient information to carry out the project. We are very happy with Mark van Koningsveld and René Braam, who are our grading supervisors.

Last but not least, we would like to thank our sponsors for their financial support, Boskalis our main sponsor in particular; and our knowledge partners. Their logos are given on the next page.

Enjoy your reading!

Koen, Mart-Jan, Igor & Menno
Concepción, 7 November 2018

(This page is intentionally left blank)

Sponsors

Main sponsor

Boskalis (Main sponsor)

Sponsors

DIMI

Arcadis

IV-Groep

DPI

Knowledge partners

Client

(This page is intentionally left blank)

Contents

Acronyms and notations

Acronyms

AGV Automated Guided Vehicle

BCR Benifit Cost Ratio

DWT Dead Weight Tonnage

GDP Gross Domestic Product

LAT Lowest Astronomical Tide

LHS Latin Hypercube Sampling

LOA Length Overall

Lbp Length between Perpendiculars

MCA Multicriteria Analysis

MSL Mean Sea Level

NOAA National Oceanic and Atmospheric Administration

NPV Net Present Value

RAO Response Amplitude Operator

RMG Rail Mounted Gantry crane

RTG Rubber Tyred Gantry crane

SIOP Seminario Internacional de Ingeniería y Operación Portuaria

STS Ship-to-Shore

SVTI San Vicente Terminal Internacional S.A.

TEU Twenty Foot Equivalent Unit

TOS Terminal Operating System

UCSC Universidad Católica de la Santísima Concepción

Notations

- The coordinates are given as UTM-coordinates.
- The Euro is used as monetary unit. The exchange rate is 1.00 Euro = 785 CLP (November 2018).
- Container throughput and capacity values are given in TEU.

(This page is intentionally left blank)

Executive summary

The San Vicente Port is a medium-sized multipurpose port located in Chile, 500 km south of the capital Santiago. The Port is the third largest port in Chile in terms of container throughput. The capacity of the terminal is 848,000 TEU/yr. The port handles different types of cargoes: solid bulk, fractional cargo and containerised cargo. Although the throughput in the region has been growing steadily, the San Vicente Port cannot engage in this growth. The current terminal capacity is not the cause of this growth problem, it is the lack of efficiency. The port of San Vicente is 'full'. The small storage area in combination with old equipment results in a less attractive market position. To regain market share in the Biobío region, improvement measures have to be taken.

This research project focuses on the improvement and future expansion of the San Vicente Port. The improvement of the port consist out of two parts, improvement of the terminal operations and improvement of nautical operations for vessels. Beside the improvement plan, an expansion for the period till 2045 is designed.

After a terminal operation analysis, it becomes clear that seven main problems can be identified. These problems are (1) Container storage, (2) Mobile cranes, (3) Container consolidation, (4) Train blockage, (5) Traffic jams, (6) Central warehouse, and (7) Parking. Multiple separate solutions are supposed to improve the terminal. It is investigated if the proposed solutions are really useful and which changes can be combined.

In the improvement plan, the rail track is moved from the front of the warehouse to the back. The empty, export and import containers are stored in separated stacks. For the export and import, Rubber Tyred Gantry crane are installed which will increase the accessibility of the containers, and as side effect also increase the capacity of the storage. Two mobile harbour cranes are replaced by Ship-to-Shore gantry cranes. The offices are merged together to one location near the gate. Extra parking space is created close to the new offices. The central warehouse in the middle of the terminal is relocated which decreases the blockage of movements inside the terminal. A new warehouse will be located next to the other warehouses near the train track. The access road to the dry bulk quay is moved to the waterfront, so that container movements are not longer hindered by dry bulk trucks.

With the terminal changes mentioned above, the efficiency of the terminal will be enlarged and service times are reduced. Besides the efficiency improvement, the capacity of the terminal will increase to 973,000 TEU/yr which is a growth of 15%.

To improve the nautical operations, both manoeuvring with tugs and mooring at the quay are investigated. When the significant wave height is above 1.5 m, tugboats are not able to operate which will cause downtime. Mooring efficiency is mostly influenced by vessel movements. If the vessel movements exceed a certain value, the loading and unloading efficiency decreases. This means that the service time of vessels along the quay will be longer. Generally, ports strive to have a optimal loading efficiency for 98% of the time (PIANC, 2012). To analyse both nautical operations, the wave climate inside the port has to be known. Only offshore wave data is available for the bay of San Vicente Port, so a wave model is needed to compute the wave climate in the port. For the so called 'offshore to nearshore transformation' the numerical wave program Delft3D is used. The Latin Hypercube Sampling (LHS) is used for this transformation. After the wave climate inside the port is computed, it has to be converted to vessel motions for which a vessel motion model is used.

Analysing the tug conditions and vessel motions, the following can be said about the nautical operations for the current situation: 13% downtime for manoeuvring operations and an optimal loading efficiency in 95% of the time. According to PIANC (2012), these numbers are below average. To improve the nautical conditions, multiple breakwater extensions are modelled to enlarge the wave sheltering in the San Vicente Port. After analysing the breakwater extensions using the same methodology as described before, it becomes clear how much a breakwater extension will improve the nautical operations. The cost benefit analysis shows, that it is uncertain if a breakwater extension is cost effective. Therefore, the breakwater extension is not included in the improvement plan. A 450 m breakwater extension will be within PIANC limits: 1.5% downtime for manoeuvring operations and an optimal loading efficiency in 98.5% of the time.

Due to the improvements the efficiency of San Vicente Port will increase, and the throughput can grow. The terminal will eventually need to expand because the capacity will be exceeded. Because inland extension is not possible an offshore expansion is investigated. Adaptive port planning is included in the future design to anticipate on the uncertainties of the future scenarios. The extreme future throughput boundaries are expressed in a pessimistic scenario (40% market share) and a optimistic scenario (70% market share). Based on the normative scenario (70% market share) an expansion plan is made which consist out of two phases. The capacity of phase 1 will be 1,284,000 TEU/yr and for the second phase 1,552,000 TEU/yr. The timeline of the expansion plan depends on the future development of the throughput. For the optimistic scenario, phase 1 will start in 2023 and the second phase will be in 2030. After 2036, new plans need to be made. For the pessimistic scenario, phase 1 will start in 2040. There will be no capacity problem after phase 1 for the period till 2045, so the second phase is not yet needed.

The following can be concluded: to improve the terminal operations, the storage, traffic flows and equipment are improved. The terminal will become more efficient and the capacity will grow with 15%. The nautical operations can be improved by a breakwater extension. However, the current analysis shows, that it is uncertain if such an extension is cost effective. Taking into account future throughput predictions, San Vicente Port will need to increase its capacity. An expansion plan until 2045 is designed taking into account adaptive port planning.

1 Introduction

Figure 1.1: Photo of the project group in front of the office of Empresa Portuaria Talcahuano San Vicente.
From left to right: Koen Gribnau, Mart-Jan Hemel, Rafael Aranguiz, Guacolda Vargas, Igor Koevoets and Menno Onrust.

Source: Own photo (12 September 2018)

Two days after we arrived in Concepción Chile, our abroad project finally started. The first step was a kick-off meeting with the port authority of San Vicente Port. The port autohority, Empresa Portuaria Talcahuano San Vicente, is the port authority of the San Vicente Port, located in San Vicente Bay, and the Talcahuano Port, located in Concepción Bay. At this meeting, the objective of our research project became clear which is presented in this chapter.

1.1. Introduction

The Chilean port system consist of several competitive ports. The San Vicente Port located near Concepción, is the largest port in terms of container throughput for its region. However, due to natural disasters like the 2010 earthquake and strategic modification of other ports in the region, the throughput and market share of San Vicente Port are decreasing. The port authority has prepared a new masterplan for the port to regain market share of the Biobío region. With this plan the port authority is trying to stop the decreasing trends and solve the terminal problems.

1.2. Objective of the report

Although the San Vicente Port has its own masterplan and future strategy, they are curious to other visions. The objective of this multidisciplinary project is to analyse operations in the San Vicente Port and design a development plan. The plan consists out of an improvement plan and a long term vision for the San Vicente Port.

This development plan can be used by the port authority of San Vicente Port, Empresa Portuaria Talcahuano San Vicente, to broaden their vision and evaluate their own masterplan. The multidisciplinairy project is an independent research which results in an open minded vision on the port system. To avoid confusion between this report and the masterplan of the port authority, this report is called a development plan instead of a masterplan.

1.3. Readers' guide

This report consists out of 9 chapters. After this introduction the report start with a region analysis in chapter 2. In this chapter the importance of the San Vicente Port for the region and Chile is clarified. Following this is an overview of the current port layout and site conditions in chapter 3. In chapter 4 the historical throughput of the port is analysed and scenarios are made for the future throughput. The project description (chapter 5) combines the information from the chapters 2-4 and introduces the analyses that are performed for the development plan. Also, the project scope is given. The analyses are presented in chapter 6 (Terminal operations), chapter 7 (Nautical operations) and chapter 8 (Port expansion). Finally, conclusions and recommendations are given in chapter 9.

We presented the findings of this report at the Seminario Internacional de Ingeniería y Operación Portuaria (SIOP). A general impression of this three day seminar is given in appendix F.
The first phase of our multidisciplinary project consists out of a climate change analysis for the Biobío region. This analysis is written as a separate report. This report is included in appendix G.

2

Region analysis

Figure 2.1: Historical (2006) aerial view of the San Vicente Port. The port consists of a multipurpose terminal. The quay has been extended so that the terminal now has 5 berths. Also, new warehouses have been constructed and old ones have been removed.

Source: Empresa Portuaria Talcahuano San Vicente (2018)

In this chapter, a region analysis is performed to get a better understanding of the San Vicente Port. The analysis is performed on three levels. First, the port is analysed on a national level. The second level describes the function of the San Vicente Port in the Biobío region, which is one of the 16 regions in Chile. Finally, the focus is narrowed to the organisational aspects of San Vicente Port. Figure 2.1 shows an overview of San Vicente Port.

2.1. San Vicente Port on a national level

Chile is a South-American country occupying a long, narrow strip of land between the Andes and the Pacific Ocean. With over 6000 km of coastline, there are many sea ports in the country. The Chilean port system can be characterised by a relatively large amount of medium-sized ports. Roughly ten can be seen as most important; the locations of these ports are shown in figure 2.2. One of these ports is the The San Vicente Port.

The types of cargo handled by the ports differ depending on the port locations. In the North, ports focus mainly on coal, copper and iron. In the centre of Chile, ports are moving mainly containers and agricultural products. Around the capital of Chile, Santiago, 66% of the Chilean population is established. It is therefore not strange that overt the half of the total shipping tonnage takes place in this region. The ports in the south of Chile are specialised in the export of forestry products and fruits.

Chile's port system is rather small in terms of container throughput compared to other ports in Latin American. San Antonio, the port with the largest container terminal in Chile, transports three times less containers (TEU) than the biggest container ports in Latin America: Santos (Brazil) and Balboa (Panama). San Vicente Port is the third largest port in Chile, in terms of container throughput (TEU). It can be classified as a medium-sized port (Merk, 2016).

Figure 2.2: Most important sea ports in Chile (Merk, 2016)

2.2. San Vicente Port in the Biobío region

Chile is divided into 16 regions that are numbered from north to south. San Vicente Port is located in the Biobío region.

2.2.1. VIII Biobío region

The Biobío region is the eight region of Chile, with multiple sea ports along its coast. Concepción is the capital of this region with 1 million inhabitants. It is located 500 km south of Santiago. Other cities in the region are: Coronel, Hualpén, Los Ángeles and Talcahuano.

There are four main seaports in the Biobío region: San Vicente Port, Coronel Port, Lirquen Port and Cabo Froward Port. San Vicent Port (40% of the market) is the largest port in terms of container throughput (TEU), followed by Coronel Port (35% of the market) (Empresa Portuaria Talcahuano San Vicente, 2017). Coronel is the largest in terms of transported cargo tonnes. In addition, there are a number of private ports that operate for a specific company.

2.2.2. San Vicente Bay

San Vicente Port is located in the San Vicente Bay. An overview of the San Vicente Bay, the city of Talcahuano and Talcuhuano Port is shown in figure 2.3. The San Vicente Bay and the Concepción Bay are separated by a peninsula and by Taiguen hill.

There are a lot of port activities in San Vicente Bay. Besides San Vicente Port, the bay offers space for the local fishing industry. Other private ports are also established in th San Vicente Bay. There is a jetty for oil, one for the steel industry and one for LNG. It should be noted that although these terminals are located in the San Vicente Bay, they are not part of the San Vicente Port. These terminals are owned and exploited by private companies.

2.3. San Vicente Port

San Vicente Port is governed by the port authority: Empresa Portuaria Talcahuano San Vicente.

2.3.1. History

The San Vicente Port is constructed in the period 1968-1974. The port is built as second port near the original port of Talcahuano, to serve vessels with larger drafts. This was needed because the port of Talcahuano is located in the shallow bay of Concepción. The San Vicente Port is a state port since the opening in 1974. In 1997 the Chilean national government modernised the State Port System creating the San Vicente Port as it is.

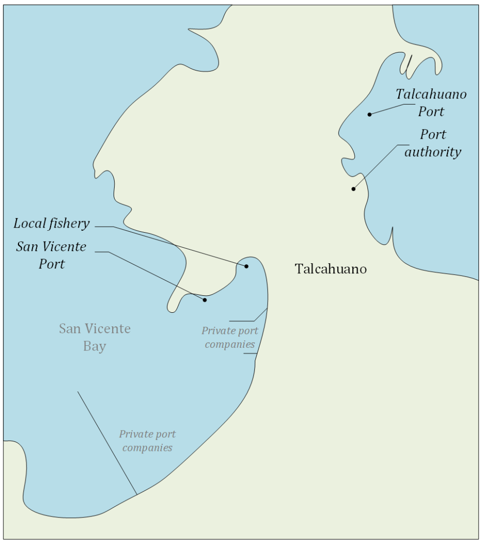

Figure 2.3: Overview of San Vicente Bay. The locations of the San Vicente Port, local fishery and private port companies are indicated.

2.3.2. Port organisation

Empresa Portuaria Talcahuano San Vicente is the port authority for both the San Vicente Port and the Talcahuano Port. Their offices are located near Talcahuano Port besides Concepción Bay, see figure 2.3.

The port authority operates according to the landlord organisation model since 1999. The port authority is the land owner and gives concessions for the use of the land to an operator. Initially San Vicente Terminal Internacional S.A. (SVTI) was awarded the concession for San Vicente Port for 15 years. In 2007, the concession was renewed for an extra 15 years, So the current end date of the concession is 31 December 2029 (Michou, 2017).

SVTI is the only operator at San Vicente Port. SVTI has two shareholders: SAAM Puertos S.A. and SSA Holdings International Chile. Both shareholders operate in multiple ports in Chile and Latin America.

2.3.3. State port

According to the Chilean foreign trade law, the Empresa Portuaria Talcahuano San Vicente is a state port organisation. This means that the port authority is not an independent commercial organisation. The ports owned by the authority serve the region. So, the San Vicente port cannot only focus on the most profitable businesses. This explains why San Vicente Port is characterised by its wide variety in goods. By law, the ports of Empresa Portuaria Talcahuano San Vicente are obligated to offer services to bulk cargo, break bulk, as well as containerised cargo. These activities may also be moved to only one of ports, as long as the port authority continues to offer these three types of transport.

(This page is intentionally left blank)

3

Overview port

Figure 3.1: Container vessel from the Meridian Shipping Service group moored at the quay as seen from the beach of San Vicente Bay.

Source: Own photo (12 September 2018)

Before our first terminal site visit, we made a drive along the San Vicente Bay. From the beach in the bay, we could observe the San Vicente Port for the first time. As can be seen in figure 3.1 we could already identify some global port components. This chapter gives an overview of the San Vicente Port. It is mostly a contemplative chapter describing the layout of the port and the design considerations.

3.1. Introduction

San Vicente Port is a multipurpose port in southern Chile with a single terminal operated by San Vicente Terminal Internacional S.A. (SVTI).

3.2. Vessels

A wide range of different vessels is served at San Vicente Port: different cargo types (container, break bulk and general cargo) and various vessel lengths, ranging from 100 meter long fishing vessels to 350 meter long container vessels. A comprehensive ship analysis can be found in appendix A. Table 3.1 shows the different vessel groups (as defined by the project group) and their percentage of appearance in San Vicente Port.

Group	**Number** [%]	**Cargo type**	**max L_{bp}** [m]	**min L_{bp}** [m]	**Vessel class**
I	19.6%	Container	350	330	New Panamax
II	6.9%	Container	300	280	Panamax
III	22.8%	Container	270	240	Supramax
IV	13.7%	Container	235	220	Handymax
V	12.7%	Bulk	220	170	Handymax
VI	14.8%	Container	190	160	Handysize
VII	10.5%	General cargo, bulk and fishery	145	100	Small vessels

Table 3.1: Vessel classes divided by cargo type and vessel length. The groups are sorted by vessel length (L_{bp}).

Considering the containerisation of shipping and the shift to larger container vessels (Quist, 2017) two scenarios regarding the vessel distribution are proposed:

1. The transported volumes by container transport will grow with respect to the other modes of transport. The distribution of vessel lengths stays the same.
2. In addition to the containerisation, a shift towards the larger vessel classes (Panamax and New-Panamax) is assumed.

3.3. Port layout

3.3.1. Offshore design

Figure 3.2 shows an overview of the offshore design of San Vicente Port. The various components are discussed below.

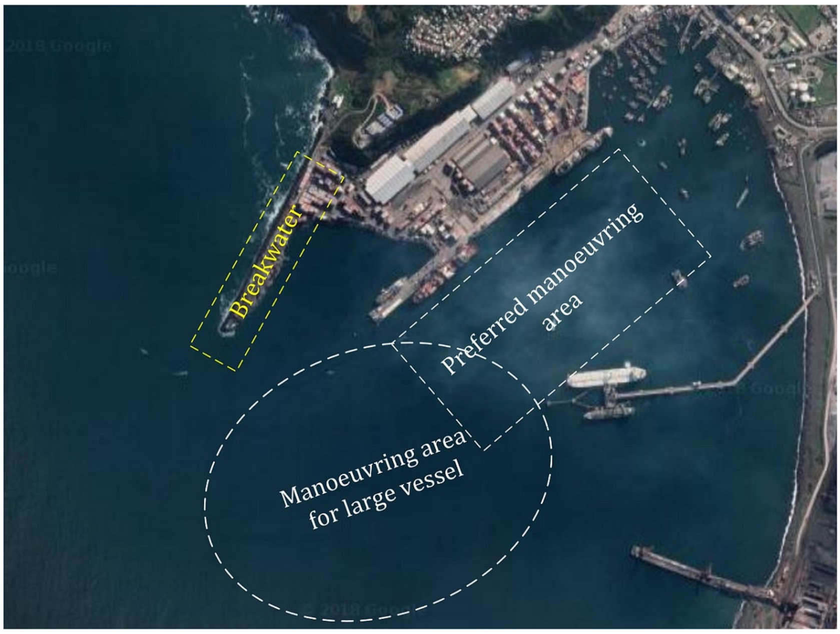

Figure 3.2: Offshore design of San Vicente Port

Port entrance

San Vicente Bays is deep enough for all vessels that want to moor at San Vicente Port, so there is no dredged entrance channel. Pilots board the vessel outside the protection of the breakwater. In rough weather, pilots have to board the vessel in Concepción Bay, located to the north of Concepción. This gives some delay in the berthing procedure.

Manoeuvring areas

Most vessels at San Vicente Port are moored on starboard side. The turning manoeuvre takes place with help of tugboats. The preferred manoeuvring area is in front of the quay, where wave conditions are calm. However, due to the limited space, only vessels shorter than 180 *m* are able to manoeuvre here (Empresa Portuaria Talcahuano San Vicente, 2018). According to PIANC (2014a) the minimal nominal diameter of a turning circle inside the manoeuvring area should be at least 2.0×LOA. There is slightly more space available, so San Vicente Port uses a conservative maximum vessel length with allowance to turn in front of the quay.

Larger vessels need to manoeuvre further away from the quay, where they are less protected by the breakwater. Because there is lots of space to manoeuvre the vessel, it is not possible to talk about a 'turning circle'.

Breakwater

A breakwater protects the port from waves from the northwest. The breakwater has a length of 680 *m* and extends 5 *m* above Mean Sea Level (MSL). The breakwater has a tetrapod armour layer; the inner slope has a riprap armour layer.

Tugboats

The tug service for the manoeuvring of vessels in the San Vicente port is provided by AGENTAL, an independent company which provides tug service to many ports in Chile. AGENTAL has a fleet of four tugboats based in Talcahuano. These tugboats also provide tug services to the port of Talcahuano, the small port of Penco and the port of Lirquen (Agental & CPT, 2018).

3.3.2. Berths

San Vicente Port has five berths. The terminal consists of a continuous quay of 864 *m* long for berths 1-4 and a 264 *m* long quay on the rear of the quay extension for berth 5. Berth 2-4 can be combined to serve two ships of 350 *m* simultaneously.

Berth 1 is 160 *m* long and is mainly used for bulk ships. A mooring buoy is present, so that longer vessels can also be accommodated. Maximum allowed draught is 11 *m*.

Berth 2 is 220 *m* long and is mainly used for container vessels. Maximum allowed draught is 12 *m*.

Berth 3 is 220 *m* long and is mainly used for container vessels. Maximum allowed draught is 14 *m*.

Berth 4 is 264 *m* long, and is operational since 2016. Maximum allowed draught is 15 *m*, so this berth is used for the largest (container) vessels.

Berth 5 is 264 *m* long, and is operational since 2016. For safety reasons, it is not allowed to serve a vessel on berth 4 and 5 simultaneously, so this berth is not used often.

3.3.3. Onshore design

Figure 3.3 gives an overview of the terminal layout. The different terminal components are indicated by different colours.

(a) Topview San Vicente Port

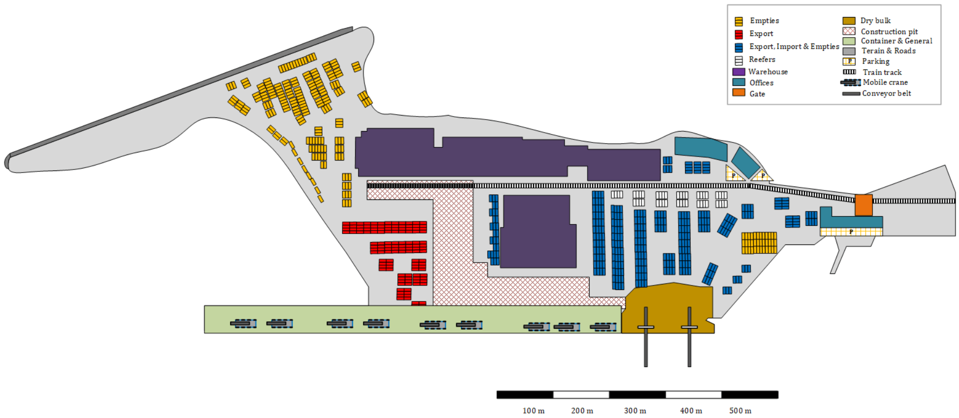

(b) Schematisation of the terminal components

Figure 3.3: Layout of the San Vicente terminal. The different components in the terminal are indicated by different colours. For convenience, the orientation of the map is rotated.

Gate

Trucks and trains enter the port at the gate (orange). There are two gates for rail and five gates for trucks, of which only four are currently used. The rails split: four rail tracks continue to run through the terminal in front of the warehouses.

Storage yard

The idea is to have empty, export and import containers separated in different stacks. However due to lack of space this is not the case everywhere in the port. Near the breakwater there are empty stacks (yellow). This section is messy because the storage area has an irregular shape. Therefore containers do not have squared stacks and containers are aligned in different directions. Some container have more than twenty container in front of it which must be moved before they can be reached. Close to the quay there is a section for export containers (red). The alignment is parallel to the quay and properly places in rows. Each row is six containers wide, the middle two cannot be reached directly. The rest of the terminal is a mix of different types containers (dark blue). Most stacks are six containers wide but some are wider. Reefers are placed next to the main road (white). Especially the storage near the offices, west of the central warehouse and east of the dry bulk section are messy: a lot of different container orientations, types of containers and storage widths are mixed. Also, a small container storage next to the waterfront can often only be reached at night. When a dry bulk vessel is present, the trucks dropping dry bulk are waiting on the road that separates this container storage from the rest of the terminal.

Bulk sector

Above berth 1 there is a dry bulk sector. There is no storage for dry bulk in the terminal. Trucks drop the dry bulk cargo immediately on the conveyor belts.

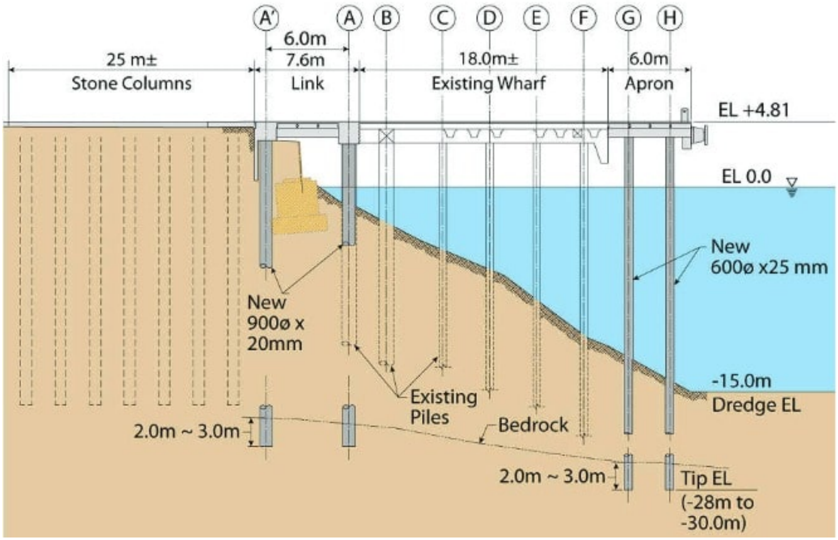

Figure 3.4: Wharf structure of the quay of San Vicente Port (Empresa Portuaria Talcahuano San Vicente, 2018)

Quay

The quay consists of platform joined with the rest of the terminal by concrete bridges, forming a wharf structure. This wharf structure is shown in figure 3.4

Terminal equipment

The terminal uses mobile harbour cranes for the loading and unloading of vessels. Reach stackers are used for container handling in the yard. Containers are transported to and from the yard by tractor-trailer units. Table 3.2 gives an overview of the terminal equipment.

Type of equipment	Amount
Reach stacker for full containers	17
Reach stacker for empty containers	7
Mobile cranes	9
Tractor units	40

Table 3.2: Terminal equipment of the San Vicente Port (Michou, 2017)

Warehouses

An important value-added-service from the port is the consolidation of containers. Goods are transported to the port by train and by trucks, where they are loaded onto containers. The terminal's warehouses (purple) provide space (and protection against weather) for storage of cargo, before they can be transported.

Especially for the forestry industry this is important: cellulose is transported to the terminal by train, where it should be protected against the weather. It is then stuffed and shipped in containers.

Container Express

Container Express is an innovative and technical platform to streamline the logistics of the port. SVTI uses a preport, 1.5 km from the terminal, where administrative checks are carried out. Trucks first go to the preport so that the processes at the gate can be accelerated and long queues can be avoided.

Port operation

The port is open 24 hours per day, 365 days per year. However, the gate is only opened 16 hours per day. Preferably, port operations are carried out during the day. The port operates in shifts of 8 hours.

Capacity

The capacity of the terminal is 848,000 TEU/yr. The capacity of the different terminal components are given in table 3.3. More information on the terminal capacity is given in appendix D.1.3.

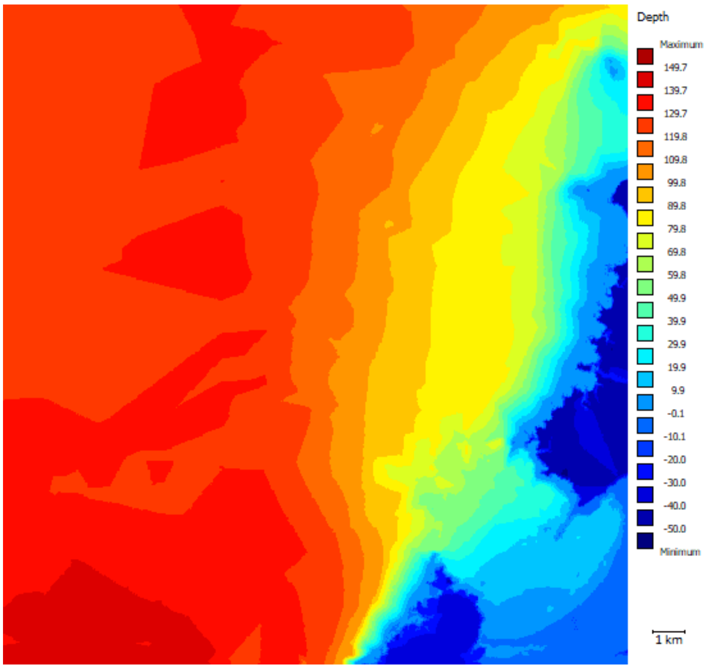

Figure 3.5: Bathymetry of the coast at San Vicente. San Vicente Bay can be seen in the southwest section of the figure.

	Capacity [TEU/yr]
Quay	1,075,000
Gate	1,477,000
Access road	6,083,000
Storage	848,000

Table 3.3: Capacity of the different terminal components of San Vicente Port.

Hinterland connection

The port is connected with the hinterland via roads and rail track. The rail track is used to bring forest products to the port. Roads are used for all type of products. Highway 164 is located a few kilometres from San Vicente Port. This highway connects together with Highway 152 the port with Highway 5, the most important highway in Chile which runs from the Peruvian border in the north through Santiago to the southern regions of Chile.

3.4. Site conditions

3.4.1. Bathymetry

The Latin-American west coast can be characterised by a steep coast, as can be seen in figure 3.5. San Vicente Bay is clearly visible in the depth profile. The average slope of the coast is 1:150. The depth in the bay is sufficient for safe entering of vessels up to 15 m draught.

3.4.2. Waves

The wave climate at San Vicente is characterised by the presence of swell waves. The waves can best be described by a two-peaked wave spectrum. A dataset with 20 years (30/01/1997-20/02/2018) of offshore wave data is used.

3.4.3. Tides and currents

The tides at San Vicente are semi-diurnal with a tidal range of approximately 1.8 m. There is no river outflow in San Vicente Bay, currents are only excited by the tides. The length of the bay is short compared to the entrance width. Therefore, these currents can be assumed negligible.

(a) San Vicente bay in 1984

(b) San Vicente bay in 2016

Figure 3.6: San Vicente is a stable coastal cell. In the period 1984 - 2016 hardly any changes of the beach can be observed.

3.4.4. Water levels

All levels are measured relative to MSL. Lowest Astronomical Tide (LAT) is at approximately -0.9 *m* (Windguru, 2018).

3.4.5. Wind

The prevailing wind at San Vicente is a moderate northerly wind, with the strongest winds in winter. Stong winds (6 Beaufort and higher) occur approximately 2.5% of the time (Windguru, 2018).

3.4.6. Sediment transport

San Vicente Bay is a stable coastal cell. There is no net sediment transport. The water in San Vicente Bay is deep enough for the vessels in the port, so no dredging activities are carried out.

3.4.7. Seismicity

San Vicente is located in a seismic active region. The port has suffered severe damage from the 2010 earthquake and subsequent tsunami. To absorb the seismic loads, the a wharf type of quay structure is chosen. Wharf structures are more flexible and have less weight than a for example a combi wall structure with a relieving platform (Peters, 2018).

3.4.8. Climate change

Extensive analysis has been done on the effects of climate change on the wind and wave climate at San Vicente. This analysis is given in appendix G and is based on the RCP 8.5 emission scenario, which is the worst example defined by the IPCC.

By 2100, a sea-level rise of 0.55 *m* can be expected, but land subsidence due to seismicity may have larger consequences. The changes of the wave climate are expected to be small: a 0.1 *m* decrease in significant wave height and a 0.05 *s* decrease in average wave period. These changes are small, so it is reasonable to neglect the effects of climate change (Gribnau, Koevoets, Hemel & Onrust, 2018).

(This page is intentionally left blank)

4

Market forecast

Figure 4.1: Storage of cellulose and other wood products in the warehouses. Wood product form a large portion of the cargo volumes of the San Vicente Port.

Source: Own photo (2 October 2018)

The San Vicente Port handles different cargo types, cellulose is one of these. Celluslose sensitive to the outdoor climate and that is why the cellulose is stored in warehouses. Figure 4.1 shows a new warehouse that was constructed recently because the market for these products is growing. This section provides an overview of the (forecasted) throughput to be used for the development plan. The (market) forecast is based on previous studies done by Empresa Portuaria Talcahuano San Vicente.
First, a description of the most important cargo types is given. Then, the market forecast is given.

4.1. Cargo types

San Vicente Port is a state port, which implies that the port must handle different types of cargoes: solid bulk, fractional cargo and containerised cargo. With the worldwide shift to container transport, more and more cargo is transported in containers. The forecast study is limited to container transport. It is expected that bulk cargo will not grow because the forest sector is close to its maximum capacity (Empresa Portuaria Talcahuano San Vicente, 2017).

San Vicente Port is mainly an export port. Approximately 85% (in terms of tonnage) of the container throughput is export. Dry bulk is mainly exported. Figure 4.2 provides an overview of the export of the Biobío region by sector. The forestry industry is the main producing sector in the region with export products such as cellulose, paper, dimensioned wood and wood chips. Wood chips are loaded on vessels as bulk cargo, the other products are consolidated in containers. Figure 4.1 shows the storage of cellulose in a warehouse at the San Vicente Port terminal. Stuffing of containers is done at the terminal, so there is a large demand of empties that need to be imported. According to the port authority approximately 87.5% of the containers are not leaving the terminal terain, but they are imported empty, stuffed at the warehouses and thereafter exported (Empresa Portuaria Talcahuano San Vicente, 2018).

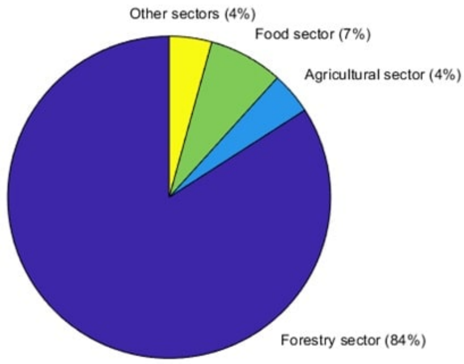

Figure 4.2: Export (in tonnes load) of the Biobío region in 2017 by sector. The forestry sector is the most important sector for export in the Biobío region. *Based on information from Empresa Portuaria Talcahuano San Vicente (2017).*

4.2. Regional market forecast

The cargo throughput of the ports in the Biobío region are expected to increase with the Gross Domestic Product (GDP) of Chile. Figure 4.3 portrays the forecasted throughput of the ports in the Biobío region in MTon. The optimistic and pessimistic scenario are indicated as a range around the predicted throughput. Also, the the cargo volumes handled at San Vicente Terminal Internacional S.A. (SVTI) are indicated in the figure.

Figure 4.3: Forecasted cargo throughput (in M Ton) for the ports in the Biobío region for the period 2017-2033. The forecast is based on a growth of the regional GDP of 3%. For past years, the cargo throughput of the San Vicente terminal is indicated. *Based on information from Empresa Portuaria Talcahuano San Vicente (2017).*

The potential for growth is strong, whereby the following trends are observed:

- Import is expected to increase more than export, so that by 2045 the percentage of export will decrease to 70%. This means that there is an increase in import of loaded containers, so that the demand for empties will decrease relative to the total number of containers.

- The forestry sector is expected to grow 20% until 2030. Then, further growth is restricted due to the supply capacity that is bounded within the hinterland.
- Large growth is expected for the export of the food sector. This will be transported as containerised cargo.

Figure 4.4 shows the forecasted growth of container transport in the Biobío region. The optimistic and pessimistic scenario are indicated as a range around the predicted throughput. In 2017, the region transports about 1.2 million TEU. The multipurpose terminal at the San Vicente Port handles about 0.5 million TEU per year. By 2045, the container throughput is expected to grow to 2.8 million TEU for the region.

[redacted]

Figure 4.4: Forecasted cargo throughput (in TEU) for the ports in the Biobío region for the period 2017-2045. For past years, the cargo throughput of the San Vicente terminal is indicated. *Based on information from* Empresa Portuaria Talcahuano San Vicente (2017).

4.3. Market forecast for San Vicente Terminal Internacional S.A.

Recent years have shown that there is a lot of competition between ports in the Biobío region. From 2008 onwards, the market share of the San Vicente Port for container handling has been declining steadily. Several events are highlighted:

- [redacted]
- The terminal was severely damaged after the 2010 earthquake. Operations were resumed quickly afterwards, but the repair works took several years.
- [redacted]
- [redacted]
- [redacted]

Although the throughput in the region has been growing steadily, the San Vicente Port cannot engage in this growth. Therefore, the San Vicente Port takes measures to improve its strategic position in the region. The first step is the purchase of two Ship-to-Shore (STS) cranes with the aim of improving the service delivered by the port. The quay has already been prepared for this after the extension in 2016.

Traditionally, transshipment is very limited in Chile. This is due to Chilean policy, but this policy is currently being discussed. For the port in the Biobío region this gives large opportunities to form a hub for the South of Chile. In addition, the worldwide shipping market is becoming more and more complex. Vessels are increasingly large, and shipping companies form alliances so multiple transporters use the same vessels.

The market forecast portrays significant growth for the export of containers in the Biobío region with throughputs of up to 3 million TEU in 2045. Although a high growth potential is forecasted, it is stressed that there is a lot competition in the region. This is a real risk for the development of San Vicente Port.

Scenarios

For the application of this development plan report, two scenarios with regards to the growth of SVTI are assumed. According to van Dorsser (2017), scenarios can be used for thinking through uncertainties in a throughput forecast. In recent years, the market share of SVTI for container transport in the region has shown large fluctuations. This has declined from approximately 75% in 2008 to 40% in 2017 (SEA, 2017). The port is currently taking action to stop this decline by improving the efficiency. A pessimistic and an optimistic scenario is selected:

Pessimistic The market share will stabilise at 40%, so no further decline is expected. The port throughput will only grow with the regional growth rate.

Optimistic The port will increase its operation efficiency. So the market share of San Vicente will start growing from the current 40% to 70% in 2025. In combination with the regional growth this means that the port will reach its capacity in 2022. [1]

[redacted]

Figure 4.5: Forecasted cargo throughput (in TEU) for the ports in the Biobío region for the period 2017-2045. For past years, the cargo throughput of the San Vicente terminal is indicated. *Based on information from Empresa Portuaria Talcahuano San Vicente (2017).*

1 [redacted]

5
Project description

Figure 5.1: A reach stacker is unloading a tractor on the main road. Due to this operation, a traffic jam occurs which requires us to stop for a few minutes.

Source: Own photo (2 October 2018)

During our second site visit (our first visit with daylight) the first problems already become clear. Container operations and traffic flows are in conflict with each other as can be seen in figure 5.1. In this chapter the project description is introduced. First, a problem description is given followed by the project procedure.

5.1. Problem description

Observing the daily operations of the San Vicente Port it looks like the port is near full capacity. Containers are stored everywhere and the stacking height is almost everywhere up to six containers. But, the historical yearly maximum throughput was about 200,000 TEU more than the throughput in the last years. So, in fact the San Vicente Port does not have a capacity problem. Nevertheless, the processes in the terminal are far from optimal. It can be state that the port has a market share problem. Due to this problem San Vicente Port is loosing clients and the regional throughput growth cannot be followed. A possible explanation for the market share problem is low terminal efficiency. A plan is needed to increase the efficiency of the terminal. An higher efficiency can attract new clients or clients from other ports due to a shorter service time. This will lead to a higher market share and thus a larger throughput. Moreover, a higher efficiency can lead to less operational costs.

5.2. The project procedure

Since several port operations are not optimal, different operations will be analysed. The port operations are separated into two parts; the nautical operations and the land based terminal operations. These two parts will be handled separately in this development plan. Both parts are analysed from an engineering point of view. The nautical operations analysis is based on the behaviour of vessels. The terminal operations part is more based on a terminal organisational point of view.

For both parts first the current situations are investigated and the inefficiency causes are indicated. Followed by a proposal of solutions for these problems. Since the exact effect of the solutions on the market share of San Vicente Port will be uncertain, scenarios are created to analyse the effects of the proposed solutions. Besides, these scenarios are used for the feasibility study of the solutions.

According to all scenarios there will be a moment that the capacity will be reached, even after improvement measures. At that moment, a terminal expansion is needed. The expansion plan is the third analysis of this development plan.

5.2.1. Development plan scope

The development plan focuses on the development of San Vicente Port. Only the terminal operations with respect to containerised cargo are taken into account. The effects of improvements and/or adaptations in the San Vicente Port itself are analysed. The development plan is prepared for the period 2018-2045.

The following point are taken into account for this project with respect to throughput:

- The yearly market growth for containerised cargo throughput for the Biobío region is according to the market forecast.
- An unchanged throughput of non-containerised cargo is assumed.
- No change is assumed in the future distribution and the number of calls of non-containerised cargo vessels.

5.2.2. Scenarios

The two market development scenarios, presented in section 4.3 can be combined with the two vessel growth scenarios presented in section 3.2 to create four scenarios. These four scenarios will be used to analyse and evaluate the nautical operations, terminal operations and expansion plan.

These combined scenarios are:

- Market share 40% with equal growth of container vessels. On average 50% of the vessel's containers capacity will be unloaded during a call.
- Market share 40% with only growth only the vessel group I and II. On average 50% of the vessel's containers capacity will be unloaded during a call.
- Market share 70% with equal growth of container vessels. On average 70% of the vessel's containers capacity will be unloaded during a call.
- Market share 70% with only growth only the vessel group I and II. On average 70% of the vessel's containers capacity will be unloaded during a call.

	Equal growth		Growth I+II	
Scenario 40%	I	81	I	137
	II	28	II	47
	III	95	III	57
	IV	58	IV	35
	V	29	V	29
	VI	45	VI	29
	VII	27	VII	27
Scenario 70%	I	102	I	175
	II	35	II	61
	III	118	III	57
	IV	73	IV	35
	V	29	V	29
	VI	60	VI	29
	VII	27	VII	27

Table 5.1: Amount of yearly vessel per group based on difference scenarios for a throughput of 1,900,00 TEU for the Biobío region.

For all analysis, nautical operations, terminal operations and the expansion plan the number of vessel and the distribution among the vessel groups is needed. The total container throughput depends on the market scenario and the distribution of the containers among the vessel depends on the distribution scenarios. An example of a future vessel distribution for the four scenarios is given in table 5.1. This distribution is based on a throughput of 1,900,000 TEU for the entire Biobío region, which is the case around 2030 according to the forecast.

5.2.3. Used guidelines and design methods

The calculations and evaluation of the results in the following analysis are primarily based on PIANC guidelines. The following PIANC reports are used:

- PIANC 24-1995: Criteria for movements of moored ships in harbours, a practical guide.
- PIANC 115-2012: Criteria for the (un)loading of container vessels.
- PIANC 121-2014: Harbour approach channels design guidelines.
- PIANC 135-2014: Design principles for small and medium marine container terminals.

Next to the PIANC guidelines, the following lecture notes of Delft University of Technology are used:

- Service systems in ports and inland waterways (Groenveld, 2001).
- Ports and terminals (Ligteringen & Velsink, 2012).
- Integraal ontwerp en beheer (Hertogh & Bosch-Rekveldt, 2015).

5.2.4. Used data sets

The following data sets are used for the analysis:

Wave data

A dataset with 20 years (30/01/1997-20/02/2018) of offshore wave data is used. The wave data is are determined from a virtual node in the Global Forecast System WaveWatch III, from the National Oceanic and Atmospheric Administration (NOAA). The location in UTM-coordinates: 18H 5000 59051.

Bathymetry

Two bathymetry data sets are used, provided by the Universidad Católica de la Santísima Concepción (UCSC) and the port authority. The first data set contains the bathymetry of a large offshore area, constructed from the GEBCO database, nautical charts and field surveys done by the UCSC (Gómez et al., 2018). The second data set contains the bathymetry in San Vicente Port, this data is collected with multibeam surveys by the port authority during the construction of berth 4 and 5.

Vessel data

The vessel data for the period Jan-Sept 2018 is used. This data is provided by the port authority Empresa Portuaria Talcahuano San Vicente. From all vessels that have been served in this period, the arrival time, berth number use, and vessel information is given. Vessel information is given about the name, registration number, Length between Perpendiculars (Lbp), Dead Weight Tonnage (DWT) and cargo type.

6
Terminal operations

Figure 6.1: A reach stacker is loading a tractor in the storage area. The container is transported towards the quay where it will be loaded on the container vessel

Source: Own photo (2 October 2018)

As mentioned in the project description, the port will need to improve their efficiency. In figure 6.1 a container is loaded on a tractor by a reach stacker. In this figure it can also be observed that containers are stacked high and close to each other. Because of this dense stacking, getting access to all containers is difficult. However with other equipment, for example RTGs, access to dense stacked containers is possible. This will make the storage area more efficient. An extensive explanation of the terminal operations and improvements can be found in appendix D.

6.1. Terminal operation analysis

The terminal operations of San Vicente Port are analysed. Problems are identified and solutions are suggested. An overview of the problems and their global location is presented in figure 6.2. Below, the main problems are discussed. These problems are discussed more extensively in appendix D.

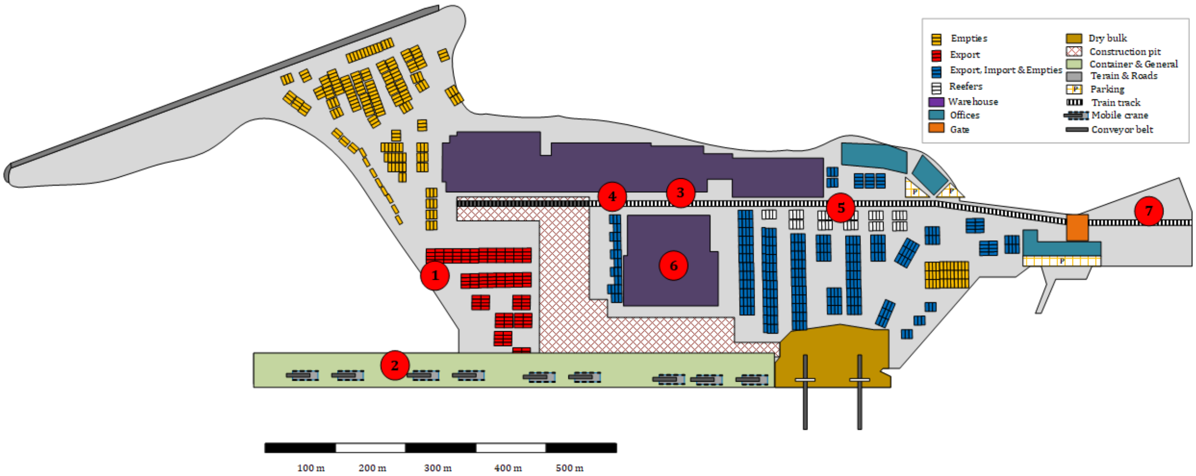

Figure 6.2: Overview of problems and their locations. (1) Container storage, (2) Mobile cranes, (3) Container consolidation, (4) Train blockage, (5) Traffic jam, (6) Central warehouse, (7) Parking.

Container storage

The container storage in the terminal is very compact. The yard is packed very densely with a high occupancy. All available space inside the terminal is used for storage of containers. The bulk storage was removed from the terminal a few years ago to create extra space for the container storage.

The problem with the container storage is that a lot of containers are unreachable. Some container blocks are more than twenty containers wide. Besides this, there are no dedicated stacks for empty, export and import containers. Containers seem randomly distributed over the terminal.

Mobile harbour cranes

San Vicente Port uses mobile harbour cranes for the loading and unloading of container vessels. These cranes have sufficient capacity, but the productivity is relatively low. This low operation speed results in a long service time for the vessels.

Sailing vessels make money; vessels at the quay cost money. Therefore, shipping companies want short service time. At this moment, there are other ports close to the San Vicente Port with Ship-to-Shore (STS) cranes that can offer shorter service times. That makes these ports more attractive.

Container consolidation

The port offers clients the possibility to consolidate containers (stuffing of goods in empty containers) at the terminal. This is cheaper for the clients, because it prevents the movement of empty containers to the clients. Container consolidation is done in front of the warehouses. The containers are placed side to side by a Reach Stacker and filled using forklift trucks.

The problem with this is that it requires Reach Stacker movements on the main road. These movements result in congestion on the main road, thus reducing the efficiency of the terminal.

Train blockage

The on-dock train terminal is located in the middle of the terminal, on the main road besides the warehouses. Three times a day, a train enters the port to deliver goods. These are mainly forestry products, which need to be stored in the warehouses for protection against the weather. When the time is right the process of container consolidation starts.

The problem of the train is that it forms an obstacle between the warehouse and the rest of the terminal. Furthermore, the container consolidation takes place on the rail track. Thus both processes cannot take place at the same time.

Traffic jam in the main road

There is a lot of traffic in the main road of the terminal. There are trucks dropping goods or just passing by and tractors (un)loading containers or driving by. Especially the (un)loading of containers for consolidation causes congestion problems in the port. Reach Stackers need to manoeuvre on the main road, and this causes blockage and traffic jams. Also, Reach Stackers block the main road when a container from the storage area next to this road is (un)loaded from/to a tractor.

Central warehouse

In the middle of the terminal is a warehouse situated. This central warehouse is the oldest warehouse of the terminal and forms an obstacle for traffic flows in the terminal. This results in a lot of movements around the warehouse.

Parking

Employees have to park their car outside the terminal. There is a parking area just before the gate, but there are insufficient parking spots. This results that cars are parked on one of the two rail tracks that enter the port. The available space in front of the gate is therefore limited, easily causing congestion in front of the gate.

6.2. Terminal improvement plan

To improve the terminal efficiency changes to the current layout are proposed. It is investigated if the proposed changes are really useful and which changes can be combined. The end result is an integrated improvement plan which will improve the efficiency of the port. As a side effect of the improvement plan, the capacity of the terminal increases as well.

6.2.1. Terminal layout

The changed layout of the terminal can be seen in figure 6.3. The most important changes are mentioned and discussed below. An extensive explanation of the changes is given in appendix D.3.1.

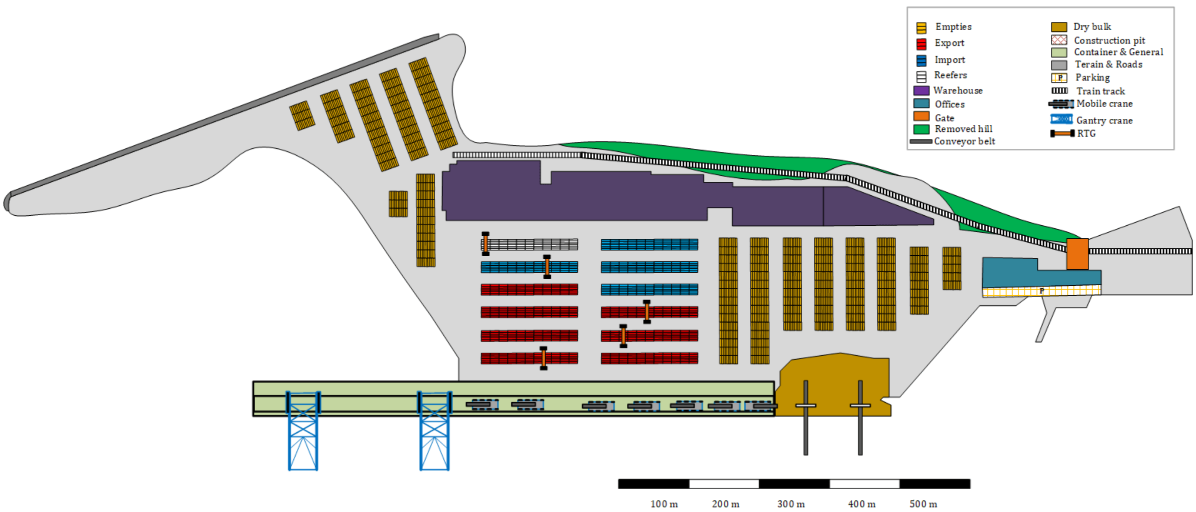

Figure 6.3: New terminal layout after implementation of the terminal improvement plan.

Rail track

The rail track is relocated from the front of the warehouses to the rear. In this way, the train blockage in the main road are solved. The movement of the rail prevents that trains are blocking the route to and from the warehouse. Some space must be generated by removing a part of the Taiguen hill behind the warehouses.

Container consolidation

Container consolidation will not change. Due to the relocation of the railway, it can be done at the same time as unloading the train. This also means that the flow of goods through the warehouse is more efficient.

Offices

The offices will be moved to another location inside the terminal. The new location is directly next to the gate at the waterfront. This location has as advantage that it is close to the terminal but it will not interrupt the terminal operation. Moreover, this location is not very suitable for container storage. Behind the offices extra parking area will be created.

Terminal equipment

Empty, export and import containers are stored in separated stacks. Rubber Tyred Gantry cranes (RTGs) are installed for the import and export stacks. This will increase the capacity of the import and export storage and makes all containers good accessible. Reach Stackers will be used for the empty containers. This is because using Reach Stackers is cheaper than RTGs and not all empty containers need to be accessible. By placing multiple containers next to each other a smaller total area is needed. The empty storage is perpendicular to the main road to prevent that reach stackers use the main road to (un)load tractors.

STS gantry cranes

STS will be installed. San Vicente Terminal Internacional S.A. (SVTI) already has two STS cranes planned for next year. These cranes have a higher productivity then mobile harbour cranes, so the (un)loading times will shorten. This will make the port more attractive. In addition, the port will save on maintenance costs for the old mobile cranes.

Central warehouse

The central warehouse is moved. The warehouses will be extended towards the east. Advantage is that the warehouses do not block movements through the storage and the new location is close to the rail track. The option to move the warehouses to another location outside the port is not considered, because this is an important service to the clients.

Route

The road towards the dry bulk area is moved. It is placed directly next to the waterfront. The advantage is that all containers can be reached during the day.

6.2.2. Capacity

Although the terminal improvement plan is meant to improve the efficiency of the terminal, the plan also increases the terminal's capacity. The capacity of the storage area will grow to 973,000 $TEU/year$, a capacity improvement of 15%. This can be seen in 6.1. The calculation can be found in appendix D.3.2. The table shows that the new STS cranes improve the quay capacity, and that the capacity of the storage yard is still normative for the capacity.

	Current [TEU/yr]	**Improved** [TEU/yr]
Access road	6,083,000	6,083,000
Gate	1,477,000	1,477,000
Storage area	**848,000**	**973,000**
Quay	1,075,000	1,385,000

Table 6.1: The capacity of the different terminal components for the current and improved layout.

7

Nautical operations

Figure 7.1: Berthing of the Caroline Maersk at the San Vicente Port.

Source: Own photo (29 September 2018)

In figure 7.1 the berthing of the Caroline Maersk, a 347 m long container vessel, at berth 4 is shown. The operation takes place in the early morning, assisted by two tug boats. The vessel is turned in the large manoeuvring area outside the port and then tugged towards berth 4. After the vessel has been approved by the inspection, the unloading procedure can start. The mooring of the vessel will take approximate 48 hours. During the manoeuvring tugs will operate in the non sheltered area of the breakwater. Large waves will influence the manoeuvring efficiency and could even give downtime to the San Vicente Port. Also, vessel movements due to waves along the quays can influence the (un)loading efficiency. In this chapter the manoeuvring and (un)loading operations are analysed and improvement measures are investigated in detail.

7.1. Nautical operation analysis

The nautical operations consists out of the manoeuvring operation and the mooring of the vessel at the berth. Both operations are affected by the nearshore wave climate. First the manoeuvring operation is analysed followed by the mooring.

7.1.1. Wave model

To analyse the manoeuvring and mooring, a wave model is used which is explained in appendix B. This model consist out of two components; a numerical model (Delft3D) which computes the offshore to nearshore transformation and a Latin Hypercube Sampling (LHS) method to convert the entire 20 year offshore wave data set to a nearshore wave dataset. The final result is a nearshore data set containing wave information for selected locations of interest near The San Vicente Port. The wave nearshore information is used to analyse the nautical operations.

7.1.2. Manoeuvring conditions

The manoeuvring limitations are determined not by the vessels self but by the tug boats. If the H_s exceed a value of 1.5 m the manoeuvring operation can not be executed. C.1. This analysis shows that manoeuvring is possible 87% of the time, which is below the common standards. This percentage includes the distribution of vessels between the two different manoeuvring areas.

7.1.3. Mooring conditions

The mooring efficiency depends on the vessel motions during (un)loading. The mooring analysis can be found in appendix C.2. The governing and only motion analysed in this appendix is the heave motion. If the heave oscillations are larger than 0.4 m there will be inefficient (un)loading.

In this analysis seven different vessel groups are analysed on their heave motion at the quay. These vessel groups are based on cargo type and vessel length. The description of the vessels groups is given in appendix A. To compute the vessel motions, the output of the wave model is used. For each wave, a wave spectrum is constructed. This wave spectrum is used to construct a motion spectra for each vessel group based on a assumed Response Amplitude Operator (RAO). The final result is a 20 year data set containing heave oscillation information of each vessel group. This information can be used to study the (un)loading efficiency of each vessel group during mooring.

On average, the conditions in the port give in 95% of the time full efficient (un)loading. PIANC (2012) indicates that on average other ports have optimal (un)loading conditions approximately 98% of the time. So, San Vicente Port has less optimal (un)loading conditions than an average Port.

7.2. Nautical operation improvement

To increase the efficiency for manoeuvring and mooring operations, improvement measures have to be taken. To improve the nautical conditions near San Vicente Port, a breakwater extension is analysed. The extension configuration is shown in figure 7.2. It can be observed that this breakwater will increase the sheltered area which is beneficial for both the manoeuvring and mooring operations. The waves in the manoeuvring areas become smaller and therefore tug boats are able to operate with less downtime. The motions of moored vessels will reduce which will increase mooring efficiency.

7.2.1. Effect of breakwater extension

The effect for breakwater extension with steps of 150 m are analysed for manoeuvring and mooring. This is shown in figure 7.3b.

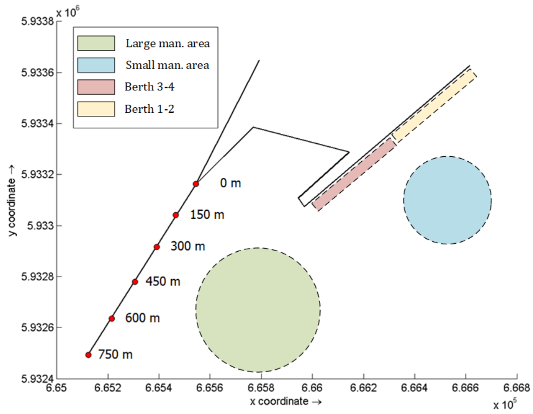

Figure 7.2: Breakwater extension configuration

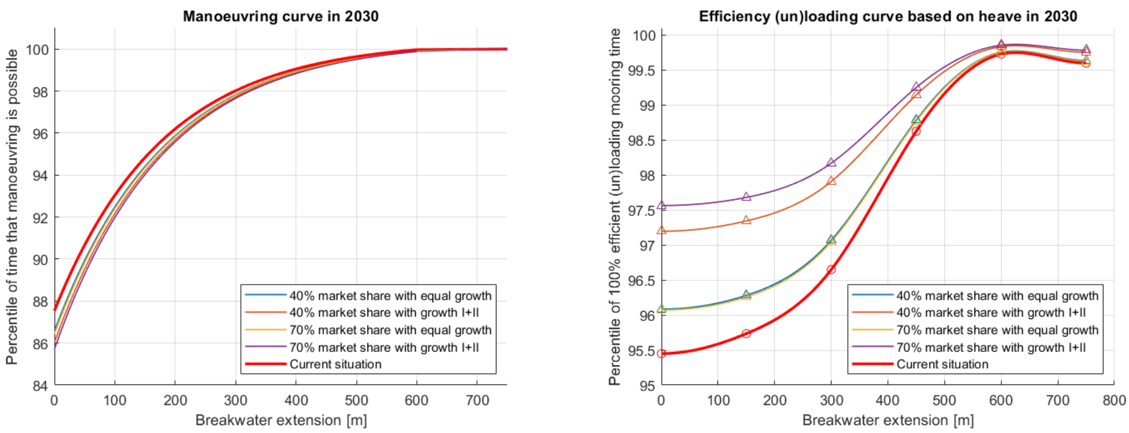

(a) Manoeuvring operations

(b) Mooring operations

Figure 7.3: Effect of breakwater extension on nautical operations including different scenarios in the year 2030

Manoeuvring

In figure 7.3a it can be observed that the current manoeuvring operations can be improved by extending the breakwater. The increase is exponential and the figure shows that an expansion larger than 500 m will not improve the time that manoeuvring is possible.

Mooring

According to figure 7.3b, the current mooring efficiency can be improved by extending the breakwater. However, the first 300 m extension have only an efficiency increase of 1 percentage point. The largest gradient in efficiency increase is found for a breakwater between 300 m and 600 m. An extension larger than 600 m will not improve the mooring efficiency anymore.

7.2.2. Influence of scenarios on nautical operations

In figure 7.3 the influence of the four future scenarios on the nautical operations are plotted. This figure is based on the vessel distribution per scenario in 2030. Figure 7.3a shows that all scenarios have a negative effect on the manoeuvring of vessels. For all scenarios, more vessels will need to manoeuvre in the manoeuvring area for large vessels which is more exposed. However, the effect of the scenarios on the current situation is rather small.

In contradiction to the manoeuvring, all scenarios have a positive effect on the mooring operations. Because there is a shift to larger vessels, and larger vessels have smaller vessel motions. This will increase the (un)loading efficiency. The influence of the future vessel distribution on mooring operations is larger than the influence on manoeuvring operations. It can be observed that the scenario, 70% market share with a growth of vessel group I & II, will have an optimal (un)loading efficiency almost 98% of the time. Moreover, this percentage is equal to the value for an average port according to PIANC.

7.3. Feasibility of breakwater extension

To investigate the feasibility of a breakwater extension, a cost-benefit analysis is preformed. The analysis can be found in appendix C.5. The costs of the breakwater extensions are determined based on the amount of required material and the construction costs. The benefit of a breakwater extension is expressed in a reduction of operational costs. This cost reduction is the result of less delays in mooring and manoeuvring time of container vessels.

A cash flow forecast with a horizon of 25 years is made for all breakwater extensions. The expenditures are based on the breakwater costs, with an estimated construction time of 3 years. The revenues are due to the above described cost reductions. The reduction is different per scenario, due to a difference in vessel distribution. With discounting techniques the present value of the cash flow is determined. As an example, the cash flow for the breakwater extension of 450 m is shown in figure 7.4. The Net Present Value (NPV) for the 25 years horizon is determined from these discounted cash flows. An overview for the calculated NPV for all scenarios and each breakwater extension is shown in figure 7.5.

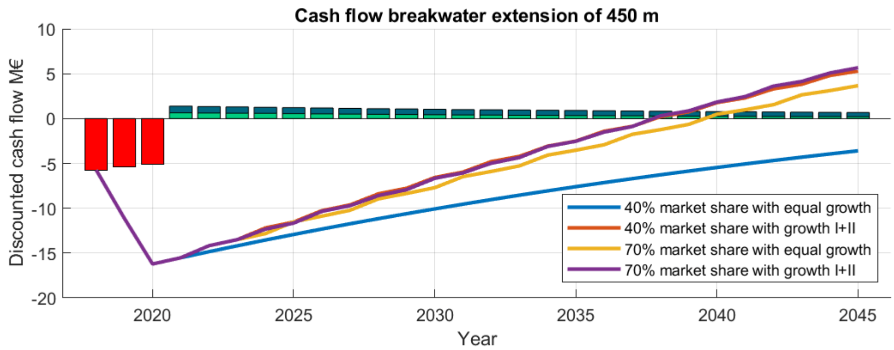

Figure 7.4: Discounted cash flow forecast for a 450-meter breakwater extension

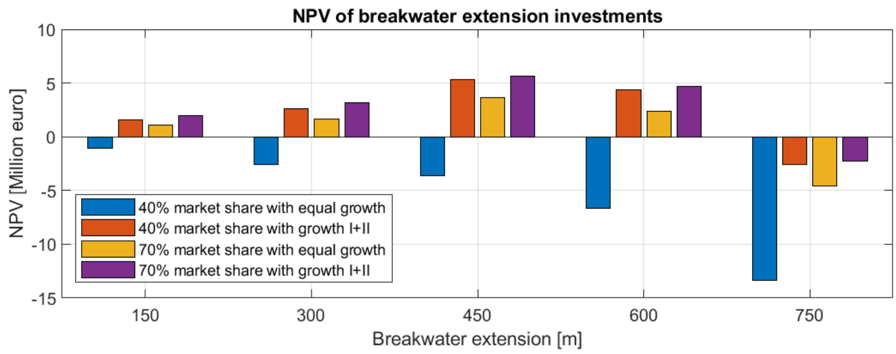

Figure 7.5: NPV of each breakwater extension for the four future scenarios

It can be observed that all NPV are negative for the scenario 40% market share with equal growth. This means that no breakwater extension is cost effective for this scenario. From figure 7.5 it can also be concluded that a breakwater extension of 750 m is not feasible for all future scenarios.

It can be observed that planning a breakwater extension is very risky. Depending on the future development of vessel distribution, a breakwater extension may be cost effective. However, it should be noted that there is a large uncertainty in the costs calculation. Thus, no breakwater extension is included in the improvement plan.

8 Port expansion

Figure 8.1: Between the breakwater and the container storage area, a small bay is present. This sheltered area can be an attractive location to start an expansion. It is protected by the breakwater and close to the quay.

Source: Own photo(2 October 2018)

When San Vicente Port grows, it will eventually need expansion to handle the demand. Because inland extension is not possible an offshore expansion is investigated. There are many possibilities to expand offshore. An obvious solution is to fill up the relative sheltered area indicated in figure 8.1. In this chapter, expansion options for the San Vicente Port are analysed. Adaptive port planning is included in the future design to anticipate on the uncertainties of the future scenarios. In appendix E the port expansion has been evaluated extensively.

8.1. Introduction

The throughput of San Vicente Port for the coming years can not be known. The different scenarios predict the fugure throughput, as is shown in figure 8.2. All scenarios show a future growth in which the throughput will eventually become larger than the current capacity and the capacity after the terminal improvements as calculated in chapter 6. When improving is not possible anymore the only solution is to expand the port.

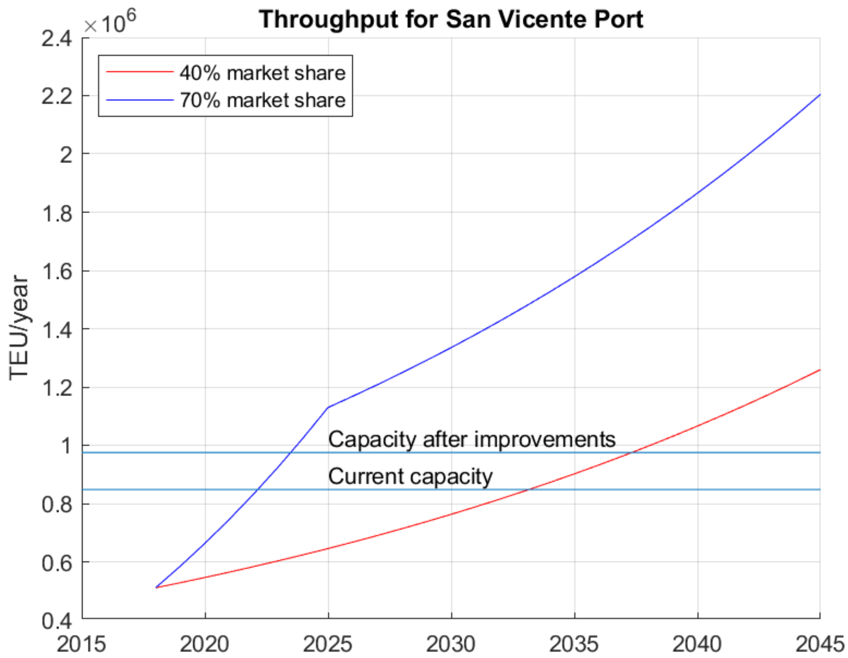

Figure 8.2: Expected container throughput (in $TEU/year$) for the 40% and the 70% scenario.

San Vicente Port is surrounded by Talcahuano city, the Taiguen hill and the local fishery port which makes inland extension not possible. The only expansion possibility is offshore. Only the possible offshore expansion location between the breakwater and the current terminal is investigated. This location is close to the terminal and the water area is less deep than outside the breakwater.

Three options for expansion between the breakwater and the current terminal are investigated in appendix E.3. Two options have a phased development. The options are compared using a Multicriteria Analysis (MCA). The selected option scores good at flexibility, which is the most important criterion. Other criteria are traffic flows, storage capacity (in phase 1), berth changes and nautical conditions.

8.2. Expansion plan

8.2.1. Adaptive port plan

Figure 8.3 shows the two phases of the expansion option with the highest multicriteria score (Option B in appendix E). In the first phase 7 ha of land is reclaimed. Berth 5 is removed; according to the quay capacity calculation this can be removed without any capacity problems. If desired, a new (temporary) quay of 300 m can be constructed at the waterfront of the reclaimed land. In the second phase, another 6 ha is reclaimed. The temporary quay of phase 1 should be removed. A construction of a new quay with a length of 400 m is possible. Again, this is not strictly necessary according to the quay capacity calculations.

The moment that the two phases of the expansion plan are needed depends on the development of the throughput. According to the two throughput scenarios, a development timeline is presented in figure 8.4. The advantage of an adaptive port design is that the design can be adapted if needed or if expected throughput will be different. This flexibility in the plans reduces the risks (Taneja, 2017). Also, the initial investment is smaller. As the timeline shows, the first expansion phase is needed in 2023 according to the 70% market share scenario. For the 40% market share scenario, this is only needed in 2040.

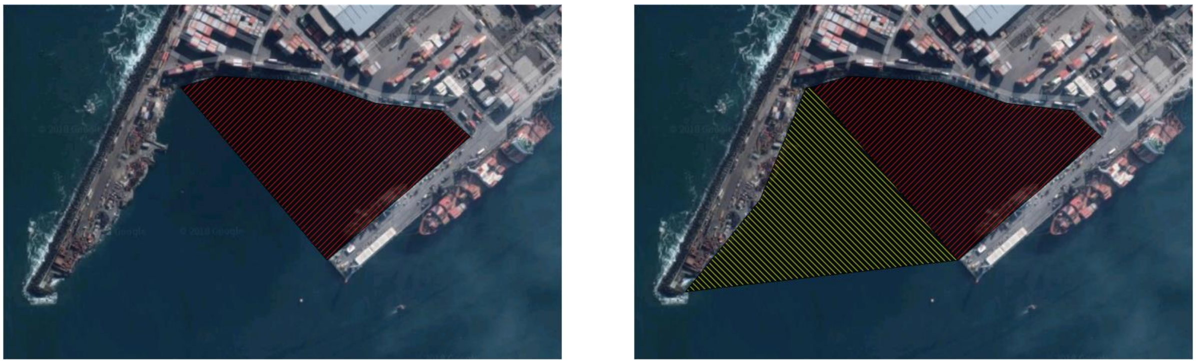

(a) Phase 1 of the expansion.

(b) Phase 2 of the expansion.

Figure 8.3: The two expansion phases. Phase 1 is shown in red and phase 2 in yellow.

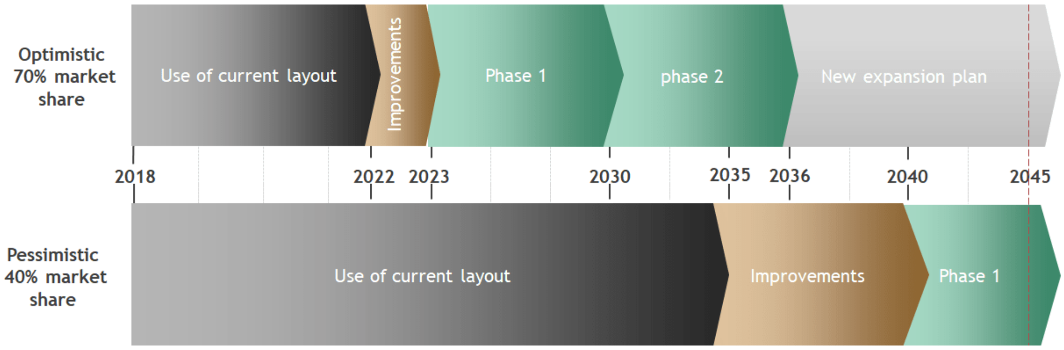

Figure 8.4: Development timeline of the port expansion plan for the optimistic and pessimistic throughput scenarios.

8.2.2. Layout

For both phases a layout is made which are presented in figure 8.5. These layouts continue on the improved layout that has been made in section 6.2.1. As a simplification, the ratio of the areas used for empty to import to export to warehouse to road is kept the same as in the improved terminal layout. In both phases, the rail track is extended and a new warehouse is build next to the current warehouses. Extra import and export stacks are added in front of the quay and the empty stacks are moved further towards the breakwater.

8.2.3. Capacity

The capacity of the terminal after the expansions are shown in table 8.1. The storage area is the governing capacity component. With the expansion of phase 1 the capacity of the terminal will grow from 973,000 TEU/yr to 1,284,000 TEU/yr. With the second phase of the expansion the capacity will be 1,552,000 TEU/yr. In the second phase also the fifth gate, which already has been constructed, must be opened. The quay capacity will grow during the different phases, because the mobile cranes will be replaced by Ship-to-Shore (STS) with a higher productivity. This is necessary to keep the waiting times for ships below the 10% of the service time, which is still considered acceptable (Ligteringen & Velsink, 2012). For this calculation only two berths are needed for container vessels. This means no extra quay is necessary to be build unless the port authority wants to reduce the waiting time to be more attractive for vessels. The port design is adaptive, so it is possible to incorporate an extra quay in the design. The capacity calculations for the expansions are explained in appendix E.4.

	Improved [TEU/yr]	**Phase 1** [TEU/yr]	**Phase 2** [TEU/yr]
Access road	6,083,000	6,083,000	6,083,000
Gate	1,477,000	1,477,000	1,847,000
Storage area	**973,000**	**1,284,000**	**1,552,000**
Quay	1,075,000	1,385,000	1,589,000

Table 8.1: The capacity of the different terminal components for the expansion phases.

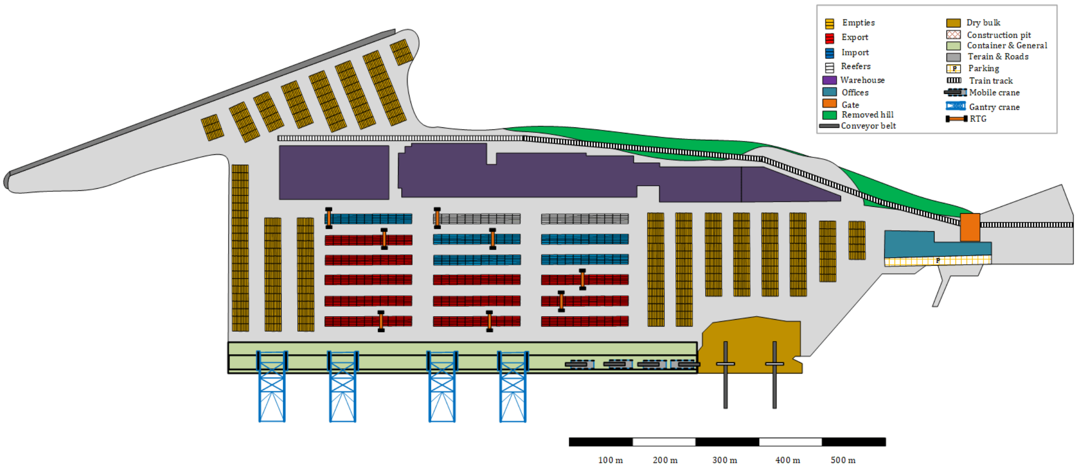

(a) Layout after phase 1 of the expansion.

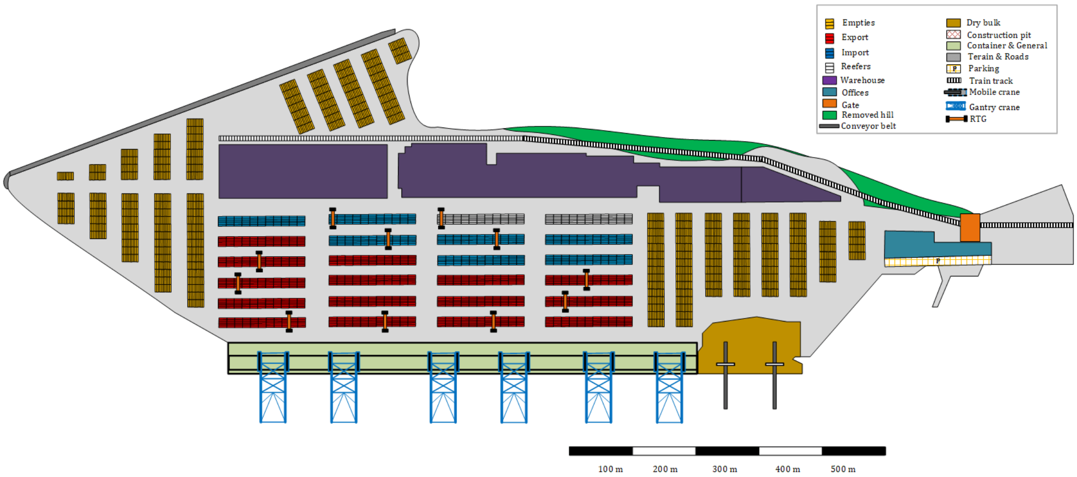

(b) Layout after phase 2 of the expansion.

Figure 8.5: The layouts for the different expansion phases.

8.2.4. Costs

The costs for the expansion are calculated based on the optimistic scenario of 70% market share. The total costs for phase 1 are €17,000,000 and for phase 2 are €12,250,000. This results in a Present Value of the expenditures of €24,100,000 and a Net Present Value (NPV) of €24,500,000. The discount cash flow can be seen in figure 8.6. The complete cost calculation can be found in appendix E.6.

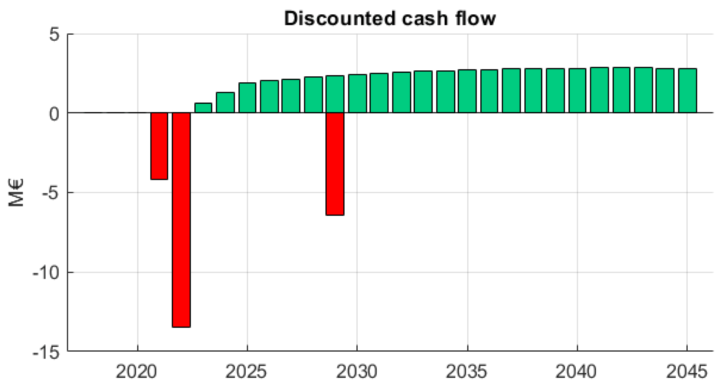

Figure 8.6: Discounted cash flow for the two phase port expansion plan based on the 70% market share scenario.

9
Conclusions and recommendations

Figure 9.1: Unloading of a container vessel by mobile cranes

Source: Own photo (2 October 2018)

San Vicente Terminal Internacional S.A. has nine mobile harbour cranes to (un)load vessels. These old cranes have a productivity of 15 movements per hour. It has been decided that mobile cranes are slowly replaced by Ship-to-Shore gantry cranes with a productivity of 27.5 movements per hour. The first two gantry cranes will be operational next year. The replacement of cranes is just a small part of the development plan for San Vicente Port. A conclusion of this development plan is given in this chapter.

Conclusions

In the development plan three analyses are executed for the San Vicente Port. The conclusions will be elaborated for each analysis separately.

From the terminal operations analysis the following conclusions can be given:

- The San Vicente Port, of which the current layout is shown in figure 9.2a, has an efficiency problem.
- The terminal improvement plan will increase the efficiency by solving the following problems: the train blockage, mobile harbour crane, container consolidation, traffic jam and central warehouse. As a side effect, the capacity will be enlarged from 848,000 Twenty Foot Equivalent Unit (TEU) to 973,000 TEU, which is a 15% increase.

From the nautical operations analysis the following conclusions can be given:

- San Vicente Port has 13% downtime for manoeuvring due to waves larger than 1.5 m.
- San Vicente Port experiences inefficient container loading and unloading due to vessel heave motions for 5% of the time.
- According to PIANC standards, ports strive for inefficient (un)loading conditions for maximum 2% of the time. Mooring conditions at San Vicente Port are below PIANC standards.
- With an breakwater extension of at least 400 m the efficiency of the mooring operations (for the current vessel distribution) will be within PIANC standards.
- According to the feasibility study it is uncertain if a breakwater extension is cost effective.
- From the studied breakwater extensions, a 450 m breakwater extension can give the highest profits, but there is also a risk of losing money.

The decision of including a breakwater extension cannot be done based om the analyses that have been preformed. Therefore, the breakwater is not included in the improvement plan. The layout of the improvement plan is presented in figure 9.2b.

From the expansion plan analysis the following conclusions can be given:

- Future container throughput will become larger than the terminal capacity (including improvement plan). A terminal expansion is needed.
- Throughput forecasts are uncertain: the development plan must take into account adaptive port planning. Therefore, the terminal expansion plan consists out of two phases. The timeline of the construction of these phases depends on the development of the future throughput.
- The first phase is an expansion of 7 ha and will give a capacity of 1,284,000 TEU/yr.
- The second phase is an expansion of 6 ha and will give a capacity of 1,552,000 TEU/yr.

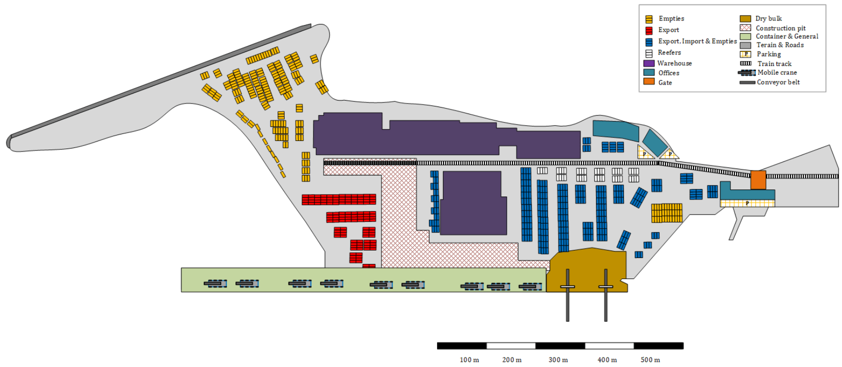

(a) San Vicente Port at current situation

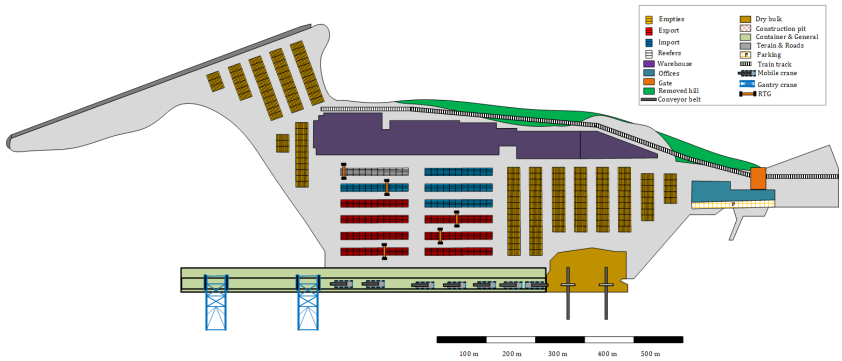

(b) San Vicente Port after improvements

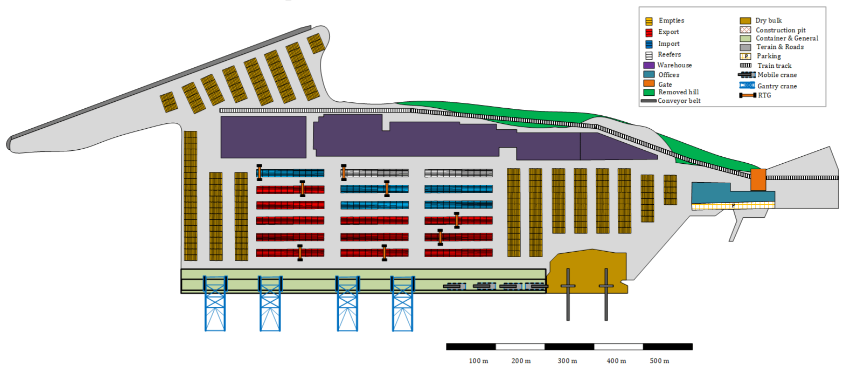

(c) San Vicente Port after expansion phase 1

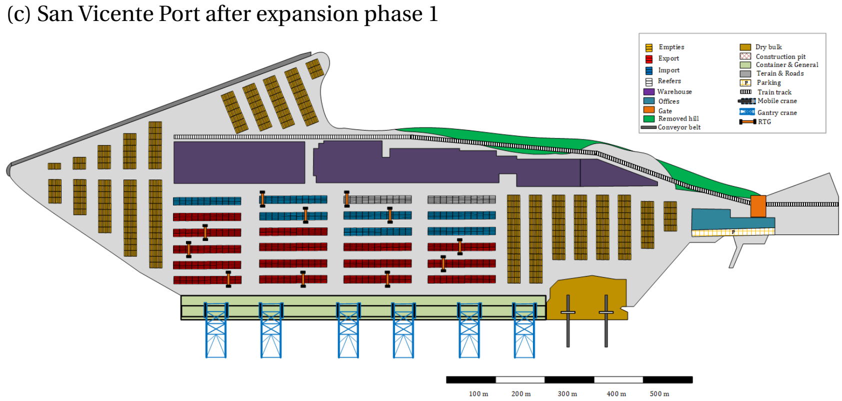

(d) San Vicente Port after expansion phase 2

Figure 9.2: Development of San Vicente Port

Recommendations

For the improvement of the development plan, recommendations per analysis are given.

The following is recommended with regards to the terminal operations analysis:

- To investigate traffic problems in the terminal it is best to use an advanced traffic model. The effects of interventions on the efficiency are difficult to define without such a model. The model can be used quantitatively to prove the efficiency increase of the various solutions.
- The technical feasibility of the new configuration of the rail tracks have to be checked. Especially the sharp bends and removal of the Taiguen hill can result in problems.
- The financial feasibility of the improvement plan has to be checked. The associated costs of moving the train, central warehouse and offices, and purchase of terminal equipment are expected to be high.
- The capacity calculation in this report is different than in the performance review of Empresa Portuaria Talcahuano San Vicente (2018), because our observations did not match the number in the calculation. A dwell time for empty containers of 10 days was assumed (compared to 3 days in the performance review); since San Vicente Port is mainly an export port, a lower dwell can be used.

The following is recommended with regards to the nautical operation analysis:

- The calculated manoeuvring downtime due to waves should be compared to real data from the port authority to validate the model.
- For the offshore to nearshore transformation a JONSWAP wave spectrum is used. However, the wave climate along the Pacific coast can be better described by a two-peaked spectrum. For a more realistic transformation, this should be included in the Delft3D simulations. Note that the Latin Hypercube Sampling (LHS) method is not applicable for two-peaked spectra. In general, the current approach is expected to give reasonable results.
- The vessel motion model is limited to vessel heave motions. Although, this will cover the general idea, the other vessel motions (like surge, roll, pitch) might also contribute to inefficient loading.
- A simple Response Amplitude Operator (RAO) is assumed due to insufficient time and resources. For a more accurate calculation of vessel motions, the RAO should be computed numerically or determined by physical model tests.
- The effect of mooring lines on the vessel motions is assumed negligible. Further research is needed for this effect.
- The cost calculation of the breakwater extension is based on a standard breakwater layout, with dimensions estimated from the current breakwater. For a better estimation of the costs, a breakwater design must be made based on an extreme wave analysis.
- It is not investigated if a breakwater extension leads to sedimentation problems (and the need of dredging) in the port.
- The limit of 1.5 m for manoeuvring is determined by the type of tugs that are used in the port. A different type of tug might have better manoeuvring limits, so manoeuvring with larger waves is still possible.
- Other solutions than a breakwater extension have not been investigated. Better mooring configurations can form a cheaper solution to improving the mooring efficiency. For example systems such as MoorMaster and ShoreTension have a positive effect on the loading and unloading efficiency. Also, a floating breakwater may be a more cost effective solution. However, it should be mentioned that floating breakwaters are usually ineffective against swell waves.

The following is recommended with regards to the expansion plan:

- It is assumed that the best location for an expansion plan is the water area between the breakwater and the quay. However, no other locations for expansion plans where investigated.

General recommendations:

- Low efficiency of the port is assumed to be the reason for the market share problem. Other reasons, such as the recovery of the port after the 2010 earthquake and the construction works of the quay expansion, are not included in the report.
- Adaptations in the port, like a breakwater extension or faster service times, make the port more attractive. This could result in a growth of the market share. This is not included in the cost benefit calculations.
- The combination of an expansion and a breakwater extension is not investigated. For the construction of an extra quay (for example for better service times), a breakwater extension might be needed, so this influences the feasibility of a breakwater extension.
- It is not possible to change the port at once, therefore it is a good idea to analyse the rivalling ports to identify the strong and weak points of San Vicente Port. Than start the improvement process with tackling the weak points first.
- The cost are based on assumptions and (outdated) Dutch price levels. Thus, there is a large uncertainty in the cost calculation. However, the used price levels give an indication of the costs. A more reliable result can be achieved with an extensive cost calculation, based on local and current price levels.

(This page is intentionally left blank)

References

Agental & CPT. (2018). *Tugs service.* Retrieved 10-2018, from `www.agental.cl`

Beyá, J. (2016). *Atlas de oleaje de chile.* Universidad de Valparaíso.

Caba, R. V. C. (2016). *Análisis de marejadas históricas y recientes en las costas de chile.* Universidad de Valparaíso.

Empresa Portuaria Talcahuano San Vicente. (2017). *Estudio: "estimación y caracterización de demanda portuaria tsv.*

Empresa Portuaria Talcahuano San Vicente. (2018). *Information received from the port authority.*

Ghassemi, H., Majdfar, S. & Gill, V. (2015). Calculations of the heave and pitch rao's for three different ship's hull forms. *Journal of Ocean, Mechanical and Aerospace.*

Gribnau, K., Koevoets, I., Hemel, M.-J. & Onrust, M. (2018). *San vicente port - climate change impact analysis.*

Groenveld, R. (2001). *Service systems in ports and inland waterways.* Delft: VSSD.

Gómez, M., Villagrán, M., Martínez, C. & Belmonte, A. (2018). Characterizing the longshore sediment transport pattern on beaches in the gulf of arauco, chile, to assess morphological shoreline evolution. *Journal of Coastal Research.*

Hertogh, M. & Bosch-Rekveldt, M. (2015). *Integraal ontwerp en beheer.* Delft: TU Delft.

Journée, J. & Pinkster, J. (2002). *Introduction in ship hydromechanics* (draft ed.). Delft University of Technology. (Lecture MT519)

Ligteringen, H. & Velsink, H. (2012). *Ports and terminals.* Delft: VSSD.

Merk, O. (2016). Ports policy review of chile. *International Transport Forum.*

Michou, D. (2017). *Memoria y balance anual 2017.* San Vicente Terminal Internacional S.A.

Onrust, M. (2018). *Framework for improved channel depth design.*

Peters, D. J. (2018). *Hydraulic structures – seismic resistance / dynamic analysis.* Delft University of Technology.

PIANC. (1995). *Pianc 24-1995: Criteria for movements of moored ships in harbours, a practical guide.* PIANC Secrétariat Général.

PIANC. (2012). *Pianc 115-2012: Criteria for the (un)loading of container vessels.* PIANC Secrétariat Général.

PIANC. (2014a). *Pianc 121-2014: Harbour approach channels design guidelines.* PIANC Secrétariat Général.

PIANC. (2014b). *Pianc 135-2014: Design principles for small and medium marine container terminals.* PIANC Secrétariat Général.

Quist, P. (2017). *Lecture cie 4330: container terminals.* Delft University of Technology.

SEA. (2017). *Market forecast report 2017.* SEA Market Forecast WSG.

Taneja, P. (2017). *Lecture cie 4330: flexible ports port planning under uncertainty.* Delft University of Technology.

Thoresen, C. A. (2010). *Port designer's handbook.*

Tutuarima, W. & Angremond, K. (1998). Cost comparison of breakwater types. *Delft University of Technology, Faculty of Civil Engineering and Geosciences.*

van Dorsser, C. (2017). *Lecture cie 4330 ports and waterways 1: Economics of port masterplanning.* Delft University of Technology.

Verhagen, H. J., d'Angremond, K. & van Roode, F. (2009). *Breakwater and closure dams.* Delft: VSSD.

Windguru. (2018). *Wind and weather information.* Retrieved 10-2018, from `www.windguru.com`

A

Ship analysis

Figure A.1: Forestal Reina during loading

Source: Own photo (29 September 2018)

This appendix gives an analysis of the different vessels that are handled in San Vicente Port. These are container, general cargo and dry bulk vessels. Vessel sizes and types are used to study the behaviour of ship movements during manoeuvring and mooring.

A.1. Vessel groups

In the period January-September 2018, 189 vessels moored at the San Vicente Port (Empresa Portuaria Talcahuano San Vicente, 2018). In figure A.2 the different vessel types are shown. It can be seen that the largest part consists of container vessels. Therefore the vessels are separated into two groups: container vessels (147 vessels) and other vessels (42 vessels). Extrapolation of this number gives, 196 container vessel and 56 other vessels on a yearly base.

The length of the vessels (Length between perpendiculars L_{bp}) with the berthing times is shown in figure A.3. According to this figure, all handled vessels in the San Vicente Port can be subdivided into seven groups. Five groups with different vessel lengths can be defined for the container vessels and two groups for the other vessels. For each group, a representative vessel is chosen and information about this vessel is provided. The vessel groups will be used for further analysis.

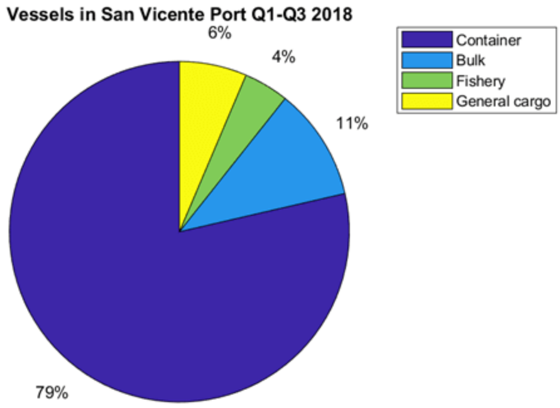

Figure A.2: Percentage of vessels types in San Vicente Port(Empresa Portuaria Talcahuano San Vicente, 2018)

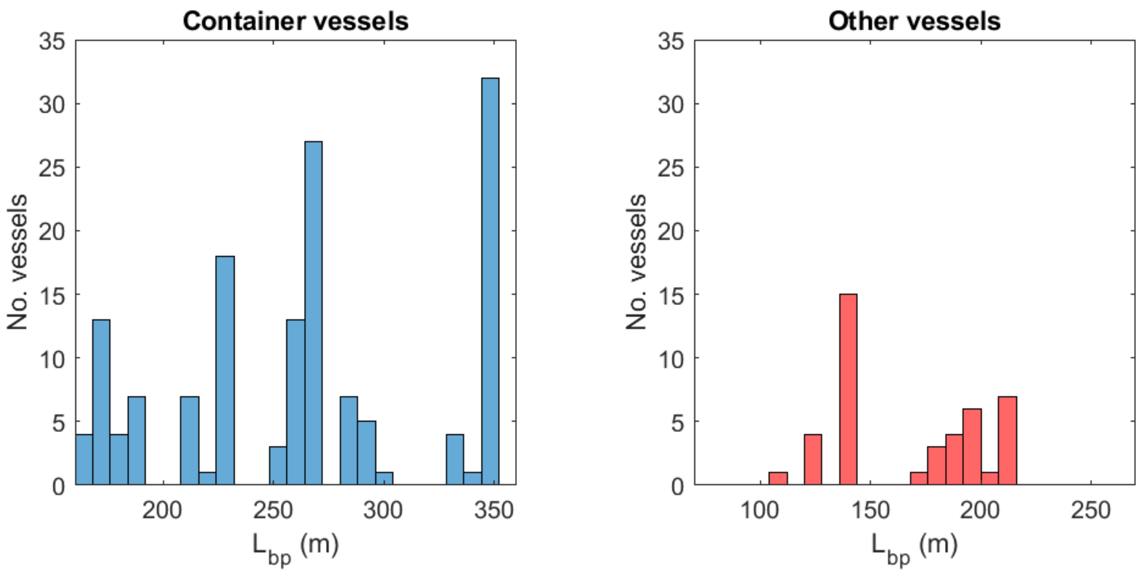

Figure A.3: Histograms of the length of the moored vessel at the San Vicente Port for the period Q1-Q3 2018

Group	**Number** [%]	**Cargo type**	**max L_{bp}** [m]	**min L_{bp}** [m]	**Rep. Vessel**
I	19.6%	Container	350	330	Caroline Maersk
II	6.9%	Container	300	280	Mongoose Hunter
III	22.8%	Container	270	240	Spirit of Lisbon
IV	13.7%	Container	235	220	Antofagasta express
V	12.7%	Bulk	220	170	Forestal Reina
VI	14.8%	Container	190	160	Meridian
VII	10.5%	General cargo, bulk and fishery	145	100	Corcovado

Table A.1: Vessel classes divided by cargo type and vessel length. The groups are sorted by vessel length (L_{bp}).

A.1.1. Group I (New Panamax)

DWT	110387
TEU	8160
$\mathbf{L_{bp}}$ [m]	347
b [m]	42.8

Figure A.4: Caroline Maersk (container ship)

A.1.2. Group II (Panamax)

DWT	58289
TEU	4922
$\mathbf{L_{bp}}$ [m]	294.1
b [m]	32.4

Figure A.5: Mongoose Hunter (container ship)

A.1.3. Group III (Supramax)

DWT	50249
TEU	4240
$\mathbf{L_{bp}}$ [m]	261
b [m]	34.34

Figure A.6: Spirit of Lisbon (container ship)

A.1.4. Group IV (Handymax)

DWT	48039
TEU	3500
$\mathbf{L_{bp}}$ [m]	224
b [m]	34.8

Figure A.7: Antofagasta express (container ship)

A.1.5. Group V (Handymax)

DWT	49892
$\mathbf{L_{bp}}$ [m]	200
b [m]	32.2

Figure A.8: Forestal Reina (Wood Chips carrier)

A.1.6. Group VI (Handysize)

DWT	30084
TEU	2339
$\mathbf{L_{bp}}$ [m]	189
b [m]	30.4

Figure A.9: Meridian (Container ship)

A.1.7. Group VII (Small vessels)

DWT	12840
$\mathbf{L_{bp}}$ [m]	138
b [m]	21

Figure A.10: Corcovado (General Cargo carrier)

A.2. Berths usage

The San Vicente Port has 5 berths. The berth usage percentage is shown in figure A.11. It can been seen that most vessels are mooring on berths 1, 3 and 4. Table A.2 presents the berth usage per vessel group. Berth 1 is only used for bulk vessels, berths 3 and 4 are used most often (mostly by container vessels), whereas berths 2 and 5 are rarely used.

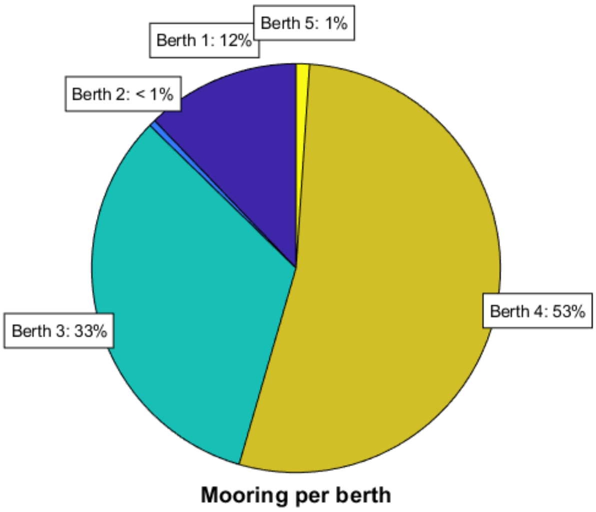

Figure A.11: Percentage mooring vessels per berth

Group	**Berth 1** [%]	**Berth 2** [%]	**Berth 3** [%]	**Berth 4** [%]	**Berth 5** [%]
I	-	-	5	95	-
II	-	-	-	100	-
III	-	2	10	88	-
IV	-	-	58	42	-
V	55	-	45	-	-
VI	4	-	79	14	3
VII	50	-	45	-	5

Table A.2: Percentage berth usage per vessel group

A.3. Manoeuvring location

Manoeuvring is needed in San Vicente Port to turn the vessels before berthing. Most vessels are moored on starboard side. The preferred location for manoeuvring is in front of the quay, because this area is well protected by the breakwater. However, the space is limited, so only vessels of up to 180 m can turn in front of the quay. Larger vessel have to turn further offshore, where conditions are more rough. Table A.3 shows the possible manoeuvring area per vessel group. Because of the chosen limits for the group sizes, only some vessels of group V and VI are able to turn in front of the quay. Based on the vessel at San Vicente Port in Q1-Q3 2018, the percentage of vessels smaller than 180 m is calculated. Only these vessels are able to turn in front of the quay.

Group	**In front of the quay**	**Manoeuvring area for $L > 180m$**
I	X	$\surd$
II	X	$\surd$
III	X	$\surd$
IV	X	$\surd$
V	$\surd$/X(18%)	$\surd$
VI	$\surd$/X (75%)	$\surd$
VII	$\surd$	$\surd$

Table A.3: Possible Manoeuvring area per vessel group, ($\surd$) possible for entire vessel group, ($\surd$/X)..% partly possible for vessel group (..%= percentage possible), (X) not possible for entire vessel group.

A.4. Future vessel distribution

San Vicente Port is a state port, which means that they are obligated to receive different types of cargo vessels. Thus, the worldwide shift from bulk and general cargo transport to containerised transport is not expected to have a large influence on the future distribution of vessels. In the future, a similar distribution of bulk vessels, general cargo and container vessels is expected.

However, due to the scale enlargement of container transport the vessel sizes are expected to increase (Quist, 2017). Currently only 25% of vessels are Panamax or larger (vesselgroup I and II), but more large vessels are expected. Due to the restrictions of the Panama sluices, no larger vessels then New Panamax will call at San Vicente Port.

For the application in this masterplan report, two scenarios are made up. In both scenarios only the container vessel groups will growth. The other vessel groups will have the same amount of yearly calls.

1. All container vessel groups will growth. The distribution of the container vessel groups will not change.
2. The larger vessels (Panamax and New Panamax) will take care of all the growth of San Vicente Port.

It should be noted that these are two extreme scenarios and that it seems likely that the truth is in the middle. However, it is impossible to predict the future.

B

Wave Model

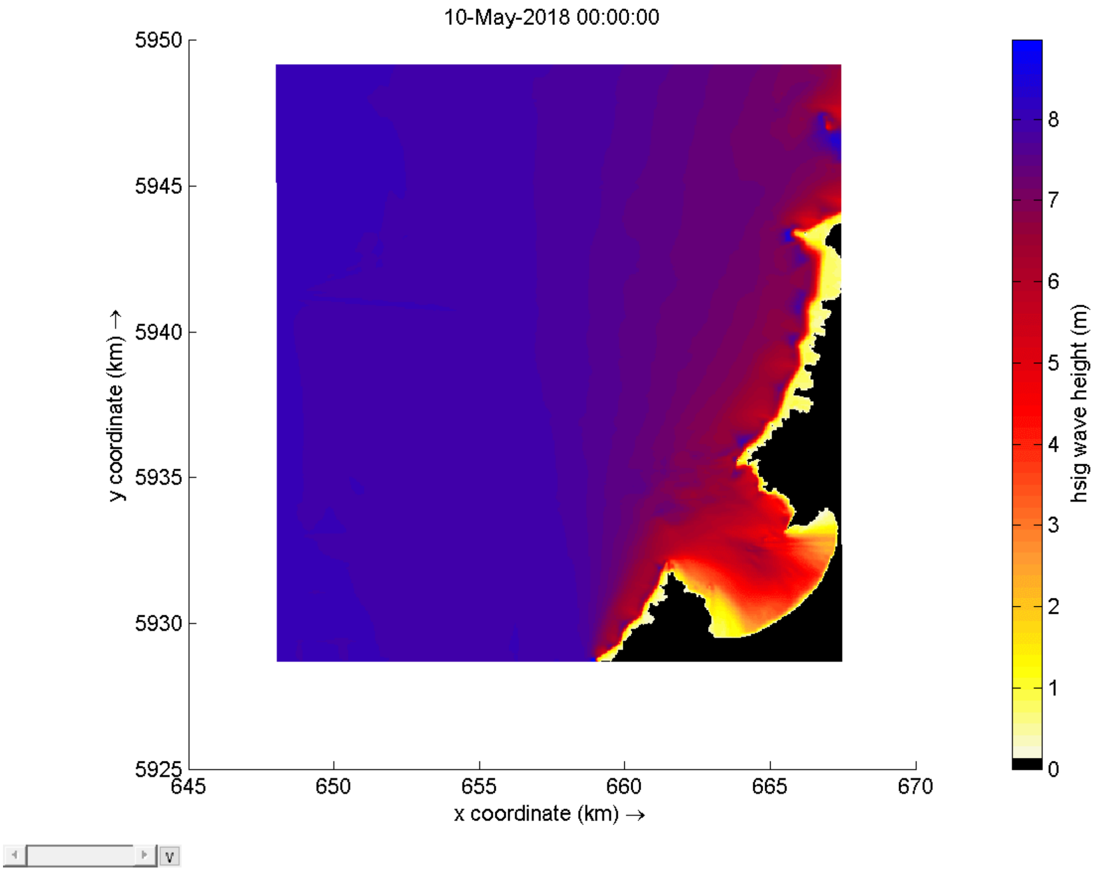

Figure B.1: Simulated wave approach towards San Vicente Port with direction 250 – 255°.

A wave model is used for analysing the wave conditions in San Vicente Bay. This appendix presents the setup of the wave model. The Delft3D standalone wave module is used in the model. The main purpose of the model is to analyse the waves in the San Vicente Bay. The waves at several locations in the bay are studied to assess manoeuvrability and the efficiency of the (un)loading operations in the port. Moreover, the model can be used to analyse the effect of a breakwater extensions on the wave conditions at the berths.

B.1. Model setup

A wave model is set up to compute the wave properties in the San Vicente Bay. The standalone wave module from Delft3D is used to perform the computation.

At Universidad Católica de la Santísima Concepción (UCSC) a Delft3D model of the Chilean coast has already been used before, so some files from the UCSC-model are adapted and reused for the San Vicente Model. The model covers an area of 18 × 18 [km], as is shown in figure B.2. Although larger grid- and bathymetry files were available, only a small study area was selected. There are two reasons for this: (1) Computational times are shorter and (2) 20 years of wave hindcast data is available at the boundary of the study area. This means that the wave hindcast data can be used as input for the wave model.

Figure B.2: Study area of the wave model.

B.1.1. Grid and bathymetry

The model consist of a single grid of 461 × 464 cells. All grid-cells have a rectangular shape; both Δx and Δy are 40 m.

The bathymetry is composed of two data files that are merged together. The large scale bathymetry, combined by UCSC (Gómez et al., 2018), contains the large scale bathymetry of the Chilean coastline. This bathymetry covers the entire study area, however the San Vicente Port is not detailed enough in this grid. In the San Vicente Port a higher level of detail is desired, so survey data along the quays, with a higher density, are merged into this bathymetry. The survey data is provided by the port authority. In order to merge the two-data files, the reference level from the survey data is first transposed from LAT to MSL.

The merged bathymetry file is interpolated over the model grid to find the depth at each grid point. This is done in Delft3D using the Triangular interpolation method. The bathymetry-file covers a larger area than the grid-file to prevent unrealistic interpolation results at the grid boundaries.

Figure B.3 shows the water depth in the model. Six observation points are indicated; these observation points are used for post-processing, see section B.4.2. In addition, one observation point is placed offshore to calibrate the model. The figure shows that the Biobío coastline is very steep. At the entrance of San Vicente Bay the water depth is already over 40 m.

B.1.2. Boundary and initial conditions

Wave boundary conditions are applied along the north, west and south boundary of the model. The east boundary of the model is the Chilean coastline, so no boundary condition needs to be applied here. The same (uniform) boundary condition is applied to all three boundaries. The wave conditions (H_s, T_p, θ, etc.) are specified at the boundaries. Delft3D uses these conditions to create a wave spectrum. A JONSWAP spectrum

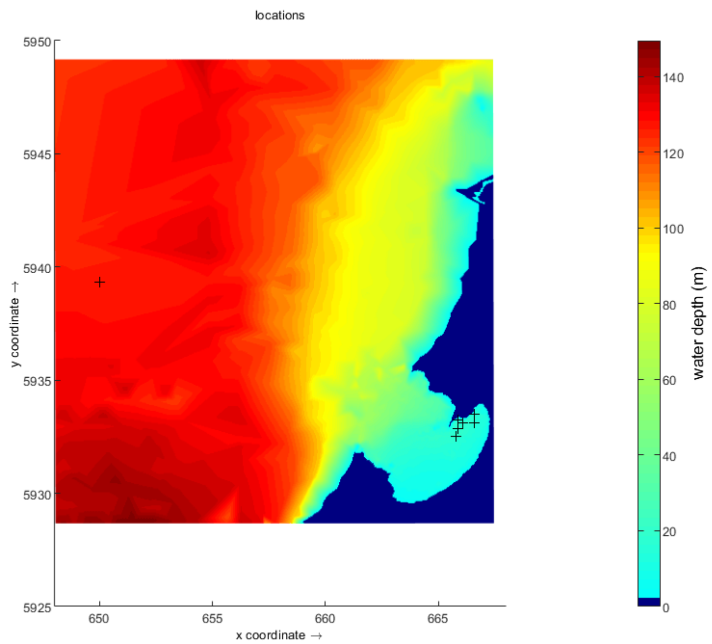

Figure B.3: Depth profile of the model area. 6 observation point in the port and 1 observation point offshore that are used for post-processing are indicated (+).

is selected with $\gamma = 1.4$; according to Beyá (2016) this value gives the best representative wave spectrum near Talcahuano.

Since the standalone wave module of Delft3D is used, only the water level is required as initial condition. The water level needs to be specified as a water level correction with respect to Mean Sea Level (MSL). MSL is used as initial water level.

B.1.3. Implementing port layout

The structural elements of the port layout, the quay and the breakwater, are implemented in the model. Since the quay and the breakwater have different properties (the quay is an open-wharf structure, whereas the breakwater is a closed non-transmissive structure), they are implemented differently in the model.

Because the quay extends above MSL, it is implemented in Delft3D as a 'sheet'-obstacle. A 'sheet'-obstacle does not allow for over- or underflow. Due to the quay's open structure transmission is possible: The wharf's pilings block about 20 % of the quay, so including some contraction a transmission coefficient of 70 % is assumed. The circular shape of the pilings means that the incoming waves will not reflect on the quay; the reflection coefficient is set to 0.0 (zero).

For the breakwater, the reflection coefficient is generally between 0.20-0.40 (Verhagen et al., 2009); a reflection coefficient of 0.3 is used in the model. The top-structure of the breakwater is wide, therefore the transmission of the breakwater is set to 0.0 (zero).

For modelling the waves in the sheltered zone, refraction and diffraction are essential to incorporate in the model. Because the breakwater is modelled as a 'sheet'-obstacle, the tip of the breakwater is sharp. As a result, Delft3D does not model the refraction and diffraction of waves around the breakwater tip correctly. For these reasons, an obstacles is not the best way to implement the breakwater. Therefore, the depth profile around the 'sheet'-obstacle is adapted to the cross-sectional shape of a breakwater. In this way, the 'sheet'-obstacle structure ensures the correct reflective and transmission properties of the breakwater while the adapted depth profile will give a representative diffraction and refraction pattern. Especially for breakwater extensions, where the sheltered zone is larger, this two step implementation is needed. This can be seen in figure B.5.

An overview of the properties of the obstacles is given in table B.1. The breakwater and quay model configuration is shown in figure B.4.

	Reflection coefficient	Transmission coefficient
Quay	0.0	0.7
Breakwater	0.3	0.0

Table B.1: Properties of the obstacles for the port layout in the model.

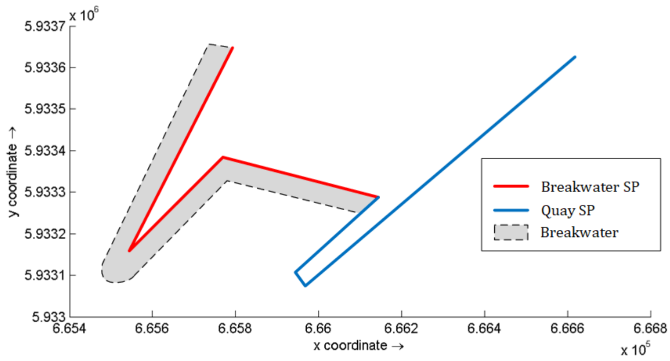

Figure B.4: Breakwater and quay model configuration. Note that SP = sheet pile.

B.2. Model verification

The model is verified with measurement data from the wave gauge in San Vicente Bay. The offshore wind and wave conditions are determined with the Global Forecast System from the National Oceanic and Atmospheric Administration (NOAA). The measurement data from the wave gauge is retrieved from the SVTI-website. The sensor is located near berths 4 and 5, see figure B.6. Only real-time wave data is publicly available, therefore a limited amount of wave conditions is used for the verification. The model will be verified for the significant wave height and the wave period. Although the peak period T_p is used for further analysis, the mean absolute wave period T_{m02} is used for verification. The reason for this is that the peak period T_p is not measured by the wave gauge.

B.2.1. Verification data

The offshore wind and wave data that are used for the verification are given in table B.2.

Date	$\mathbf{H_s}$ [m]	$\mathbf{T_p}$ [s]	Wave direction [°]	$\mathbf{v_{wind}}$ [m/s]	Wind direction [°]
08-10-2018 09:00	2.7	11	263	5.0	244
08-10-2018 22:00	2.1	10	268	4.0	248
09-10-2018 09:00	2.0	13	233	5.0	182
09-10-2018 12:00	2.6	18	228	4.0	195
09-10-2018 17:00	3.5	17	231	9.0	210
09-10-2018 23:00	3.5	17	229	8.0	191
10-10-2018 09:00	2.7	15	229	5.0	168

Table B.2: Offshore wave and wind data (Windguru, 2018).

The wave measurement data inside San Vicente Bay that is used for the verification is given in table B.3.

B.2.2. Model verification

The wave conditions presented in table B.2 are used as boundary conditions for wave simulations. The wind velocity and direction are used as additional input for the entire model area. The model result for the location of the wave gauge (UTM-coordinate: 18H 6659 59330) are presented in table B.4.

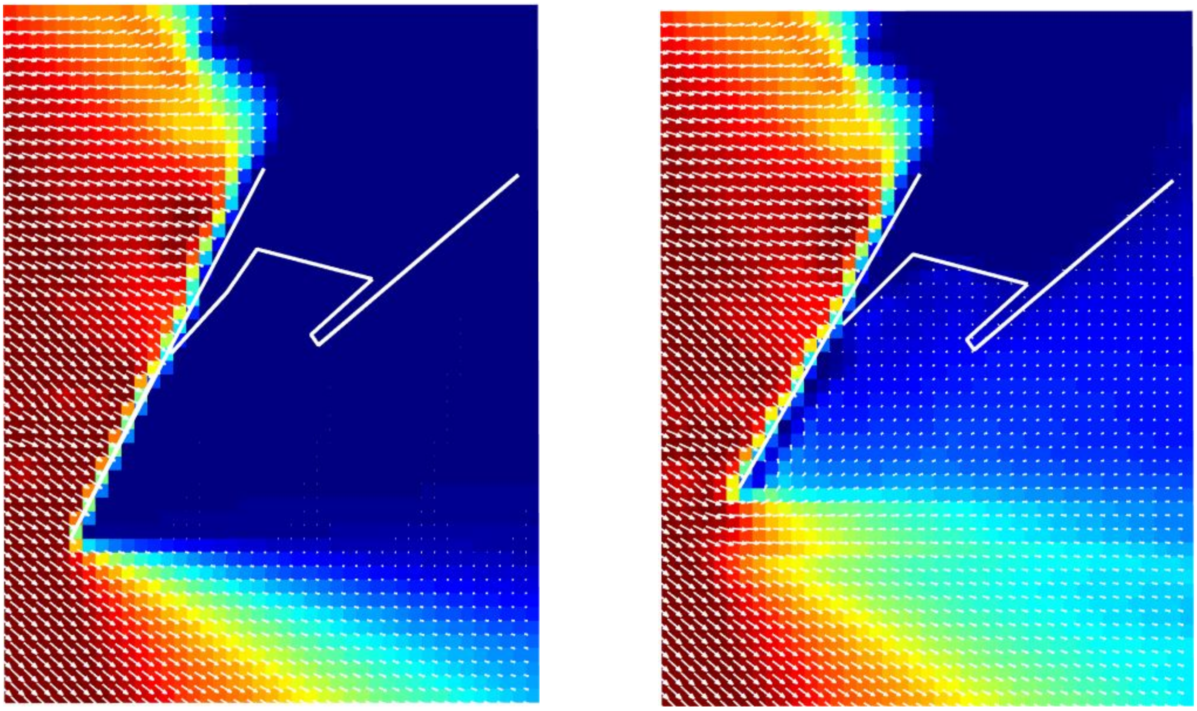

Figure B.5: Comparing the model results for a implementation of an extended breakwater of a) only a 'sheet'-obstacle and b) a 'sheet'-obstacle and depth profile adaptations

Date	$\mathbf{H_s}$ [m]	$\mathbf{T_{m02}}$ [s]	**Wave direction** [°]
08-10-2018 09:00	1.20	5.6	261.2
08-10-2018 22:00	0.73	5.1	261.2
09-10-2018 09:00	0.54	5.0	255.0
09-10-2018 12:00	0.64	4.2	253.4
09-10-2018 17:00	0.69	3.2	259.0
09-10-2018 23:00	0.70	4.0	255.1
10-10-2018 09:00	0.51	4.9	267.0

Table B.3: Wave Gauge data, UTM-location: 18H 6659 59330. Source: SVTI

Date	$\mathbf{H_s}$ [m]	$\mathbf{T_{m02}}$ [s]	**Wave direction** [°]
08-10-2018 09:00	0.88	5.33	255.2
08-10-2018 22:00	0.69	4.96	255.2
09-10-2018 09:00	0.56	3.60	247.8
09-10-2018 12:00	0.67	4.96	251.4
09-10-2018 17:00	1,02	3.66	246.1
09-10-2018 23:00	0.96	4.33	246.5
10-10-2018 09:00	0.61	4.88	267.8

Table B.4: Model result for verification waves

Figure B.7 shows a plot of the model data compared to the measured data. The model results for wave 2, 3, 4 and 7 are quite similar to the wave gauge data. The wave height for verification wave 1, 5 and 6 are not similar to the model result. Nevertheless, the wave period for this wave is similar. In the $T_{m02} - T_{m02}$ plot can be seen that the wave period is quit well approximated by the model.

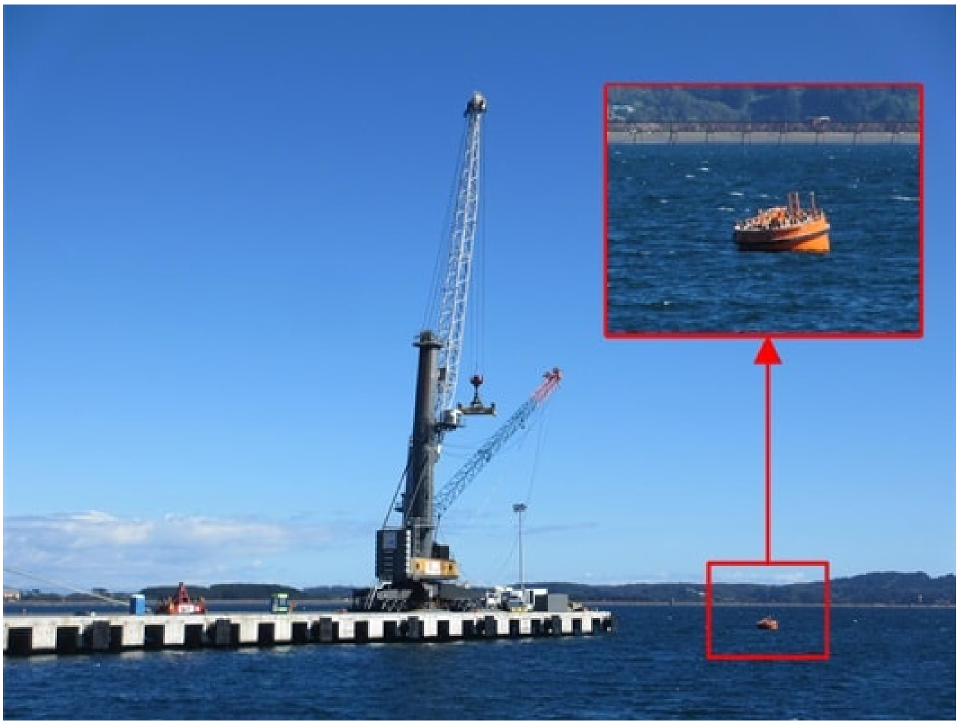

Figure B.6: Wave gauge in the San Vicente Bay. The measuring buoy is located near the berths.

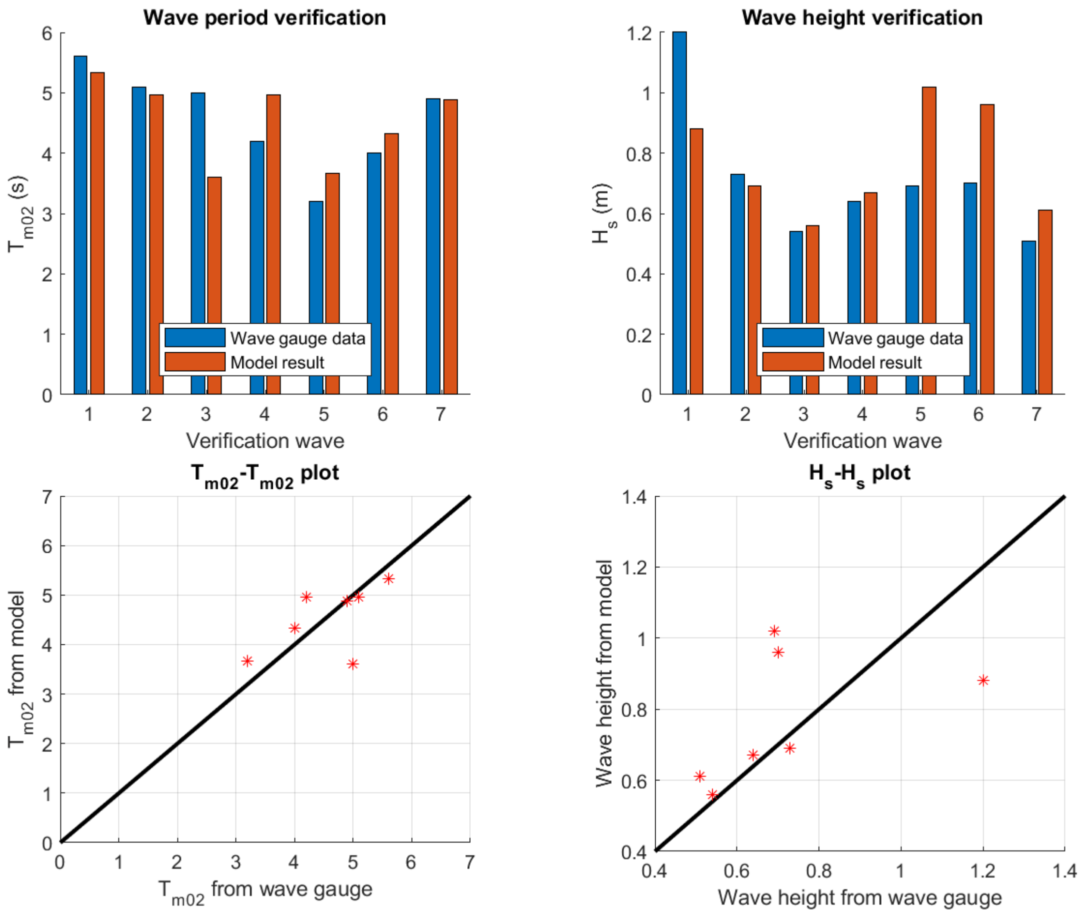

Figure B.7: Comparing the model results with the wave gauge data for the verification waves

B.3. Wind input effect

In a later stage the offshore wave data will be transformed to nearshore wave conditions. Only offshore wave data is available. Wind data is lacking and cannot be used for the transformation. An analysis is done to study the effect of wind on the wave conditions in the simulations. Two simulations are run (with and without wind) using the wave and wind conditions on 10/10/2018 09:00. The following two conditions are used as model input:

	$\mathbf{H_s}$ [m]	$\mathbf{T_p}$ [s]	**Wavedirection** [°]	$\mathbf{v_{wind}}$ [m/s]	**Winddirection** [°]
Wind	2.7	15	229	5.0	168
No Wind	2.7	15	229	0	0

The wave properties along the line indicated in figure B.8 will be analysed. The variation of H_s and T_p along this line is shown in figure B.9. Please note that the right in the figure is the most offshore location. The figure shows that wind does not effect the offshore significant wave height.

This is because there is limited fetch in the model, thus no extra wind growth is possible. Nearshore, a small difference can be observed in the wave height, this can be explained by the fact that in the simulation with wind, wind waves are generated inside the bay. These wind waves give an increase in wave height.

For the T_{m02} a larger difference can be seen. An explanation for this is that for the simulation without wind the energy input in the wave-energy spectrum is stopped. The wind adds energy at the high frequency part of the energy-frequency spectrum. Wind input gives more waves with a shorter period. The lack of these energy input gives thus longer periods, which can be observed in figure B.9.

Instead of the T_{m02} the peak period will be used for post-processing. The peak period is affected by the quadrupled wind-wave interactions, which transfers energy from high frequencies to lower frequencies. This energy transfer is not present without wind. However, the peak period of a JONSWAP spectrum with a low γ-value is not much affected by the quadrupled wind-wave interaction. This can also be concluded from the model simulations: in both cases, with and without wind the peak periods along the line are almost the same, namely between 15.0 and 15.5 s.

So, the conclusion is that there is only little difference between the models with and without wind input. The relevant output parameters for post processing (H_s and T_p) are only little effected by the wind input. Therefore, it is justified to run the model without wind input.

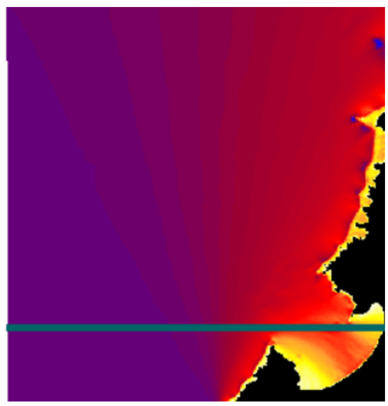

Figure B.8: Line used for wind input analysis

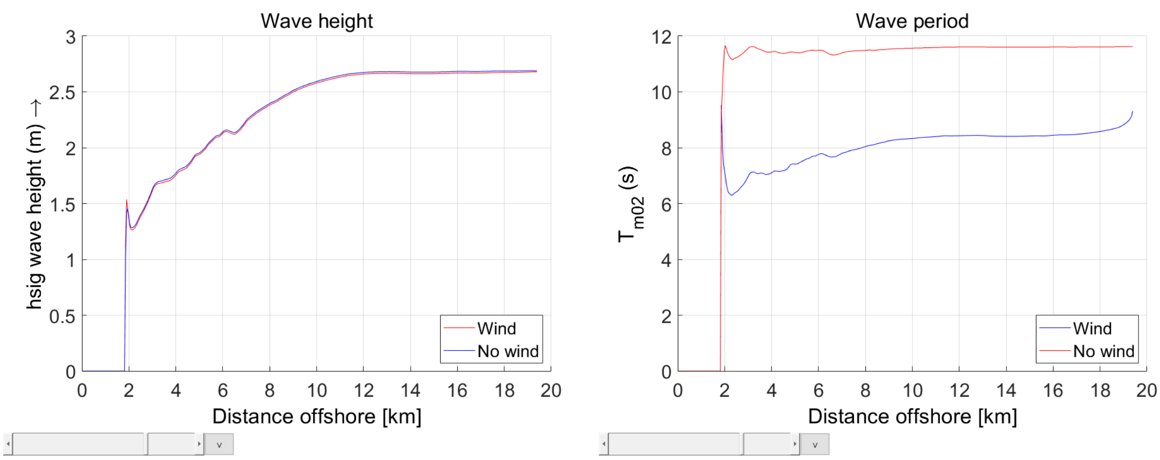

Figure B.9: Comparing the model results for simulation with wind input (blue) and without wind input (red). a) Significant wave height and b) Peak period

B.4. Offshore to nearshore transformation

Now that the model has been set up and verified, it is used to calculate the wave properties in the San Vicente Bay. The model is used to transform the entire offshore wave dataset to a nearshore dataset. In a later stage, the transformation is used to analyse the effect of different breakwater interventions.

B.4.1. Transformation input

The input for the offshore to nearshore transformation, is a wave dataset from the period 30/01/1997-20/02/2018. This dataset gives the significant wave height, peak period and wave direction every 3 hours. The dataset is hindcasted using the WaveWatch III (NOAA) model, based on wind data. The location is (500000.00 m E; 5905127.63 m S) which is offshore from Talcahuano and can be applied for simulations at the San Vicente port. The dataset is provided by UCSC.

B.4.2. Observation points

Six observation points are placed in the port. The offshore dataset is transformed to these locations. The six observation points in figure B.10 are are given the following names:

- Dry bulk quay side (Qback)
- Small vessel manoeuvring area (SM)
- Container quay side front (Qfront)
- Area between breakwater and container quay (Bay)
- Large vessel manoeuvring area north (LM1)
- Large vessel manoeuvring area south (LM2)

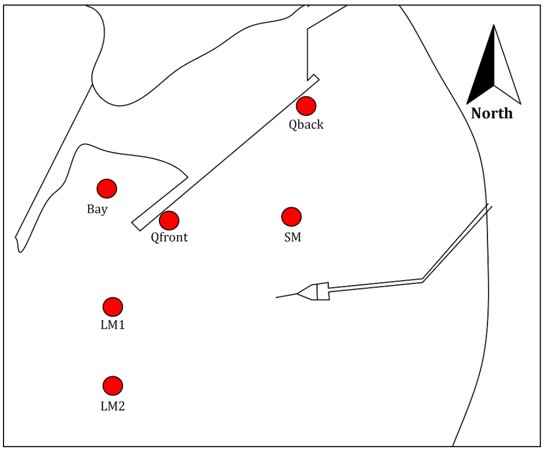

Figure B.10: Observation points in the port. The offshore wave information is transferred to these nearshore locations using the Delft3D model.

B.4.3. Latin Hypercube Sampling method

To transform the entire offshore dataset to a nearshore dataset the Latin Hypercube Sampling (LHS) method is used. LHS is used to reduce the number of Delft3D simulations that are required to achieve a reasonable accuracy. In this way, the entire offshore wave climate can be converted to a nearshore wave climate with a small number of Delft3D simulations.

Selecting wave directions

For better accuracy, LHS is applied to smaller sets of the offshore dataset. The dataset is divided into sets with a 5° range of the wave direction. Each wave direction has its own propagation pattern in combination with different wave heights and periods. Because of this, it is necessary to separate all directions and preform the LHS separately. A visual example is shown in figure B.11.

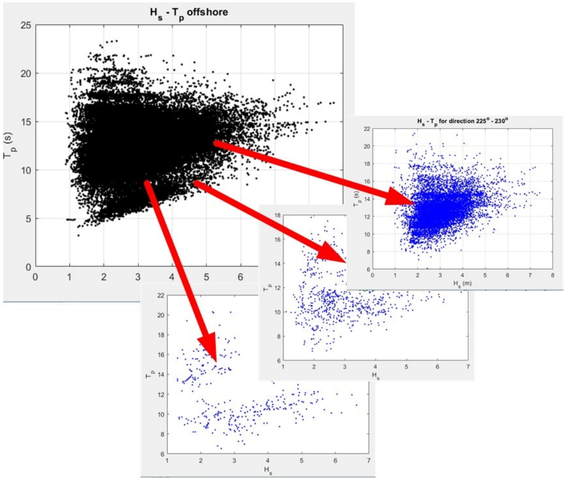

Figure B.11: The offshore dataset (black) containing all directions is divided into sets with a 5° range. Note that only 3 of the 20 wave directions are shown for this example.

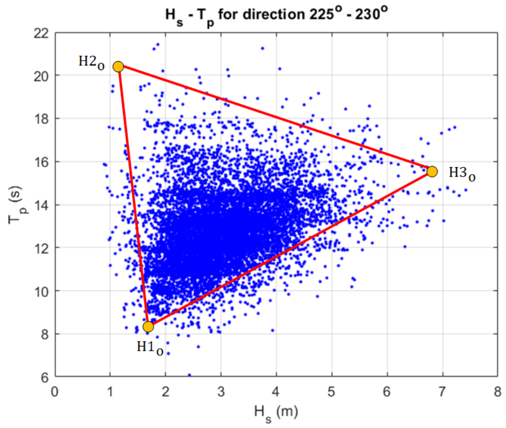

Figure B.12: Interpolation method for 225° – 230° range

Because of its location in San Vicente Bay, the port is sheltered from waves outside the 250° – 315° range. This sheltered range of the shadow zone of the bay does not include refracting waves. Therefore, a transitional area of 35° in the southwest direction is added to include these refracting waves. The breakwater protects the port against refracting waves from the northwest. Thus, the following 20 wave directions are used in the LHS method: (215° – 220°), (220° – 225°)....(310° – 315°).

Wave sampling

A $H_s - T_p$ plot is created for all wave directions, and a triangle is fitted around the data points. The $H_s - T_p$ plot for direction 225° – 230° is shown in figure B.12 as an example. The figure shows the offshore dataset which is the starting point for the transformation. The corners of the triangle are defined by the following offshore waves: $H1_o$, $H2_o$ and $H3_o$, where o is indicating an offshore condition. The waves $H1_o$, $H2_o$ and $H3_o$ do not necessarily need to be in the offshore wave climate.

Delft3D simulations

An offshore-to-nearshore transformation is preformed in Delft3D for all selected waves $H1_o$, $H2_o$ and $H3_o$. The waves are grouped in 20 directions, which means that a total number of 60 Delft3D simulations are required. The waves $H1_o$, $H2_o$ and $H3_o$ are used as model boundary conditions. They are then converted by the numerical model to $H1_n$, $H2_n$ and $H3_n$, where n is indicating an nearshore condition, for each observation point.

The wave spectrum

The offshore waves $H1_o$, $H2_o$ and $H3_o$ are used as boundary conditions in the Delft3D model. They are implemented in the model as a JONSWAP spectrum, see section B.1.2. Although the overall methodology is correct, the fact that a JONSWAP spectrum is used here is incorrect. Waves at the Chilean coast can best be described by a two-peaked spectrum. The transformation of such a spectrum towards the coast is different than that of a JONSWAP spectrum. Thus, the offshore-to-nearshore transformation using the numerical model is not representative for the linear transformation of the offshore dataset using the LHS method. For the purpose of this report, this approximation is considered sufficiently good.

Interpolation

For each location, a transformation function $f(H_s, T_p)$ can be found. This transformation function is unique for each nearshore location and wave direction and can be used to transform the entire offshore dataset. The transformation function can be obtained with linear interpolation in two directions (H_s and T_p) between the offshore to nearshore ratio of H1, H2 and H3. The transformation function is than applied to all offshore data.

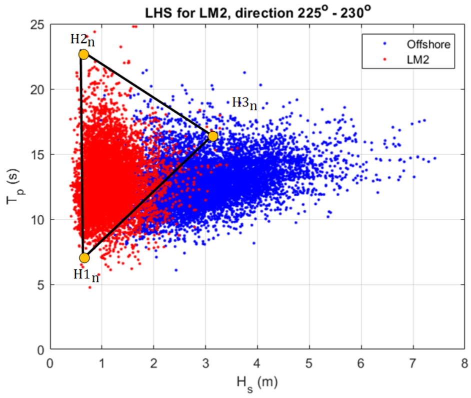

Figure B.13: Interpolation method for 225° − 230° range. In blue the offshore wave climate, in red the nearshore wave climate for location LM2.

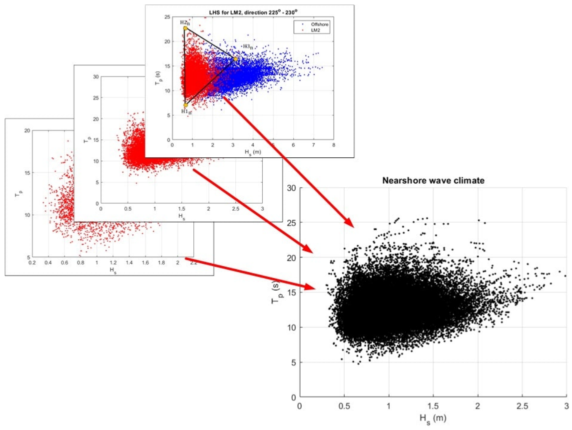

Figure B.14: All different nearshore directions are merged together to form a complete nearshore dataset (black) for a specified nearshore location. Note that only 3 of the 20 wave directions are shown for this example.

Figure B.13 shows an example transformation for waves from the 225° − 230° directional range at location LM2. The neashore waves $H1_n$, $H2_n$ and $H3_n$ are indicated. The linear transformation is applied to the offshore dataset (blue) to obtain the nearshore dataset (red). It can be observed that the wave field for the offshore dataset is shifted towards the left, thus the wave heights become smaller. This change in wave properties is specific for each wave direction and location.

After completing all transformations for the wave direction, the different directions are merged together to form a complete nearshore dataset at a specified nearshore location. A visual example of the merging of wave directions is presented in figure B.14.

The wave information in the port can be used for vessel stability during manoeuvring and mooring operations.

C

Manoeuvring and mooring analysis

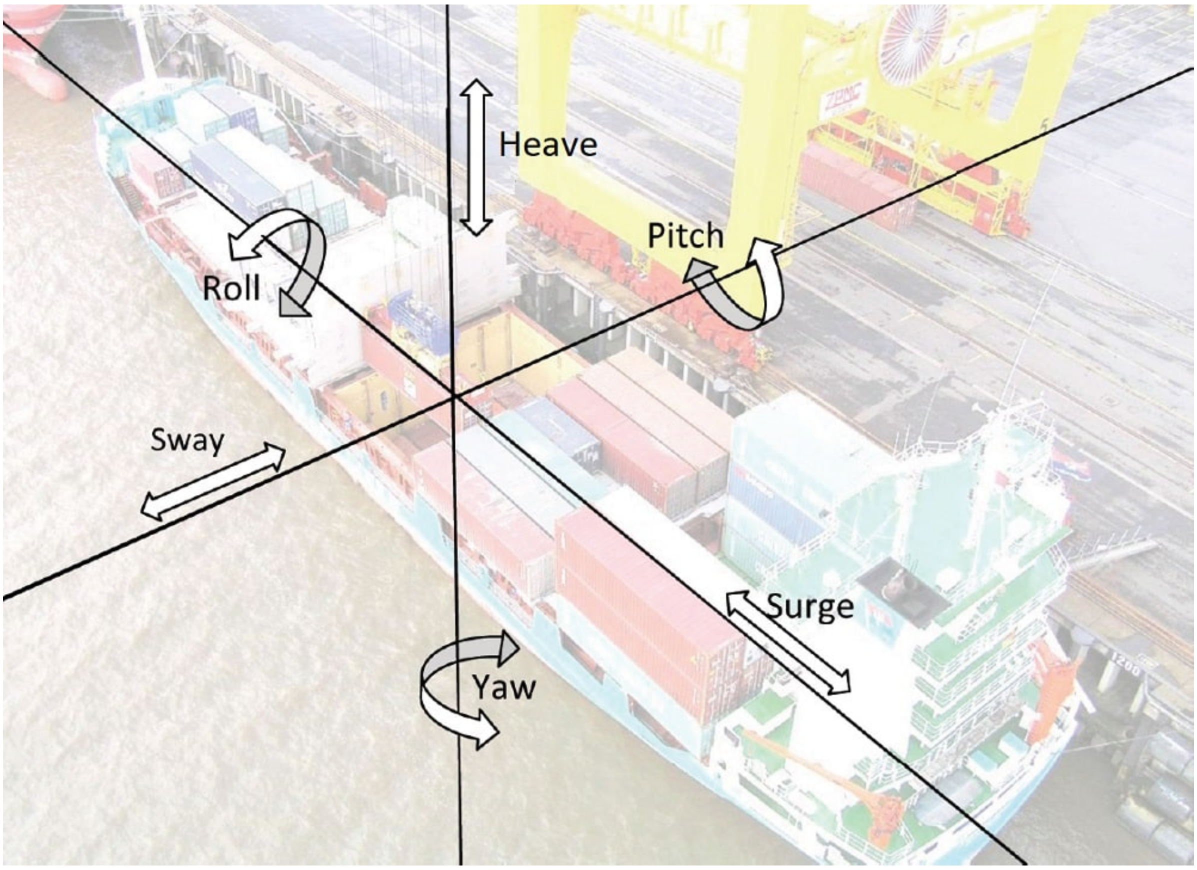

Figure C.1: Principle vessel motions. Three translational motions (heave, surge and sway) and three rotational motions (pitch, roll and yaw) are identified. Vessel motions have a large influence on the (un)loading efficiency.

Source: PIANC (2012)

Vessels exposed to wave forcing start to move. These motions have a negative impact on manoeuvring and mooring. In this appendix, these processes are observed in detail to assess the possibility of the manoeuvring operation and the efficiency of the (un)loading operation. To improve manoeuvring and mooring conditions, a breakwater extension is investigated. First the current situation is studied; thereafter the influence of a breakwater extension on manoeuvring and mooring is investigated.

C.1. Manoeuvring analysis

Vessel manoeuvring in ports is complicated due to the limited navigability of sea-going vessels at low forward speeds. Therefore, vessels are assisted by tugs for the manoeuvring operation. Waves, wind and currents hinder the tug operation and are limiting the possibility to manoeuvre.

C.1.1. Operational limits

PIANC (2014a) recommends the following operational limits for manoeuvring with tug assistance:

$$
\begin{aligned}
V_w &\leq 10 m/s && \text{(wind velocity at 10 } m \text{ height)} \\
V_f &\leq 0.10 m/s && \text{(flow velocity at half the draught)} \\
H_s &\leq 1.5/2.0 m && \text{(significant wave height)}
\end{aligned}
$$

The limit for **wind** means that manoeuvring is not possible at 6 Beaufort and above. At San Vicente Port this occurs approximately 2.5% of the time, see section C.1.2.

The **currents** at San Vicente Port are small. San Vicente Bay does not have a river discharge, so flows are only induced by the tides. Since San Vicente Bay has a relatively wide entrance and a small length, flow velocities are assumed negligible.

Waves hinder the tug operations. The wave maximum operational significant wave height depends on the type of tug that is used. Since the exact limits of the tugs used at San Vicente Port are not known by the project group, a limit of $1.50 m$ is assumed. Tugs will not operate when there are waves larger than $1.50 m$. In the end, the pilots are responsible for making the decision to continue the manoeuvre.

C.1.2. Downtime due to wind

Figure C.2 shows the distribution of wind velocities per month. 6 Beaufort is exceeded approximately 2.5% of the time. Consequently, nautical operations are stopped and the manoeuvring downtime due to wind is 2.5% of the time.

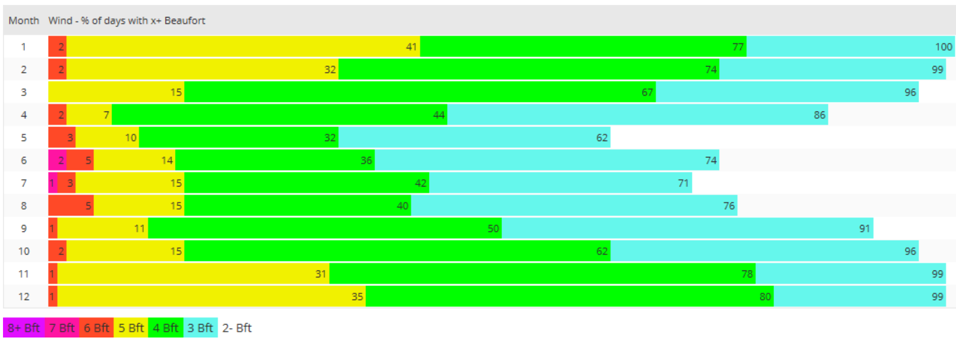

Figure C.2: Distribution of wind velocities per month. The wave climate at San Vicente Bay is mostly moderate, with strong winds in winter. Retrieved from www.windguru.com.

C.1.3. Downtime due to waves

An offshore-to-nearshore transformation is performed on 20 years of hindcast data to obtain a good representation of the nearshore wave climate, see appendix B. The previously mentioned limits are applied to the waves at two locations: (1) the manoeuvring area for large vessels and (2) the manoeuvring area for small vessels. The results are presented in table C.1, showing that manoeuvring is possible 87% of the time. The manoeuvring downtime due to waves is thus 13% of the time. A visual example for the large manoeuvring area is presented in figure C.3.

Basin SM [%]	**Basin LM1** [%]	**Weighted average** [%]
100	83.50	87.43

Table C.1: Time that manoeuvring is possible at the manoeuvring area for large vessels (LM1) and the manoeuvring area for small vessels (SM). Also, the weighted average is presented based on the distribution of vessels. Hereby, the assumption is made that manoeuvring of small vessels is possible when the waves in front of the quay are sufficiently small, also when the waves further offshore are larger then the operational limit.

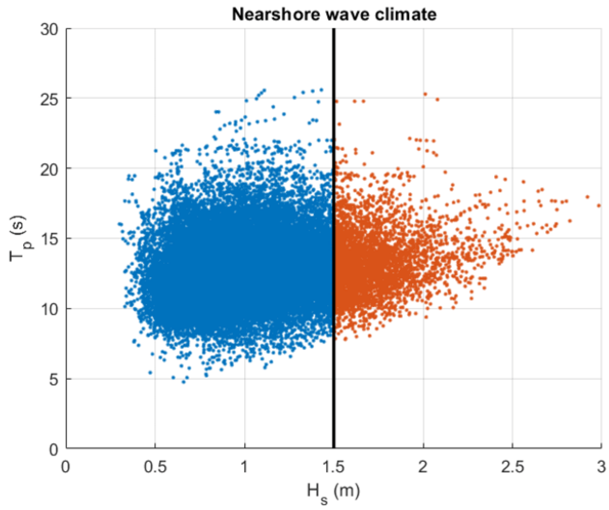

Figure C.3: Example of the nearshore wave dataset for the manoeuvring area for large vessels. In blue, significant wave height smaller than 1.5 m. In red, significant wave height larger than 1.5 m. 83.50% of the significant wave heights in the dataset is smaller than 1.5 m, in these conditions manoeuvring operations are possible.

C.2. Mooring analysis

Although vessels moored along the quay are restricted in their motions, motions are still possible. There are two main reasons to perform a calculation of these motions: (1) to calculate the efficiency of the (un)loading operation, and (2) to calculate the line forces. In San Vicente Port, one occasion is known where the forces were so large that the lines snapped. This analysis will focus on the efficiency of the (un)loading operation. To be able to understand the efficiency of this operation, section C.2.1 will give an introduction to the behaviour of vessels in waves.

C.2.1. Behaviour of vessels in waves

The motion of a vessel can be split into three mutually perpendicular translations of the centre of gravity and three rotations around the centre of gravity. These motions are illustrated in figure C.1 on the cover of this appendix. The behaviour of a vessel in waves is thus a six-degree-of-freedom system that can be described by equations of motion (Journée & Pinkster, 2002). The physics involved with vessel motions in waves in shallow water are complex in character. That make them difficult to predict accurately, especially for moored vessels.

The response of a vessel to wave forcing can be assumed linear (Journée & Pinkster, 2002): the ratio between response amplitude and wave amplitude is constant. This ratio is referred to as Response Amplitude Operator (RAO). Each degree of freedom has its own RAO. Figure C.4 shows that with respect to the motional behaviour three frequency areas can be distinguished (Onrust, 2018):

- The low frequency area where the ship follows the wave motions. These waves generally have a wavelength that is much larger than the length of the ship. The RAOs have a value of 1: the amplitude of ship motions is equal to the wave amplitude.
- The natural frequency area with motions in resonance: ship motion amplitudes in this frequency range are larger than the corresponding wave amplitude. The RAOs have a value larger than 1.
- The high frequency area with very small vessel motions. The high frequency waves generally have a wavelength that is smaller than the length of the vessel, so wave forces are averaged out. The RAOs have a value of 0.

RAOs can be obtained using model tests or by numerical simulation. When a RAO has been obtained, the motions of the vessel can be calculated using the following equation:

$$S_z(\omega) = \left|\frac{Z_a}{\zeta_a}(\omega)\right|^2 \cdot S_\zeta(\omega) \tag{C.1}$$

In which:

$S_z(\omega)$	=	the motion spectrum of the vessel	$[\mathrm{m^2/Hz}]$
Z_a/ζ_a	=	the RAO	$[\mathrm{m/m}]$
$S_\zeta(\omega)$	=	the wave spectrum	$[\mathrm{m^2/Hz}]$

The significant motion is then: $Z_s = 4\sqrt{m_0}$, where m_0 is the spectral moment of the vessel motion spectrum. This calculation can be done for all ship motions.

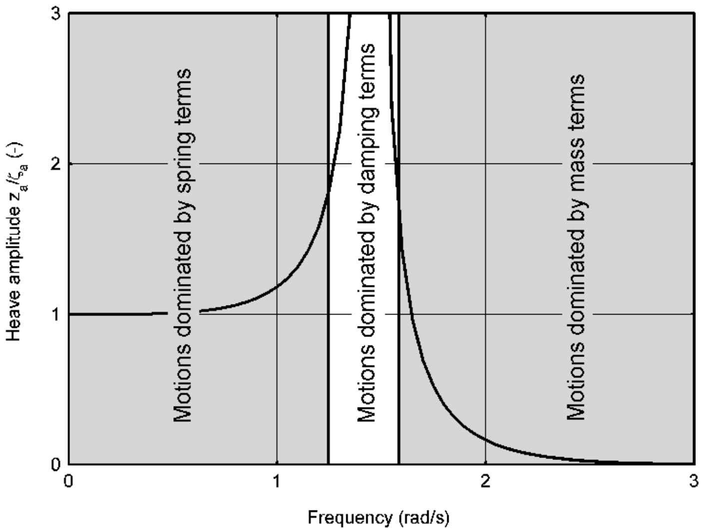

Figure C.4: Example of the influence of frequency on the RAO for heave. There are three frequency areas with a different terms dominating the equations of motion. Please note that the vertical axis shows the heave RAO (Z_C/ζ_C), not the heave amplitude (Z_C) (Journée & Pinkster, 2002).

C.2.2. Operational limits

Container (un)loading is sensitive to waves: the spreader of a crane needs to be positioned right above the containers to be able to lift them. This is a precise task; ship movements should be limited in order to (un)load effectively.

Efficient loading and unloading of other cargo types is also limited by waves, but these limits are less strict. Because these (un)loading processes are less precise. Table C.2 shows the limitations for container-, bulk, general cargo and fishery (un)loading to realise a 100% efficiency. Bulk has two different limitation criteria, one for loading and one one for unloading. Loading is done with conveyor belts while unloading is done by a grab crane. The last one needs more precision and therefore the criteria is more strict. In addition, there is also a limit for the wind velocity, but this is mainly determined by the type of equipment used.

Principal motion		**Container**	**Bulk**	**General cargo**	**Fishery**
Surge	[m]	0.5	2.0-5.0	2.0	1.0
Sway	[m]	0.6	1.0-2.5	1.5	1.0
Heave	[m]	0.4	1.0	1.0	0.4
Roll	[°]	1.5	6.0	5.0	3.0
Pitch	[°]	0.5	2.0	2.0	3.0
Yaw	[°]	0.5	2.0-3.0	3.0	3.0

Table C.2: Maximum motion amplitudes for container vessels, bulk vessels, general cargo vessels and fishery vessels in order to achieve 100% (un)loading efficiency. Note that bulk has two efficiency requirements for surge, sway and yaw [unloading - loading]. These depend on the type of loading; loading is with conveyor belt and unloading with cranes (PIANC, 2012) (PIANC, 1995).

C.2.3. Wind at the quay

The SVTI terminal uses conveyor belts for the loading of bulk vessels and mobile harbour cranes for the other loading and unloading operations. The wind limit is assumed to be 10 m/s, which corresponds to 6 on the Beaufort scale. Similar to the nautical operations, see section C.1.2, this means that the loading and unloading operations are stopped 2.5% of the time.

C.2.4. Vessel movements at the quay

Figure C.5 shows a typical mooring configuration for a container vessel. There are four breast lines at the bow, four at the stern, and two spring lines at the two ends of the ship. The lines restrict the motions of the vessel. Since the focus of this research is on quay efficiency and not line forces, this means that some motions can be neglected in the study.

Figure C.5: Mooring configuration of the Caroline Maersk. The photo shows the stern of the vessel, where 4 breast lines and 2 spring lines are visible. (Own photo, 29 Sept. 2018)

Sway and yaw are assumed to be restricted by the breast lines at the bow and stern. Surge is limited by the spring lines and according to Thoresen (2010) pitching is small and insensitive to wave period. This means that the roll and heave are the governing motions for efficiency.

Roll motion

Rolling is the rotational motion along the longitudinal axis of the vessel. Rolling is most sensitive to beam waves with a period close to the natural rolling period. These are primarily swell waves in the 13 – 19 seconds range. However, figure C.6a shows the waves at the quay are very unidirectional, whereas offshore they had a larger directional spreading. Diffraction and refraction around the tip of the breakwater (indicated by the pink line in figure C.6b) change the direction of the waves in San Vicente Bay, in such a way that the waves propagate almost parallel to the quay. The figure illustrates that the quay is transmitting waves: the reason for this is that it is a wharf structure.

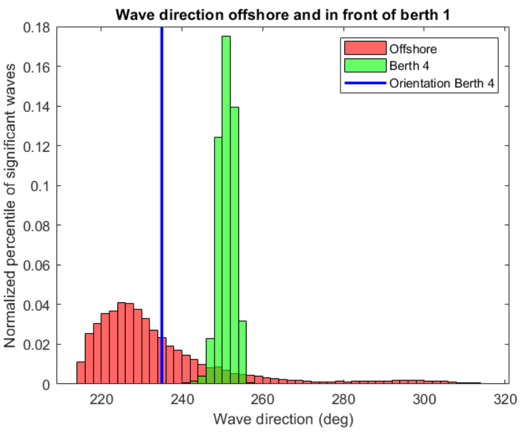

(a) Wave directions offshore and at berth 4. The orientation of the quay is indicated by the blue line.

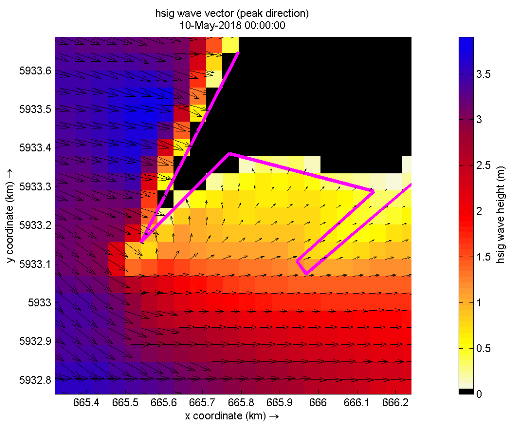

(b) Wave deflection at breakwater tip

Figure C.6: Deflection of the waves in San Vicente Port. In the offshore to nearshore transformation, the directional spreading of the waves decreases. There is a lot of wave deflection around the tip of the breakwater.

The quay at San Vicente Port has an orientation of 235° N, and the mean wave direction is 255° N. This means that the angle of the waves relative to the moored vessels is only 20°. Although roll motions will still occur, it is assumed that the motions will not be governing the efficiency of loading and unloading.

Heave motion

Heave is the vertical translational motion of the vessel. Heave is most sensitive to long-period waves with a wavelength equal to the vessel length. Resonance will lead to amplification of the vessel motion, so the vessel motion can be large than the forcing wave height. For long period waves, the heave motion tends to be equal to the wave height and for short period waves the heave motions will be small (Thoresen, 2010), (Journée & Pinkster, 2002). The wave climate at San Vicente Port consists of swell waves that have a large influence on the heave motions. Thus, heave is expected to be governing for (un)loading efficiency.

Response Amplitude Operator

To analyse the heave motion, the influence of the waves on the vessel needs to be quantified. The RAO strongly depends on the type of vessel (length, breadth, metacentric height), draught, mass, forward speed, wave properties (frequency, incoming wave direction), water depth, mooring conditions, etc (Ghassemi et al., 2015). The RAO should be determined using model test or a numerical model, but this is too elaborate for the purpose of this report. The RAO is given in figure C.7 is adopted taking the following into account:

- The goal of this research is to get an idea of the vessel motions at the quay, not to calculate the real motions of the vessel. Therefore, it is justified that roll is neglected and that the RAO is overly simplified.
- The motions of a free floating vessel are studied, so it is assumed that the mooring does not have an effect on the heave motion.
- The only parameter in the RAO is the length of the vessel.
- For waves longer than the vessel length ($1.5 \cdot L_{bp}$) a value of 1 is used.
- For waves shorter than the vessel length ($0.5 \cdot L_{bp}$) a value of 0 is used.
- For waves with a length equal to the vessel length, a value of 2 is used. A linear gradient around the peak is used.

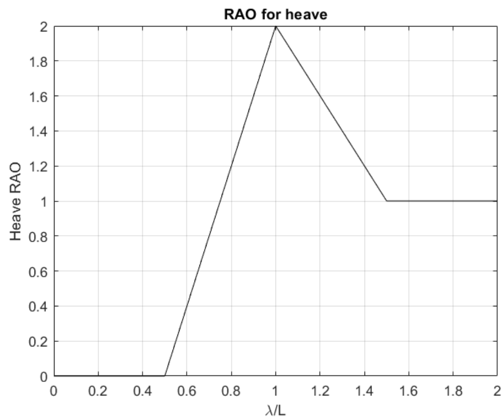

Figure C.7: Assumed Response Amplitude Operator for heave motion.

Vessel motion model

The vessel motions are calculated with the vessel motion model. In which the method described above is processed. For clarification an example of a calculation with this model is performed.

20 years of historical data is used to get an overall idea on the motions of vessels in the port and the frequency of large motions that cause inefficient loading. Appendix B describes how the waves in the port are found.

Vessels respond differently to waves with different frequencies. This behaviour is described by the RAOs. A JONSWAP wave spectrum is created from the nearshore wave data. Subsequently, equation (C.1) is used to find the vessel motion spectrum for each vessel group. Figure C.8 shows an example of such a calculation. A wave spectrum with a wave height of 1.1 m and a peak period of 17 s is displayed in figure C.8a. The corresponding motion spectra for the different vessel groups, and their corresponding significant heave, are shown in figure C.8b. The oscillation of a vessel of group I due to the heave motion is 0.32 m. This means that the heave motion is below the 0.40 m limit and that 100% efficient (un)loading is possible. The oscillation of a vessel of group II due to the heave motion is 0.59 m. In this case, 100% efficient (un)loading is not possible.

This calculation is executed for all 61,630 wave conditions in the entire nearshore wave climate, for all the 7 vessel groups for the locations Q_{front} and Q_{back}, to determine the (un)loading efficiency per vessel group.

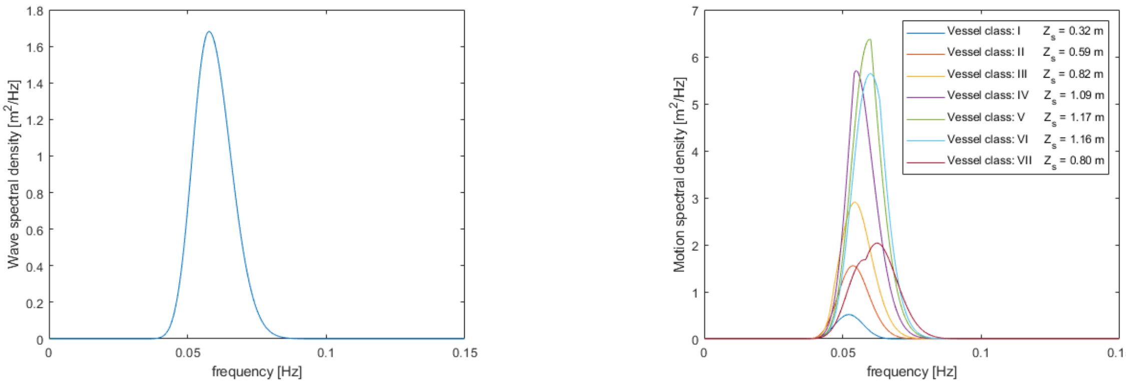

(a) Wave spectrum

(b) Motion spectra for different vessels

Figure C.8: Example calculation for vessel motions. A JONSWAP wave spectrum is created with $H_s = 1.1m$ and $T_p = 17s$. The motion spectra for the different vessel groups are calculated. Due to the different lengths of the vessels, their motion spectra are very different. The significant heave per vessel group is given.

C.2.5. Conclusions on heave motions

The heave motions is calculated for the different vessel groups that have been described in appendix A. The motions from the vessels are computed at two locations and afterwards averaged using their berth allocations from Q1-Q3 2018.

A visual example of the averaged heave motions for a group IV type of vessel is shown in figure C.9. The heave motion of the vessel is calculated for all significant waves in the 20 year data set. Please note that vessel group VII is divided into bulk, general cargo and fishery because they have different (un)loading criteria.

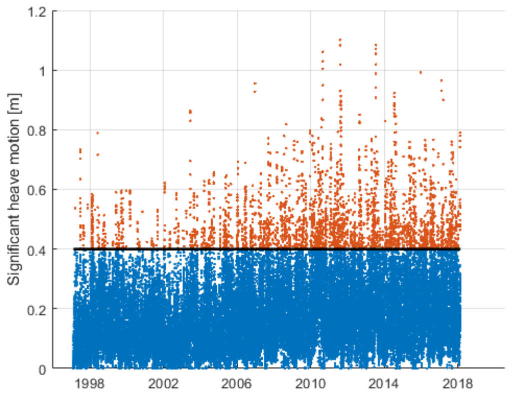

Figure C.9: Heave motions for vessel group IV for a period of 20 years. Heave motions that are larger than 0.4 m are plotted in red.

Vessel type	**Heave criterion** [m]	**Berth 1-2** [%]	**Berth 3-4** [%]	**Weighted average** [%]
I	0.4	100.00	99.97	99.97
II	0.4	100.00	99.68	99.68
III	0.4	100.00	98.78	98.80
IV	0.4	100.00	94.82	94.82
V	1.0	100.00	99.96	99.98
VI	0.4	99.99	83.37	84.04
VII_B	1.0	100.00	100.00	100.00
VII_G	1.0	100.00	100.00	100.00
VII_F	0.4	100.00	61.65	80.83

Table C.3: Percentage of time that optimal loading efficiency based on heave can be achieved. This calculation is done for two locations: berths 1-2 and berths 3-4. These are then averaged using the berth usage by these vessels in the past year, see appendix A. Note: B = bulk, G = general cargo, F = fishery

Table C.3 shows that a high loading efficiency can be achieved at berths 1 and 2. The reason for this is that it is relatively sheltered from waves, so the wave heights here are small. At berths 3 and 4 the waves are larger, so optimal loading efficiency cannot be achieved all the time. Small vessels are most sensitive to the swell waves so show the largest movements.

On average, the conditions in the port are good for efficient (un)loading in 95% of the time. PIANC (2012) indicates that on average other ports have optimal (un)loading conditions approximately 98% of the time. So, San Vicente Port has lower optimal (un)loading conditions than average. As a measure to improve the (un)loading efficiency at the berths, the extension of the current breakwater is studied.

C.3. Breakwater extension

In this section, the influence of a breakwater extension on manoeuvring and mooring is investigated based on the current situation. An extension of the breakwater will change the wave properties at the manoeuvring basins and berths of San Vicente Port. The manoeuvring and mooring efficiency will change which is attractive for the port. First, the manoeuvring is elaborated followed by mooring. Please not, the downtime due to wind cannot be affected by breakwater extension. Therefore the downtime due to wind will not be taken into account for the breakwater extension analysis.

C.3.1. Breakwater configuration

As mentioned earlier, the orientation of the original breakwater is 235°. The extension of the breakwater will have the same orientation as the original breakwater. In total five different extensions are investigated. These are extensions of 150m, 300 m, 450 m, 600 m and 750 m. The configuration of these extensions are shown in figure C.10. In this figure, the shape of the port is shown as well. The extended breakwater has the same properties as the original one, described in B.1.3. Moreover, the properties of the quay are not changed.

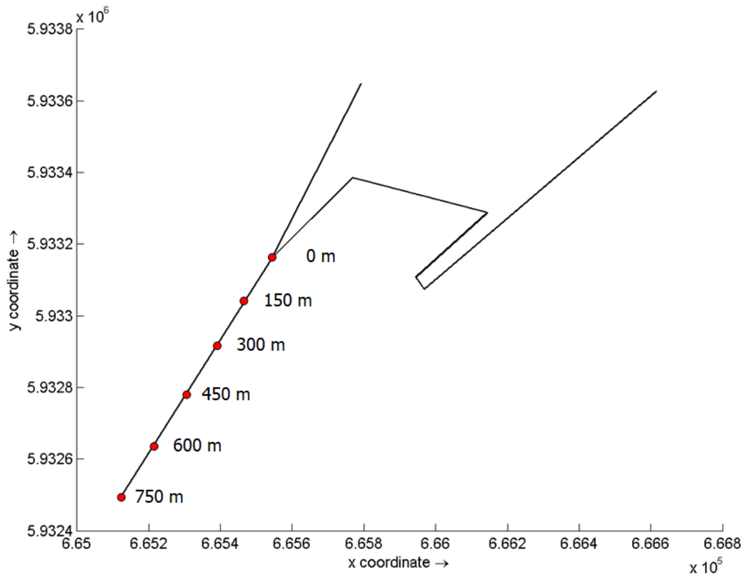

Figure C.10: Location of breakwater extension

C.3.2. Manoeuvring

To analyse the effect of a breakwater extension on the manoeuvring, several model simulations need to be preformed. For each breakwater extension, an offshore-to-nearshore transformation is done based on the 20 years hindcast data. The methodology is explained in appendix B.4. The nearshore wave climate is known for the locations shown in figure C.11.

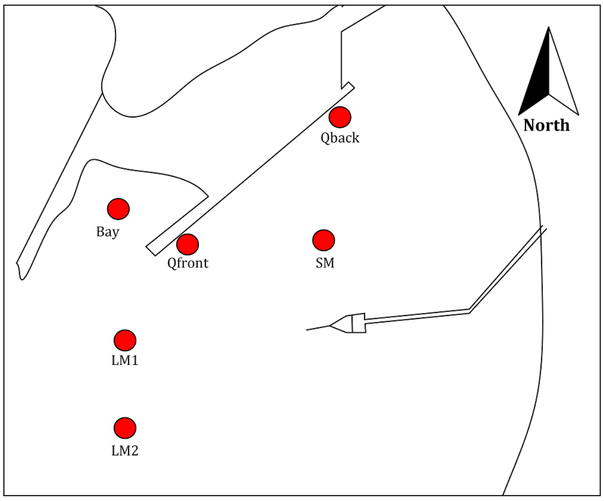

Figure C.11: Nearshore measurement locations in the port

By elongating the breakwater, the manoeuvring basins become more sheltered which will improve the manoeuvring conditions. The time that manoeuvring is possible will increase with breakwater length. This can be seen in figure C.12 which gives the weighted average of possible manoeuvring time for location SM and location LM1. For a breakwater extension of 600 m or longer, no further improvement in manoeuvring conditions can be expected.

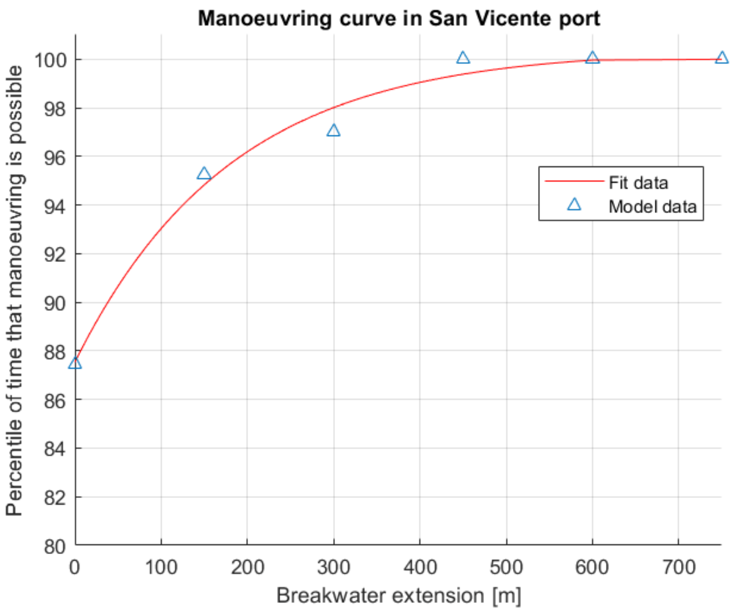

Figure C.12: The time that vessels are able to manoeuvre $H_s < 1.5m$. This includes the small and large manoeuvring basin.

C.3.3. Mooring

To analyse the influence of a breakwater extension on the (un)loading efficiency, the same data is used as in section C.3.2. The influence of the breakwater extension on the (un)loading efficiency is shown in figure C.13. In here the (un)loading efficiency is plotted for each vessel group. It can be observed that a longer breakwater gives a larger (un)loading efficiency for all vessel groups. However, small vessels benefit more from a breakwater extension than larger vessels. In the figure, the weighted average efficiency is plotted based on the percentage of vessels in San Vicente Port. The largest gradient in efficiency increase can be found in the range of a 300 m - 450 m breakwater.

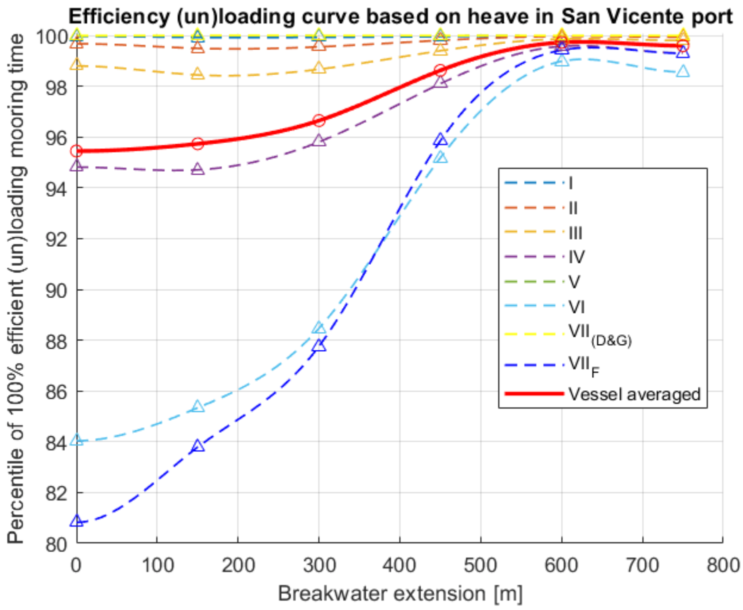

Figure C.13: Efficiency (un)loading curve based on heave in San Vicente port. This includes berth 1-4, berth 5 is neglected.

C.4. Breakwater extension costs

To investigate the feasibility of a breakwater extension, an estimate of the costs needs to be done.

C.4.1. Layout

The original breakwater has a tetrapod armour layer; for simplicity it is assumed that the extended breakwater will also have a tetrapod armour. For the determination of the costs, a typical tetrapod armoured breakwater cross-section is used presented in figure C.14 Tutuarima & Angremond (1998). The breakwater has a berm width of 25 m with a crest height 5 m above Mean Sea Level (MSL). As a simplification, the tetrapods are placed double layered on both sides of the crest. The outer slope has a steepness of 1:1.33 and the inner slope has a steepness of 1:1.5. For simplification, the filter layers and core are build out of quarry run. The height of the tetrapod is measured during site visit. The height is approximately 2.1 m.

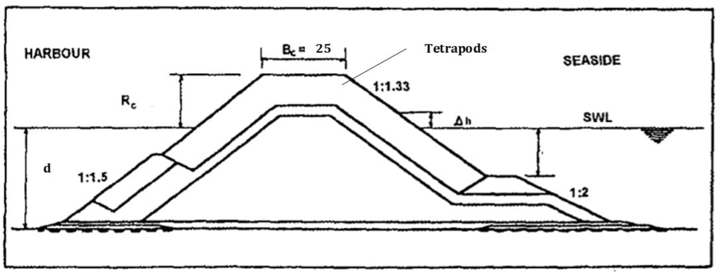

Figure C.14: Typical tetrapod armoured breakwater cross section

C.4.2. Costs

A list of basic costs for breakwater materials can be found in table C.4. The costs are subdivided in four activities. For each activity, the quantity needs to be determined to obtain the total cost of all different breakwater extensions.

Activities	Unit costs [€]
Quarry production (all gradings)	$7.00/ton$
Transport of rock (over land)	$0.20/tonkm$
Tetrapods	$150.00/m^3$
Mobilisation demobilisation	$2.0M$

Table C.4: List of basic costs according to Tutuarima & Angremond (1998)

C.4.3. Quantities

The size of the breakwater cross section is depending on the depth profile. A larger depth will give a larger total height and a wider base which means more materials are needed in larger depths. The water depth is plotted in figure C.15, it clearly shows that the breakwater cross-section will be larger when it is located further away from the original breakwater.

For each section of 150 m, the average height (distance above water + below water) of the breakwater is determined. The sections are named after the distance between the extension and the original breakwater. The sections are shown in figure C.16.

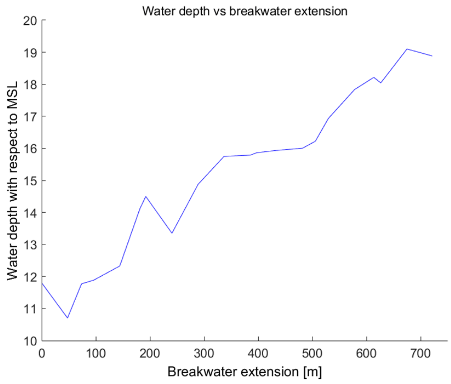

Figure C.15: Depth depending on breakwater extension

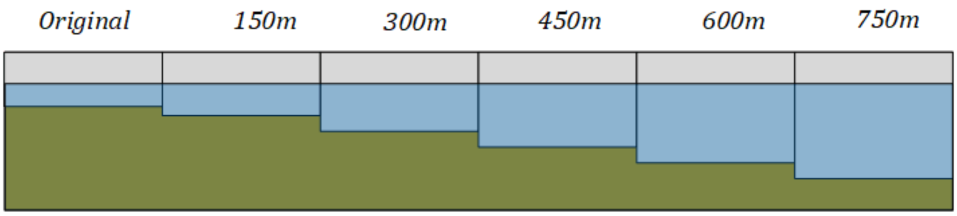

Figure C.16: Breakwater sections, longitudinal view

For all sections the cross sectional properties, quantities and costs per 150 m placement are calculated. These can be found in C.5. The volume of a tetrapod is determined by the following formula: $V = 0.280H^3$. Because, the tetrapods are double layered, in total $2 \times 0.588m^3$ tetrapod is present on each square meter of slope. Because the breakwater expansion is in steps of 150 m, the cost per cross-section is determined for 150 m. The grading that are needed for the breakwater construction come from a quarry nearby. This is the Canteras Lonco quarry, located 23.1 km from the San Vicente Port.

Cross sectional properties	**150 m**	**300 m**	**450 m**	**600 m**	**750 m**
Properties					
Depth [m]	12.0	15.0	16.0	16.5	19.0
Total height [m]	17.0	20.0	21.0	21.5	24
Volume core [m^3]	833.9	1066.0	1149.0	1191.6	1415.0
Outline for armour [m^2]	61.3	72.1	75.7	77.5	86.5
Quantities					
Tetrapods (2x layer) [m^3]	72.1	84.8	89.0	91.2	101.8
Quarry [ton]	1667.9	2132.0	2298.0	2383.2	2830.0
Transport Quarry [tonkm]	38527.8	49249.2	53084.5	55051.2	65374.8
Costs for 150 m [M€] excluded (de)mobalisation	4.5	5.6	6.0	6.2	7.2

Table C.5: Costs for a 150 m section for cross sections 150,300,450,600 and 750 m

C.4.4. Breakwater extension costs

For each 150 m section the costs are known. To obtain the cost for each extension the sections need to be summed depending on the length of the extension. The result is presented in table C.6.

Breakwater extension length [m]	**Cost** [M€]
150	6.5
300	12.2
450	18.2
600	24.4
750	31.6

Table C.6: Breakwater extension cost

Please note that this cost estimate is done based on the market prices of 1998. For the current situation, the placement of a breakwater could be more expensive due to the change in price levels. Moreover, techniques for transport and construction have been improved the last two decades, which reduced the price.

C.5. Feasibility of breakwater extension

To analyse the feasibility of breakwater extensions, only the reduction in operational cost as results of delays in mooring and manoeuvring time of container vessels are take into account.

The expected delays are:

- An average delay of 0.5 hour for each inefficient (un)loading hour. ($f_{delay} = 0.5$).
- An average delay of 3.0 hour for each time that a vessel cannot manoeuvre in the manoeuvring area($f_{delay} = 3.0$).

The hourly operational costs of the San Vicente Port are 7,500,000 CLP (Caba, 2016). So, a delay of 1 hour will lead to approximately €10,000 extra operational costs.

C.5.1. Scenarios

Due to market development and changes in vessel type usage, the amount of vessels and the distribution between the vessels groups will change. Based on an average yearly container throughput increase of 3.0% for the Biobío region, two throughput scenarios are made for San Vicente. Moreover, two vessel group distribution scenarios are made.

The market scenarios are:

- Pessimistic: decrease in market share to 40%, with a vessel (un)loading percentage of 50%
- Optimistic: increase market share to 70%, the market share of 2008, with an (un)loading percentage of 70%.

The scenarios for the vessel group distribution are:

- Equal growth in absolute amount of vessel
- Only growth of group I+II, same amount of vessels in the remaining groups.

Combining these scenarios gives four scenarios for the yearly amount of vessels per vessel group. With the above described scenarios, the following yearly amount of vessel per group can be expected for the San Vicente Port, if the total throughput of the Biobío region will be 1,900,000 TEU. Which will be the case around 2030.

	Equal growth		Growth I+II	
Scenario 40%	I	81	I	137
	II	28	II	47
	III	95	III	57
	IV	58	IV	35
	V	29	V	29
	VI	45	VI	29
	VII	27	VII	27
Scenario 70%	I	102	I	175
	II	35	II	61
	III	118	III	57
	IV	73	IV	35
	V	29	V	29
	VI	60	VI	29
	VII	27	VII	27

Table C.7: Amount of yearly vessel per group based on difference scenarios

C.5.2. Manoeuvring and mooring operations based on future scenarios

Both manoeuvring downtime and mooring efficiency are affected by changes in the market share and vessel distribution. The influence on the four scenarios is shown in figure C.17.

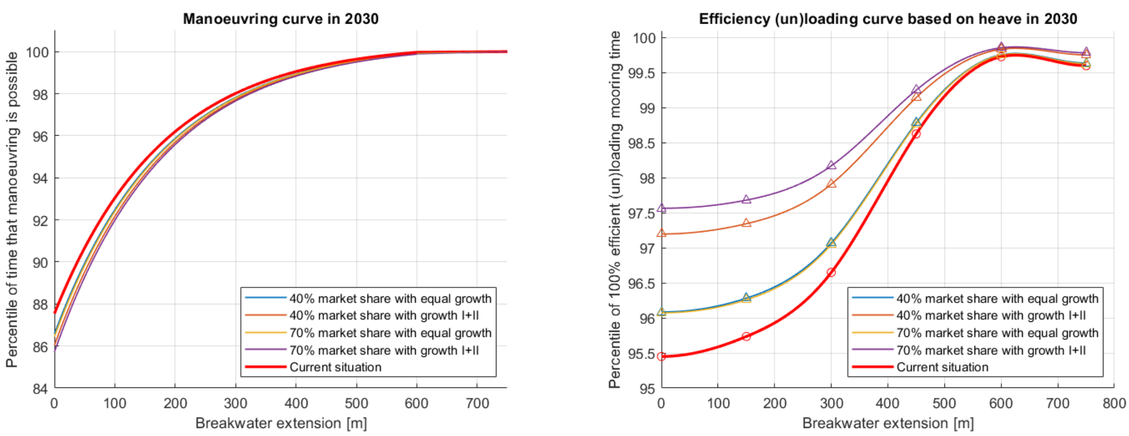

(a) Manoeuvring operations

(b) Mooring operations

Figure C.17: Effect of breakwater extension on nautical operations including different scenarios in the year 2030

C.5.3. Delays

Combing the vessel scenarios with the results obtained from the breakwater extension gives the total yearly delays. In order to calculate the mooring delays, the service time per call per vessel is needed. This is done for the two difference market scenario in table C.8.

Vessel group	Pessimistic market scenario	Optimistic market scenario
I	51.6	72.3
II	31.1	43.6
III	26.8	37.5
IV	22.1	31.0
VI	14.8	20.7

Table C.8: Service time in hours per vessel group

The mooring delay can be calculated with:

$$t_{mooringdelay} = \sum n_i \times t_{service.i} \times p_{not100\%.i} \times f_{delay} \tag{C.2}$$

In which:

$t_{mooringdelay}$	=	the total delay due to inefficiency (un)loading	[hrs]
n_i	=	amount of vessels in group i	[#]
$t_{service.i}$	=	service time of vessel in group i	[hrs]
$p_{not100\%.i}$	=	percentage of time with inefficient (un)loading	[−]
f_{delay}	=	delay factor (=0.5)	[−]

The yearly delay due to manoeuvring problems can be calculated with:

$$t_{manoeuvringdelay} = \sum n_i \times p_{notmanoeuvring.i} \times f_{delay} \tag{C.3}$$

In which:

$t_{mooringdelay}$	=	the total delay due to manoeuvre downtime	[hrs]
n_i	=	amount of vessels in group i	[#]
$p_{notmanoeuvring.i}$	=	manoeuvring downtime percentage of group i	[−]
f_{delay}	=	delay factor (=3.0)	[−]

The yearly delay costs are obtained if the delay time is multiplied with the delay cost rate of 10,000 $€/hr$. To determine the reduction in delay cost, the difference in yearly delay cost between the breakwater extensions and the original breakwater have to be calculated.

C.5.4. Cash flow

To analyse the feasibility of the breakwater the present value cash flow for the breakwater extensions have to be determined. The present value of the cash flow can be obtained from the yearly reduction in delay costs.

$$PVCF_{2018} = CF_i/(1+R)^t \tag{C.4}$$

In which:

$PVCF_{2018}$	=	Present value of cash flow in 2018
CF_i	=	Cash flow in year i
t	=	years ahead
R	=	discount rate

A real discount rate of 4% is applied (Tutuarima & Angremond, 1998). For inflation 2% is used. This results in a nominal discount rate of 6.08%.

The cash flow for the breakwater extensions are presented in figure C.18. These cash flows are determined for a lifetime of 25 years and an assumption for the construction period of 3 years for each breakwater extension. In the figure, the present value of both construction cash flow and the cash flow based on savings due to decrease in delay costs are shown. The cash flow is indicated as a range, obtained from the four different vessel scenarios. The cumulative cash flow for these scenarios are presented as well.

C.5.5. Net Present Value and payback period

The Net Present Value (NPV) is the summation of the yearly cash flow. The range of NPV for the breakwater extensions are presented in table C.9.

Breakwater extension length [m]	**NPV** range [€]
150	2.0 – -1.1
300	3.1 – -2.6
450	5.7 – -3.6
600	4.7 – -6.7
750	-2.2 – -13.3

Table C.9: Net Present Value of breakwater extension

The payback period is different per scenario and per breakwater extension. The expected payback year is presented in table C.10. As can be seen, for the 40% market share with equal vessel growth scenario, no breakwater extension will be paid back within 25 years.

Breakwater extension	40%; equal growth	40%; only I+II	70%; equal growth	70%; only I+II
150	-	2038	2040	2037
300	-	2039	2041	2038
450	-	2037	2039	2037
600	-	2039	2042	2039
750	-	-	-	-

Table C.10: Payback year for different scenarios. Note that no payback of a breakwater extension is indicated by (-)

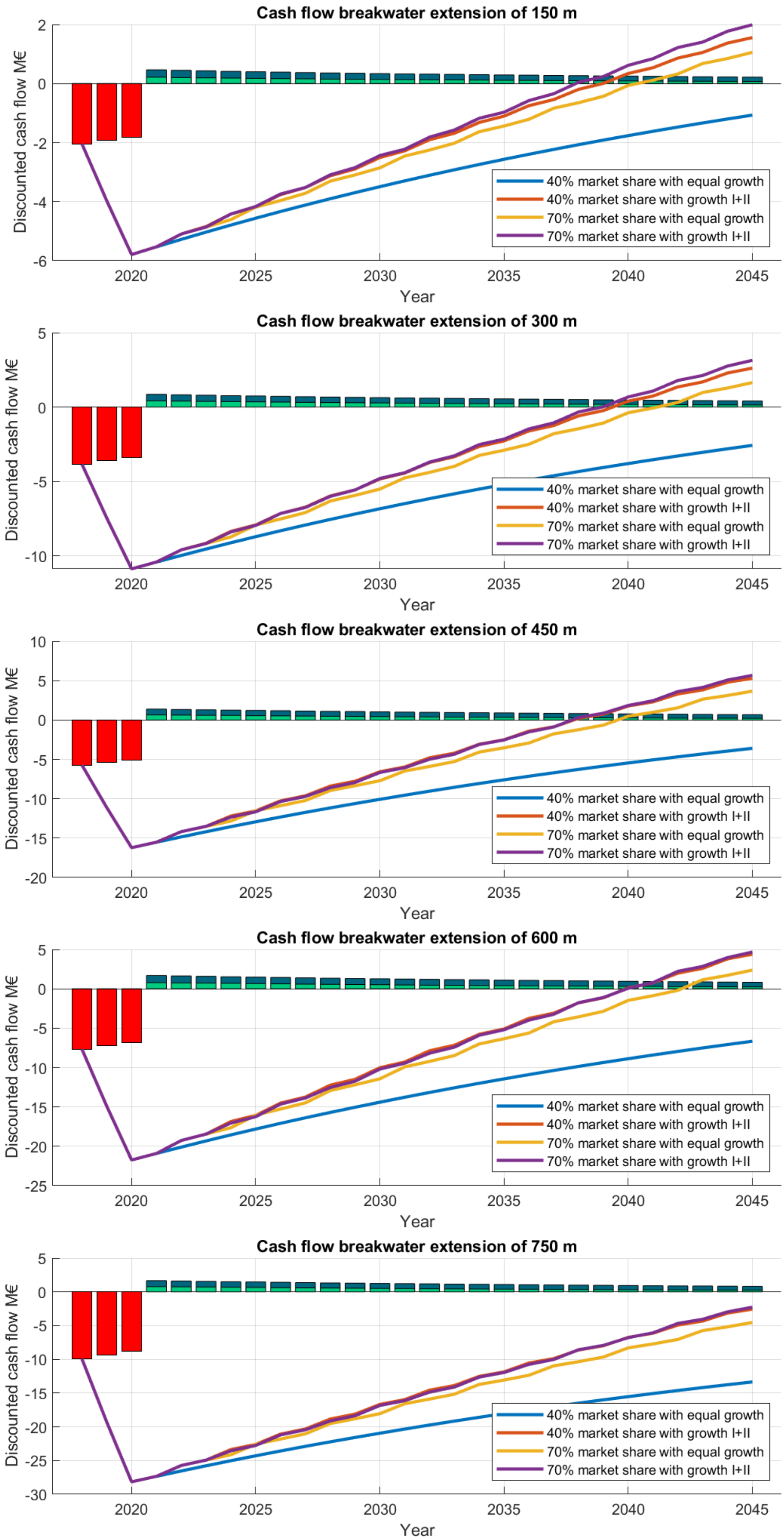

Figure C.18: Discounted yearly and cumulative cash flow for breakwater extensions.

D

Terminal operations

Figure D.1: Container consolidation with forklift trucks.

Source: Own photo (2 October 2018)

In figure D.1 the container consolidation is shown. This terminal operation is executed between the warehouses. Besides container consolidation, many other terminal operations are present in the San Vicente Port. These operations are analysed and if possible improved. A total overview of this analysis can be found in this appendix.

D.1. Current terminal analysis

Figure D.2 shows a schematisation of the San Vicente terminal. The terminal is compact. There are warehouses (5.1 *ha*) for storage of goods. The port is mainly an export port, so most of these goods are consolidated and shipped in containers. The container storage has a size of 20.7 *ha*.

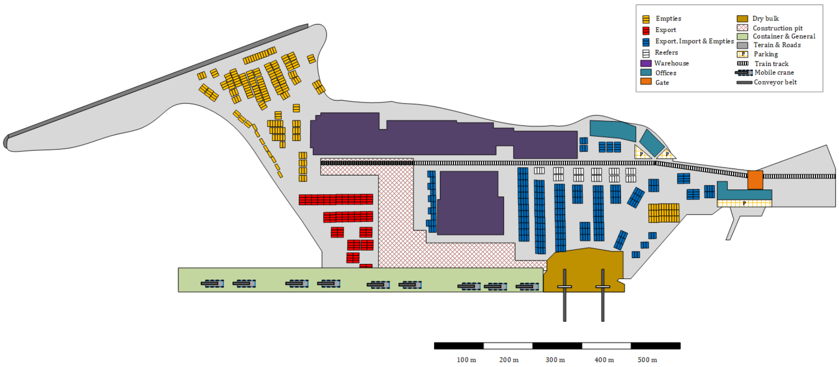

Figure D.2: Schematisation of the terminal layout of the San Vicente terminal.

D.1.1. Bulk and break bulk cargoes

Although the terminal services container-, bulk- and break bulk vessels, the terminal layout is mainly adjusted to the shipping of containers. The reason is that the cargo volumes of containerised cargo are larger than the other two (Empresa Portuaria Talcahuano San Vicente, 2018). Since San Vicente Port is a state port, the other two cargo types are also handled.

Break bulk is handled using the mobile harbour cranes; the cargo is stored on empty terminal terrain. Most general cargo is shipped in containers. The terminal has a berth dedicated to bulk cargo. Conveyor belts are used for the loading of vessels. Because of the compact layout of the terminal, San Vicente Terminal Internacional S.A. (SVTI) decided to remove the storage of bulk from the terminal. Bulk is transferred directly from trucks to the vessel. This results in large queues of trucks in the terminal.

The focus of this report is on containers. The (space) demands for bulk and break bulk are noted, but these cargo types are not discussed in detail.

D.1.2. Container flow

In 2016 nearly 200 container vessels moored at San Vicente Port (Empresa Portuaria Talcahuano San Vicente, 2018). The container flow and modal split of the San Vicente Port for 2016 is shown in figure D.3.

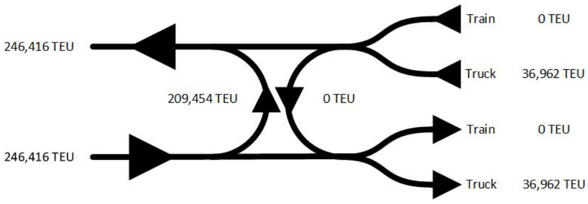

Figure D.3: The container flow and modal split of San Vicente Port for 2016 (Empresa Portuaria Talcahuano San Vicente, 2018).

An average container ship (un)loads 2,366 TEU (Empresa Portuaria Talcahuano San Vicente, 2018). The TEU-factor of the port is equal to 1.86 and the ratio loaded to unloaded containers is 50:50. This gives on average 636 containers that are unloaded and 636 containers that are loaded per container vessel. The port offers companies the opportunity to bring bulk or general goods to the terminal, which will be put in empty containers inside the terminal. The port called this operation container consolidation. 85% of the incoming containers, all empty containers, remains inside the terminal for container consolidation. After the consolidation all of these containers are transported to another port by vessels. The remaining 15% of the imported containers leaves the port by truck, but even those nearly 37,000 containers per year are not all full containers, among these containers there are also empties. The export containers of San Vicente Port are only full containers, no empties are exported.

San Vicente Port has multiple warehouses on the terminal. These warehouse are used to fill containers. The export goods are brought to the port via train and truck. Every day three trains with a length of 500 m long, deliver good to the port. The rest of the goods is transported to the port by trucks. The goods are stored inside the warehouses before forklifts use the goods to fill the containers.

D.1.3. Capacity

The capacity of the terminal is the smallest capacity of the different terminal components. The capacity of the access road, the gate, the storage area and the quay are discussed in this report. Table D.1 gives an overview of the capacity. As can be seen the storage is governing for the terminal capacity. The capacity calculations are shown below. Also, the required berth length is calculated. The equations used originate from the book *Ports and Terminals* by Ligteringen & Velsink (2012).

	Capacity [TEU/yr]
Access road	6,083,000
Gate	1,477,000
Storage area	**848,000**
Quay	1,075,000

Table D.1: The capacity of the different terminal components.

Access road

The following equation gives the capacity of the access road:

$$N_r = R_{cap} \times f_{TEU} \times t_{hr} \times m_r \times 365 \tag{D.1}$$

In which:

N_r	=	access road capacity in container movements per year	[TEU/yr]
R_{cap}	=	access road capacity	[vehicles/hr]
f_{TEU}	=	TEU factor	[−]
t_{hr}	=	gate opening hours per day	[hr]
m_r	=	average occupancy rate of the access road	[−]

This calculation is based on the performance review by Empresa Portuaria Talcahuano San Vicente (2018). The properties of the access road are shown in table D.2. The road capacity is 1400 vehicles per hour. To allow other road users to use the road, the maximum occupancy rate of the access road is 40%. The capacity of the access road is 6,083,000 TEU/yr.

R_{cap} [vehicles/hr]	1400
f_{TEU} [−]	1.86
t_{hr} [hr]	16
m_r [%]	40
N_r [TEU/yr]	**6,083,000**

Table D.2: Properties and capacity of the access road to the terminal (Empresa Portuaria Talcahuano San Vicente, 2018).

Gate

The gate capacity of the terminal can be calculated with the following equation:

$$N_g = \frac{m_g \times n_{gate} \times f_{TEU} \times t_{hr} \times 365}{T_s} \tag{D.2}$$

In which:

N_g	=	number of container movements per year through the gate	[TEU]
T_s	=	service time at the gate	[hr]
m_g	=	average occupancy rate of the gate	[−]
n_{gate}	=	number of gates	[−]
f_{TEU}	=	TEU factor	[−]
t_{hr}	=	gate opening hours per day	[hr]

This calculation is based on the performance review by Empresa Portuaria Talcahuano San Vicente (2018). The properties of the gate are shown in table D.3. A high occupancy of 85% is used; this is justified due to the presence of the preport (Container Express). This also results in low service times at the gate of only 1.5 minutes. The capacity of the gates is 1,477,000 TEU/yr.

T_s [hr]	0.025
m_g [%]	85
n_{gate} [−]	4
f_{TEU} [−]	1.86
t_{hr} [hr]	16
N_g [TEU/yr]	**1,477,000**

Table D.3: Properties and capacity of the gate in the terminal (Empresa Portuaria Talcahuano San Vicente, 2018).

Storage area

The storage area capacity of the terminal can be calculated with the following equation:

$$N_c = \frac{A \times r_{st} \times 365 \times m_s}{\overline{t_d} \times A_{TEU}} \tag{D.3}$$

In which:

N_c	=	number of container movements per year	[TEU]
A	=	available surface area	$[\mathrm{m}^2]$
$\overline{t_d}$	=	average dwell time	[days]
A_{TEU}	=	required area per TEU including equipment travelling lanes	$[\mathrm{m}^2/\mathrm{TEU}]$
r_{st}	=	average stacking height / nominal stacking height	[−]
m_s	=	acceptable average occupancy rate	[−]

For the calculation of the storage yard capacity, the calculation deviates from the performance review by Empresa Portuaria Talcahuano San Vicente (2018). The storage capacity is determined for each container type (empty, import and export). The properties of the storage area are shown in table D.4.

The storage area is divided according to the division of containers in section D.1.2 and the current layout of the terminal. The port authority mentions that there are 20.7 ha of container storage, with 4 to 5 ha free for container stacking and 2.9 ha correspond to covered warehouses (and 2 ha more outside the port). However, Google Maps shows that there is actually only 14 ha of storage area available at the terminal.

In their performance review, the port authority mentions a maximum allowed stay time of five days and an average dwell time of dray days. However, with a static capacity 26,000 TEU, the port does not receive enough vessels to renew all stored containers in three days. Also, the dwell time for empty containers is usually much larger according to Ligteringen & Velsink (2012). Thus, an average dwell time of three days is used for import and export containers, but a dwell time of ten days is used for empty containers.

The stacking height and the acceptable average occupancy are obtained from the port authority (Empresa Portuaria Talcahuano San Vicente, 2018). The required area per Twenty Foot Equivalent Unit (TEU) are estimated based on the current configuration (nominal stacking height of 5 compared to 1.8 in the performance review). This results in a total dynamic capacity of about 848,000 TEU/yr, which is considerably lower than the 1,149,750 TEU/yr that the port authority calculated.

	empty	**import**	**export**
A $[\mathrm{m}^2]$	39,600 & 44,000	18,267	36,533
$\overline{t_d}$ [days]	10	3	3
A_{TEU} $[\mathrm{m}^2/\mathrm{TEU}]$	4.11 & 7.8	7.8	7.8
$r_{st} * m_c$ [−]	0.6	0.6	0.6
N_c [TEU/yr]	**334,500**	**171,000**	**342,000**

Table D.4: Properties and capacity of the storage in the terminal. The density of empty containers depends on the location, there are two stacks with different density. (Empresa Portuaria Talcahuano San Vicente, 2018).

Quay

The calculation for quay capacity is done in two steps. First, the quay capacity is determined. Second, the waiting time is checked using queuing theory.

The quay capacity of the terminal is determined by the crane capacity. The crane capacity per berth is calculated with equation (D.4). By multiplying this with the number of berths, n, the quay capacity is obtained.

$$c_b = P \times f_{TEU} \times N_{cb} \times n_{hy} \times m_b \tag{D.4}$$

$$C = n \times c_b \tag{D.5}$$

in which:

n	=	number of berths	$[-]$
C	=	Quay capacity in TEU	$[TEU/yr]$
c_b	=	average annual productivity per berth	$[TEU/yr]$
P	=	net production per crane	$[moves/hr]$
f_{TEU}	=	TEU factor	$[-]$
N_{cb}	=	number of cranes per berth	$[-]$
n_{hy}	=	number of operational hours per year	$[hr/yr]$
m_b	=	berth occupancy factor	$[-]$

This calculation is based on the performance review by Empresa Portuaria Talcahuano San Vicente (2018). The properties of the quay are given in table D.5. The number of berths is 2.5. There is enough space for three vessels, but there are not enough cranes to (un)load them all at the same time. The port authority uses a maximum occupancy of 44%, so that waiting times remain small. This is within PIANC limts: the maximum occupancy according to PIANC (2014b) is 50%. The capacity of the quay is 1,075,000 TEU/yr.

P [moves/hr]	15
m_b [−]	0.44
N_{cb} [−]	4
n [−]	2.5
f_{TEU} [−]	1.86
n_{hy} [hr]	8760
C [TEU/yr]	**1,075,000**

Table D.5: Properties and capacity of the quay in the terminal (Empresa Portuaria Talcahuano San Vicente, 2018).

Based on the current capacity of the terminal, the waiting times are estimated using queuing theory. Storage yard capacity is normative for the capacity of the terminal, so a capacity of 848,000 TEU/yr is used. First, the required number of berths must be estimated. This is done using equation (D.4). The maximum occupancy of 50% is used (PIANC, 2014b). The properties in table D.6 are used in the calculation.

C [TEU/yr]	848,000
P [moves/hr]	15
N_{cb} [−]	4
f_{TEU} [−]	1.86
n_{hy} [hr/yr]	8760
m_b [−]	0.5
n [−]	**1.73 > 2**

Table D.6: Properties and number of berths required in the terminal (Empresa Portuaria Talcahuano San Vicente, 2018).

Two berths are required. Although there are 2.5 berths available according to the port authority, 2 berths are used for queuing theory calculation. There are two reasons why this is justified: (1) the port can only serve two large vessels (Panamax and New Panamax) simultaneously and (2) this will give an overestimation of the waiting times. The queuing theory equations are given below:

$$u = \frac{\rho}{n} \tag{D.6}$$

$$\rho = \frac{\lambda}{\mu} \tag{D.7}$$

$$\frac{1}{\mu} = \frac{c_c}{f_{TEU}} \cdot \frac{1}{P \cdot N_{cb}} + T_{mooring} \tag{D.8}$$

$$\lambda = \frac{N_{sy}}{n_{hy}} \tag{D.9}$$

in which:

u	=	utilisation	$[-]$
ρ	=	Berth occupancy	$[-]$
λ	=	Average arrival rate	$\left[\text{hr}^{-1}\right]$
μ	=	Average service rate	$\left[\text{hr}^{-1}\right]$
c_c	=	Average unloading per call	[TEU]
$T_{mooring}$	=	Time required for mooring	[hr]
N_{sy}	=	Number of vessels per year	[vessels/yr]

The utilisation is determined using the numbers in table D.6 and table D.7. The utilisation is 0.26 for both vessel distribution scenarios. Due to the larger vessels in the large vessel scenario, this scenario serves fewer vessels. This does not effect the utilisation: for both scenarios the utilisation is the same.

N_{sy} [vessels/yr]	247	227
$T_{mooring}$ [hr]	2	2
c_c [Containers/vessel]	1845	2008
u $[-]$	**0.26**	**0.26**

Table D.7: Properties and utilisation of the terminal (Empresa Portuaria Talcahuano San Vicente, 2018). The first column gives the utilisation for the equal growth scenario, the second column for the large vessel growth scenario.

Now the queuing theory can be applied. The tables from Groenveld (2001) are used; the number of berths and the utilisation are input parameters. The result is the waiting time. Depending on the required service, a waiting time is acceptable. According to Ligteringen & Velsink (2012) a waiting time of 10% of the service time is considered acceptable. For larger waiting times, additional berths are required and for small waiting times, fewer berths should be considered. The used queuing system is M/E2/n which can usually be assumed for port systems without a tidal window (Groenveld, 2001). With $n = 2$ and $u = 0.26$ a waiting time of 5.5% of the service time is achieved. This is below 10% and is thus considered acceptable.

The required berth length can be calculated with the following formulas:

$$L_q = \begin{cases} L_{s,max} + 2 \cdot 15 & \text{for } n = 1 \\ 1.1 \cdot n \cdot \left(\bar{L_s} + 15\right) + 15 & \text{for } n > 1 \end{cases} \tag{D.10}$$

in which:

L_q	=	The required length of the quay	[m]
$L_{s,max}$	=	The length of the design vessel	[m]
$\bar{L_s}$	=	The length of the average vessel calling this port	[m]

At least two berths are required. The average vessel at San Vicente Port has a length $\bar{L_s}$ of 262 m. So, the required quay length $L_q = 624$ m. Berth 1 is dedicated to bulk cargo, so this berth cannot be used for containers. The total remaining quay length is 940 m, so there is sufficient quay length.

D.1.4. Terminal problems

During our site visit at San Vicente Port we investigated the terminal efficiency. We found that, in the current situation, the terminal has some problems which affects the capacity and efficiency. Roughly seven major terminal problems can be identified, which are discussed below. Also, they are indicated in the current port layout in figure D.7. For each problem, a photo is added with a problem description to get a good insight in the situation. Please note that the parking problem is not indicated in this figure. A more detailed description of the problems is given below:

Train blockage

San Vicente Port has an on-dock rail terminal, where three trains are served each day. These block trains usually have a length of 500 m, and are mainly used for transport of forestry products to the port.

Ideally, the rail yard has a buffer zone of 40 m between the stacking yard to the tracks (PIANC, 2014b). In San Vicente Port, this is much more compact, as can be seen in figure D.7. The rail tracks are located between the warehouse and storage area, which also serves as the main road in the terminal.

There are four rail tracks in the terminal. The first track is located below the cantilever roof of the warehouse, but is never used: goods in the warehouses are stored on this track. Usually, the second rail track is used which is close to the warehouses. While goods from the trains are unloaded into the warehouses, the train forms a large obstacle in the terminal:

- The train yard is located in the middle of the terminal. This implies that traffic from one side of the terminal to the other is not possible during train unloading. In addition, the main road in the terminal is partly blocked.

- Container consolidation (stuffing goods in empty containers) is done in front of the warehouses. For this process, empty containers are aligned on the second rail track with their opening towards the warehouses. These processes cannot take place at the same time.

Traffic jam in the main road

A schematic overview of the transport routes inside the terminal is shown in figure D.4. It can be seen that most routes through the terminal use the main road (in grey), which is located in front of the warehouses. It is not the road capacity that forms a problem here, but the concentration of processes in this area.

The capacity of the main road (30 km/hr) is roughly 500 large $vehicles/hr$. On an average day, there are only about 150 $vehicles/hr$ here (estimation based on the number of container movements per day). Even during peak periods, when the number of vehicles is doubled, the road has sufficient capacity.

The problem with the main road is congestion due to stopping trucks and other obstacles. Trucks stop to deliver goods to the warehouses, trains reduce road capacity, and Reach Stackers block the road to (un)load containers, for example for the consolidation of containers.

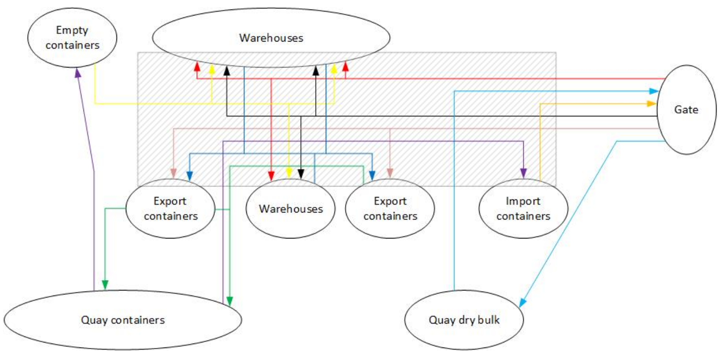

Figure D.4: Schematic overview of the movements of the vehicles in San Vicente Port

Containers are stored along the main road, for which Reach Stackers need to manoeuvre in the main road. Also, a lot of containers are stored temporarily in the area near the gate. This area is located next to the main road, so for handling these containers Reach Stackers need to manoeuvre in the main road. This causes congestion, as can be seen in figure D.5.

Figure D.5: Congestion in the main road due to Reach Stacker operation. The Reach Stacker will pick up the grey container from the trailer and place it in the area behind the warehouse (in the left of the figure). This process was observed during the site visit and took about 2 minutes.

A quick calculation shows that if a truck or a Reach Stacker blocks the road, a queue of vehicles arises. If this blockage lasts for about 1 minute, the queue will be 2.5 vehicles long and the average waiting time is 30 seconds. Per blockage this gives a delay of 75 seconds. Assuming a total amount of 300 movements in the main road per day, the total delay per day is approximately 375 minutes. This situation can be improved by reducing the number of processes in the main road.

Container consolidation

An important service of the port is the consolidation of containers. Clients transport their goods to the terminal and than these are temporarily stored in the warehouses. At the terminal they are loaded into containers.

As indicated in figure D.6, the empty containers are put side to side in front of the warehouses. The empty containers are brought by tractor-trailer units on the main road. A Reach Stacker will pick up the container and this procedure will block the main road. This blockage is creating traffic jams on the main road which is not beneficial for the efficiency.

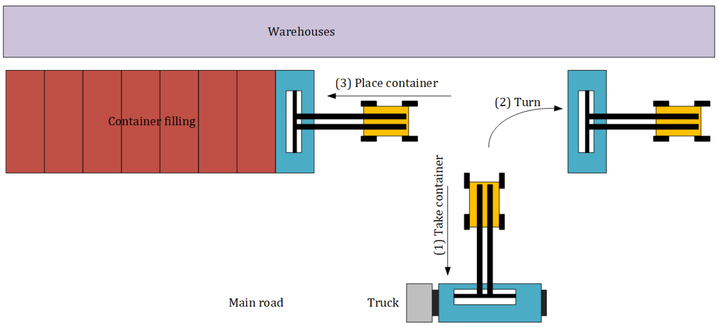

Figure D.6: Filling procedure

Container storage

San Vicente Port is very compact. The occupancy rate of the container storage and the packing density are high. Containers are placed so closed to each other that Reach Stackers are not able to reach all containers. For empty containers this is not a big problem (only the brand and type matters) but for import and export containers it is. For import containers it is important that they are all easily accessible because it is unknown when clients come to get their imported containers. Export containers must be loaded in a particular order and this order is different than the order that containers are brought to the terminal. Besides, there are containers all over the terminal, without a strict alignment. This results in loss of capacity and an even lower accessibility.

Currently, the containers seem randomly scattered over the terminal. There are no designated stacks for import and export containers and the stacks have irregular shapes. In some places, improvement of the pavement is necessary.

Mobile harbour cranes

(Un)loading is executed by mobile cranes. These cranes have enough capacity for the current throughput, but a low efficiency compared to Ship-to-Shore (STS) gantry cranes. This results in longer (un)loading times for vessels and makes the port less attractive compared to other ports with gantries (for example Coronel Port). Moreover, the maintenance of STS cranes is cheaper. The current cranes are old and a lot of repairs are needed. The maintenance is expensive, because there are not many spare parts left.

Central warehouse

In the middle of the container storage area a warehouse is located. This warehouse is the oldest of all warehouses. The warehouses are important for the port, but this central warehouse is an obstacle for traffic. All traffic must drive around it which results in busy roads and it is taking extra time to move between storage stacks.

Parking

There is a shortage of parking places for employees. Both inside and outside the terminal, there are insufficient parking places. Therefore, employees park their cars on one of the railways entering the port: only one of the two railway gates is operational. In addition, the limited space in front of the gates means that congestion in front of the gate is easily caused.

Bulk traffic congestion

As mentioned before, there is no storage of bulk cargo in the SVTI terminal. This means that all bulk is directly transferred from trucks to the ship. During loading of bulk vessels, a queue of truck forms near berth 1: the road towards this sector is completely blocked. The containers that are stored in this sector cannot be reached during the day. Relocating these containers can only be done at night.

D.1.5. Current improvements

Currently, there are multiple parts of the terminal under construction. When the construction works are finished the rail track inside the terminal will be elongated by about 120 m. Also, an area for storage of containers between the warehouses and the quay will become available when the construction works are finished. Furthermore, there will be more connecting bridges between the storage and the quay.

In addition to the mentioned construction works, SVTI has ordered two STS gantry cranes. These cranes will be placed next year (2019), and form the first step of an efficiency improvement. The service time will decrease, which is good for the strategic position of San Vicente Port in the region. In order to keep up with the improved handling speed at the quay, more tractor-trailer units and Reach Stackers are needed. This, means that there are more movements in the terminal with the corresponding congestion problems.

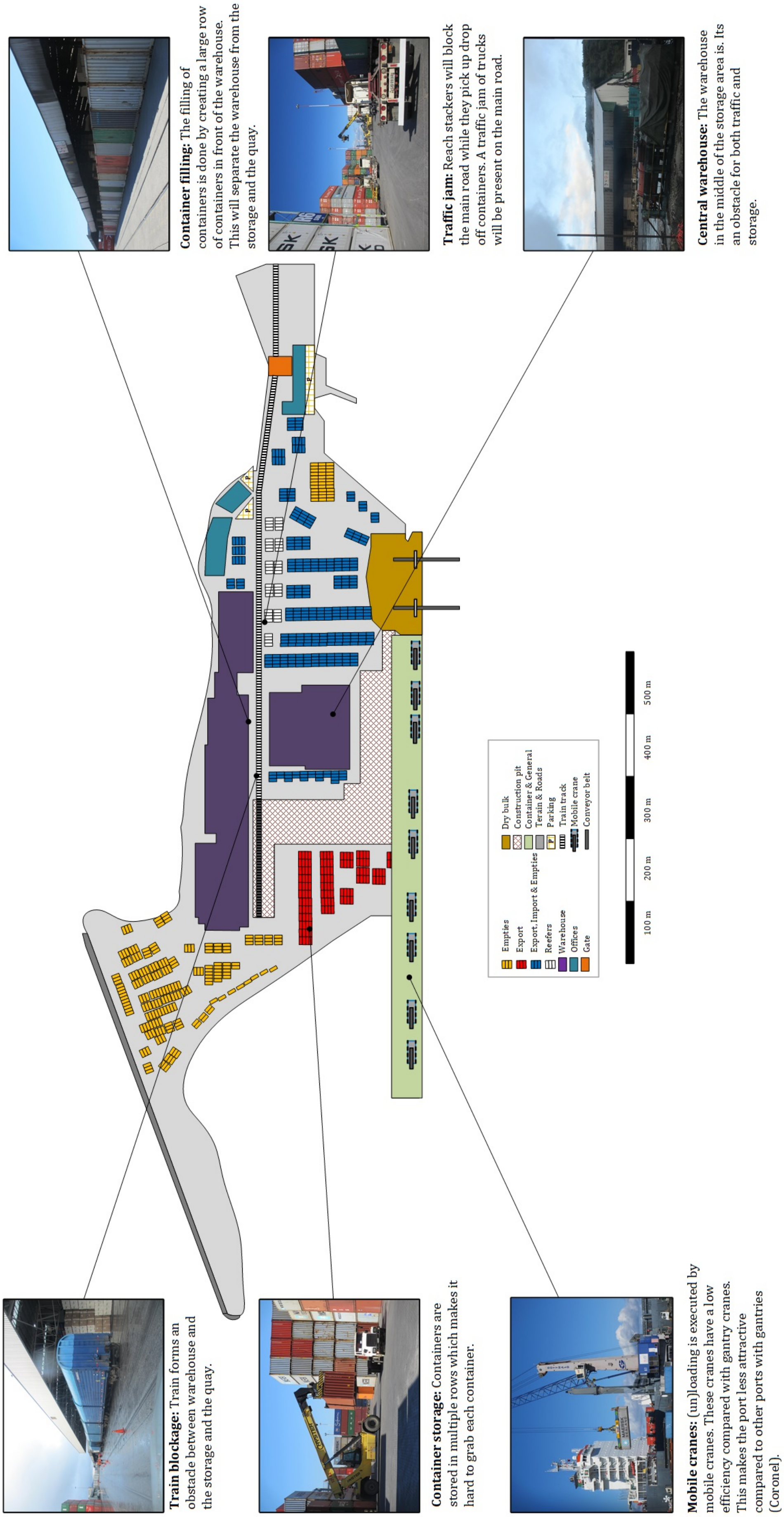

Figure D.7: Port terminal problem overview

D.2. Solutions to terminal problems

Several solutions are proposed that (partially) solve the terminal problems. All solutions have there pros and cons.

D.2.1. Train blockage: relocate rail tracks

The trains causes a lot of hinder when they are unloaded in front of the warehouse. Moving the rail tracks to the back of the warehouses, as shown in figure D.8, would solve this problem. Another advantage is that the flow of goods inside the warehouse is in one direction. Goods enter the warehouse from one side and leave on the other side. This flow makes more movements per hour inside the warehouse possible than loading and unloading the warehouse at the same side.

With the present layout, it is not possible to unload a train and to consolidate containers simultaneously. However, with the relocated rail tracks this becomes possible. It is even possible to immediately fill containers, this saves movements with the forklifts and space inside the warehouse.

The main disadvantage of this solution is that, at this moment, there is not enough space behind the warehouses. Parts of a stone hill would have to be removed. This costly operation is the biggest downside. Also, the offices that are located at the hillside of the terminal have to move. A possible location for the offices is shown in figure D.8, where a yellow arrow indicates the movement of the office to a location near the water front.

Another disadvantage is that the warehouses become a large open structure, which makes it harder to effectively protect the goods which are stored against the weather. A large overhang or walls that hinder the traffic flows would be required.

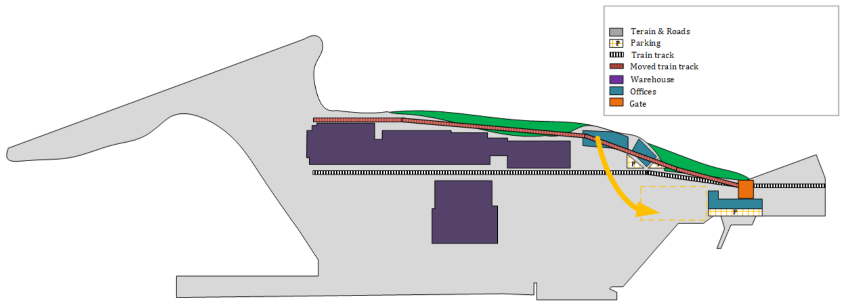

Figure D.8: Train blockage solution

D.2.2. Container storage: other terminal equipment

Other terminal equipment is an option to improve capacity and efficiency of the container storage. Different types of terminal equipment are discussed. First, equipment for the stacking operation is discussed. Then, equipment for the horizontal transfer operation is mentioned.

Equipment in the stack: Rubber Tyred Gantry cranes (RTGs) and Reach Stackers

Currently, Reach Stackers are used for the stacking operation. They are relatively cheap and can easily operate in an irregular shaped areas, such as the SVTI terminal. Another advantage is their flexibility and that they can be used anywhere in the terminal. Reach Stackers (or empty handlers) are particularly useful for stacking empty containers: empties can be stored very densely. For import and export containers this is not possible due to the fact that it is desired to be able to reach all containers.

Straddle carrier are considered as an alternative to Reach Stackers. Like Reach Stackers, they are very flexible and can easily handle the irregular shape of the terminal. Also, the need for tractor-trailers would become unnecessary. Disadvantages of this type of equipment are the low storage density.

RTGs are characterised by a high stacking density. With their tires, they are flexible and are able to move between stacks. Disadvantage is that large rectangular areas are required, whereas the SVTI terminal has an irregular shape. In addition, the costs are considerably higher then the previously mentioned equipment types.

When using Rail Mounted Gantry cranes (RMGs), even higher stacking densities can be achieved. They can store 7-8% more containers in the same area compared to RTGs. In addition, this system is very suitable for full automation. The disadvantage is the high investment costs.

Table D.8 shows the capacity of the terminal if the equipment for the stacking operation would change.

	$\mathbf{A_{TEU}}$ [m^2/TEU]	**Empty** [TEU/yr]	**Import** [TEU/yr]	**Export** [TEU/yr]
Reach Stackers	4.11 & 7.8	445,500	171,000	342,000
Straddle Carriers	10	183,000	133,500	267,000
RTG	6.9	265,500	193,500	386,500
RMG	6.4	286,000	208,500	417,000

Table D.8: Storage capacity with different terminal equipment. The properties are kept the same as in the calculation for the capacity of the current port except the A_{TEU} which is mentioned in the table. For Reach Stackers two number are mentioned in A_{TEU}: The first is for empty containers and the second is for import and export containers.

For the stacking of import and export containers, the current situation with Reach Stackers is not ideal. The storage density is relatively low, and a lot of containers are unreachable. RTGs or RMGs would improve this situation. Due to the high initial costs of RMGs and the flexibility of RTGs, RTGs are the preferred terminal equipment for import and export containers.

For the stacking of empty containers, Reach Stackers are the best solution. The storage has an irregular shape, and Reach Stackers can easily account for this. In addition, very high stacking densities can be achieved for empties, which is ideal given the compact layout of the terminal. Moreover, they are the cheapest solution and can also be used for the consolidation of containers.

Horizontal transfer equipment: tractor-trailer

For horizontal transfer of containers, three options are investigated.

Automated Guided Vehicles (AGVs) are essential in fully automated terminals. Disadvantages are the high costs, the wide apron which is required and that the vehicles are only limited to designated paths.

Tractor-trailer units are the second option. These are used in most small ports, because of the low cost and high manoeuvrability.

Last are Straddle carriers. They have a high manoeuvrability but compared to tractors also high costs.

A full automated functioning terminal is not realistic for the medium sized San Vicente Port. The costs will be too high to make it profitable. Therefore, AGVs are no option for the horizontal transfer operation. Straddle carriers can do both the stacking and the horizontal transfer operation but for this port space is valuable. Therefore, for the horizontal transfer operation the tractor-trailers are the best options.

D.2.3. Mobile cranes: switch to STS gantry cranes

As mentioned in section D.1.5, SVTI is planning to buy two STS gantry cranes in the coming year. An example of a STS crane is shown in figure D.9. Also, plans are made to sell the old mobile cranes. The gantry cranes have a higher productivity and are more efficient. Moreover, the maintenance costs are lower than the costs of the old mobile cranes. This all will increase the attractiveness of the port.

Figure D.9: Example of a gantry ship to shore crane

D.2.4. Container consolidation

For the container consolidation procedure, two solutions are proposed.

Route through warehouses

To improve the traffic flows in the main road in front of the warehouses, a new traffic flow is proposed. For this new traffic flow, less hindrance is expected from Reach Stackers that are blocking the main road. Figure D.10 illustrates this solution: Tractors that need to pick up a consolidated container or to drop an empty container for consolidation are directed through the warehouses. This way, the tractors do not hinder the traffic while they are waiting for the Reach Stacker. The manoeuvre by the Reach Stackers is much simpler, so this would improve the operation.

A disadvantage of this solution is that a modification to the warehouse is needed to make this new route possible. Because tractors are not stopping at the exact place where the containers must be dropped Reach Stackers will need to drive longer distances. The same applies to the tractors, because of the longer route.

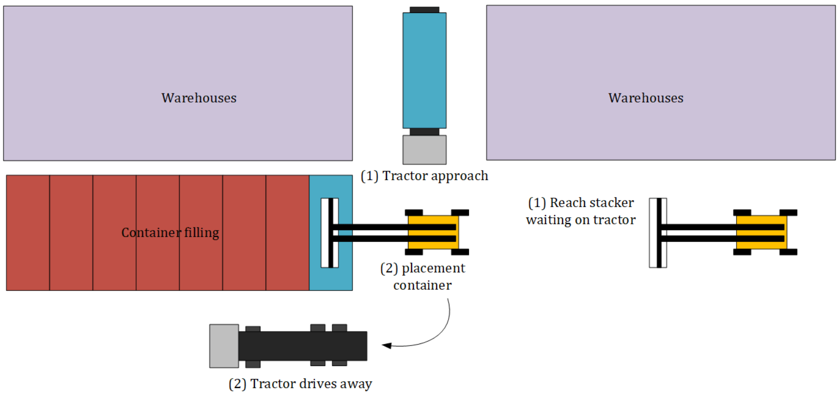

Figure D.10: Route trough warehouse solution

Consolidate containers behind warehouse

Not being able to fill containers simultaneous with emptying the train, is a problem which can be solved if the containers are filled somewhere else. Behind the warehouses, there is a small space which is currently used to store some goods and containers. By moving the container consolidation to this area, the number of processes in the main road is decreased. Less containers need to be filled in front of the warehouse so that it is possible to perform the train unloading and container consolidation processes simultaneously. Main disadvantage is that there is not enough space for filling all containers so the area in front still need to be used. Because the space behind the warehouse is small the containers must be picked up in reverse order compared to dropping the containers. This is not efficient.

Gantry crane in front of warehouses

Reach Stackers working in front of the warehouse cause delays for trucks and tractors driving in the main road. To prevent that Reach Stackers are working in the main road, a gantry crane can be placed in front of the warehouses that will be used to place the containers there. This can be seen in figure D.11.

Tractors need to drop the containers at a drop-off point. From there the gantry crane moves the containers to the filling place in front of the warehouses. Because of the length of the warehouse multiple gantry cranes and drop-off points are needed. The best place for drop-off points is at the end of the warehouses because these locations can be reached when a train is present. Disadvantage is that the gantry crane also needs space which means the train must be relocated from the second to the third rail track.

The capacity of the main road is sufficient, even with the train on rail track 3. With the advantage that there is less Reach Stacker activity in the main road, no traffic problems are expected. The replacement of the train also has an advantage. It is now possible to fill containers at the same time as to unload the train, even though this is not easy.

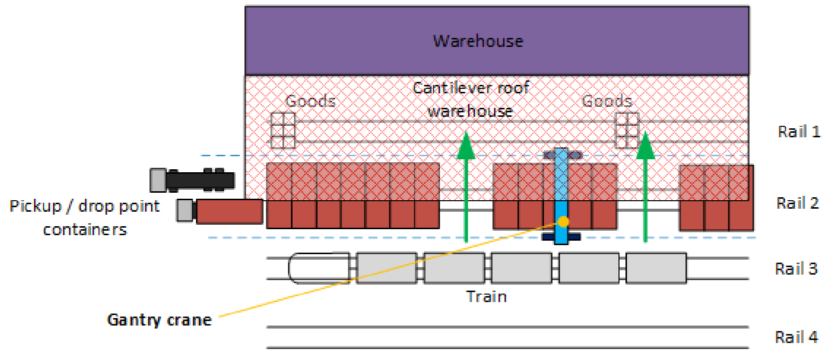

Figure D.11: Gantry crane in front of warehouse

D.2.5. Traffic jam in the main road

To reduce traffic jams, two solutions are proposed. However, the solutions to the container consolidation problem also contribute to improvements in the main road.

One-way roads

Blocked roads give delays to vehicles. By creating one-way roads in the terminal there is more space for overtaking when a vehicle is blocking the road. Figure D.12 shows a layout for one-way roads in the terminal. More space does not mean that vehicles can always overtake each other: even in one-way roads, there is no space when a Reach Stacker is (un)loading a tractor in a container lane. The main disadvantage is that the distances that vehicles need to drive will increase. To prevent that there will be too much activity on the quay an extra road is needed next to the quay. This loss of space will cost storage area for about 300 containers.

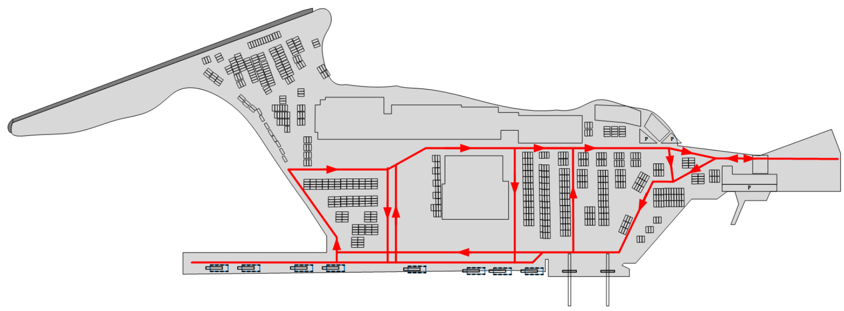

Figure D.12: One-way road solution

Widen the main road

Most vehicle movements through the terminal are via the main road. When too much vehicles are making their movements on this road it will cause delays to other traffic. By widening the road it will be possible for all vehicles to do their jobs without hampering each other. Without delays everything will be more efficient. There is space for storage of goods in front of the warehouse, the train or containers, movements with Reach Stackers and driving lanes for trucks and tractors. Downside of this idea is that some valuable container storage and a part of the central warehouse gets lost. The loss of one rows of container is about 300 containers and 2000 m^2 storage.

D.2.6. Central warehouse: relocate

The warehouses are an important part of the port because it delivers service to the customers. Thus, the terminal's warehouses are important. However, the central warehouse is old and is located in the middle of the terminal. Relocating the central warehouse to a less obstructing locating would improve the terminal's traffic flows. Possible new locations are shown in figure D.13.

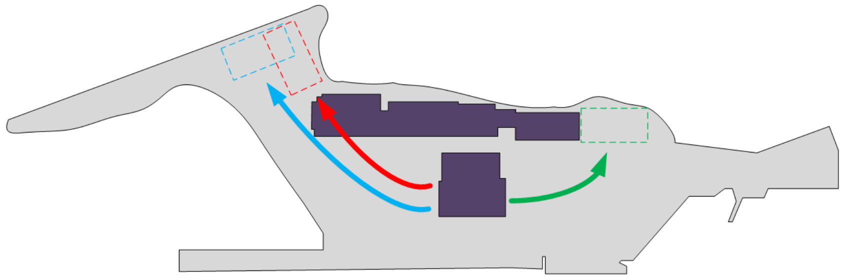

Figure D.13: Moving the central warehouse

D.2.7. Parking: new spots

Extra parking space should be constructed. This can be inside or outside the terminal, but the best is to do it close to the offices. That will avoid that people have to cross roads on which traffic is driving with heavy equipment or loads. In this way, safety is guaranteed. If no space is found for extra parking the current situation can also be preserved. The blocking of one of the two rail tracks is not causing large problems in front of the gate. Because only one rail track is needed one rail track can be blocked and the limited space for trucks in front of the gate is not causing problems because the preport is used. This preport send the trucks gradually to the gate.

D.2.8. Bulk traffic congestion: move road to waterfront

The containers that are stored between the road towards berth 1 and the waterfront cannot be reached at day because of the traffic in this road. A simple solution would be to move the road towards the waterfront. The containers can be relocated inside the terminal where now the road towards berth 1 is. This does not completely solve the problem, but improves the accessibility of containers.

D.2.9. Combination matrix

It is not possible to combine all proposed solutions. The combination matrix (table D.9) shows which solutions can be combined. Some combinations are not logical: for example, one-way road and widening of the main road try to solve the same problem. This is not shown in the matrix but is taken into account when the choice is made. The $\surd$ does not mean that it is a good solution. For example, it can be seen that widening the main road does not obstruct any other solutions, but it still decreases the capacity of the storage yard.

		A	**B**	**C**	**D**	**E**	**F**	**G**	**H**	**I**	**J**
A	Replace rail track		√	√	X	X	√	√	√	√	√
B	Change equipment	√		√	√	√	√	√	√	√	√
C	Ship-to-shore gantry cranes	√	√		√	√	√	√	√	√	√
D	Route through warehouse	X	√	√		X	√	√	√	√	√
E	Fill containers behind warehouse	X	√	√	X		X	√	√	√	√
F	One-way roads	√	√	√	√	X		√	√	√	√
G	Widen main road	√	√	√	√	√	√		√	√	√
H	Gantry in front of warehouse	√	√	√	X	√	√	√		√	√
I	Remove central warehouse	√	√	√	√	√	√	√	√		√
J	Extra parking	√	√	√	√	√	√	√	√	√	

Table D.9: A combination matrix which shows which solutions can be combined and which cannot

D.3. Terminal improvement plan

A combination of solutions is selected for improving the efficiency of the terminal. Thereby, the capacity of the terminal increases as an extra advantage. The solutions which suites the wishes of the port authority, terminal operator and clients as good as possible are combined in the improvement plan. The new lay out can be seen in figure D.15.

D.3.1. Terminal layout

Rail tracks behind warehouses

The rail tracks will be relocated behind the warehouses with the goal of simplifying the processes on the main road.

For this shift of the tracks, space must be made available behind the warehouses. Part of the hill must be removed, and the terminal's offices need to be relocated. There should be sufficient space between the rail tracks and the warehouses for efficient unloading of the trains. When there are no trains in the port, this area can also be used for trucks to drop of their cargo. Container consolidation can occur at the same time as the train operation.

Offices on the other side of the main road

The offices need to be replaced to another area. It is chosen to place the offices just after the gate entrance on the left. The shape of this area is not suitable for container storage. By placing it at the entrance of the terminal it is prevented that the employees must drive over the entire port but they are still on the terminal to monitor and control everything. Extra parking spots can be placed behind the offices.

Terminal equipment: RTGs, Reach Stackers and tractor-trailers

There will be designated stacks for import, export and empty containers. Import and export containers will be stacked using RTGs, because of the high stacking density, flexibility and accessibility of containers. The stacks will be parallel to the quay; a typical stacking arrangement will be used (figure D.14). All containers can be reached from the top instead of the side so more containers can be placed next to each other. This will increase the capacity of a stack with RTGs, compared to Reach Stackers.

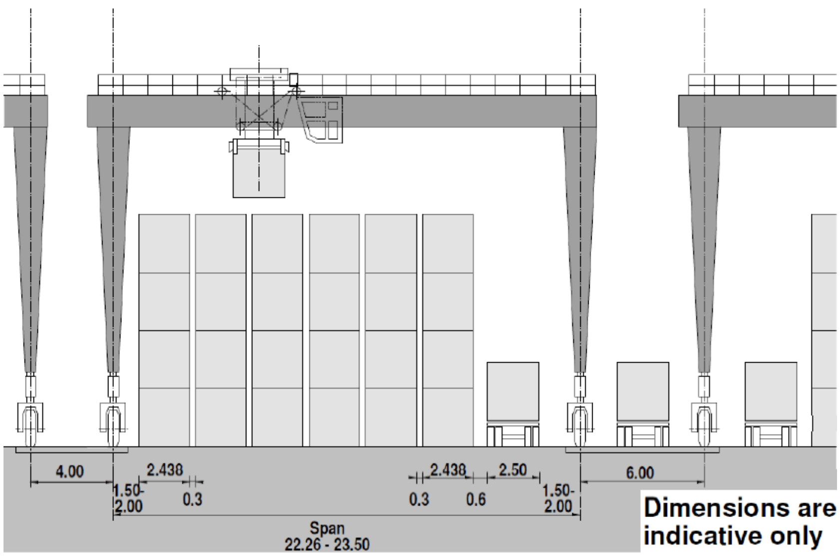

Figure D.14: Typical stacking arrangement for RTGs (PIANC, 2014b).

Because the accessibility of the empties is less important it is not needed to buy new equipment for the Reach Stackers. The density of empty stacks can be improved by placing more containers next to each other so the same or even better density compared with RTG can be achieved. Tractors will be used for the horizontal transfer operation.

Storage yard configuration

Container storage will be tightly aligned in front of the quay. Export, import and empty container stacks will be stored in different parts of the port. This configuration will help to store more containers and process the containers more efficient. The alignment of the export and import stack is parallel to the quay. This is done because of the new equipment that is used. It is more efficient to place RTG stacks parallel to the quay than perpendicular (PIANC, 2014b).

The empty stack be placed perpendicular to the quay. The empties are placed perpendicular to be sure that Reach Stackers will not use the main road for (un)loading containers on tractors.

Ship-to-Shore gantry cranes

Two STS gantry cranes are bought, because of their high productivity. This allows for quicker loading and unloading of vessels, and lower service times. This will increase the attractiveness of the port. In addition, this will keep maintenance costs for the mobile harbour cranes down. As a bonus, this results in a higher quay capacity.

Warehouses

Removing warehouses from the port terrain is not possible because it is too important for the port authority.

The port currently houses a lot of empty containers which requires just as much space as a filled container and with the new RTG cranes it will be not a problem to reach the export containers when they are stored. By filling containers immediately when the goods are brought inside the port saves movements with forklifts and saves space inside the warehouses. The problem with this is the maximum stay time for export containers. If this rule is broadened, the opportunity is opened to store more goods in containers then in the warehouses. Than, less warehouse space is needed so the central warehouse can be demolished. The warehouses can be extended towards the east to provide more storage.

Due to the proposed location of the trains, it is possible to create a flow of goods inside the warehouses from one side to the other. Goods enter at the back and will leave at the front. One exception is possible when the train is inside the port, then trucks must be unloaded at the front but this should be minimised.

Bulk traffic congestion: move road to waterfront

The route to the dry bulk sector is shifted towards the waterfront. This prevents that there are containers that are not reachable during day. The containers can be relocated on the other side of the road.

Traffic rules and Terminal Operating System

There is a lot of traffic in the main road, so this area gets congested easily. By applying strict traffic rules, the port provides a smooth traffic flows. It is too expensive to create extra space for separated (un)loading and driving lanes. Stopping in this area should be prevented, except for Reach Stackers and tractors that need to (un)load a container in front of the warehouses. Reach Stackers should not (un)load containers from the stacks in the main road. A good Terminal Operating System (TOS) can help to efficiently use the storage yard. The advantage of such a system is that fewer containers are moved unnecessarily and dwell times remain small. TOS can be used to reduce travel and waiting times by pooling tractors across the port. It will match available tractors to available work in real-time, so tractors are not fixed to a single mobile harbour crane or STS crane.

D.3.2. Terminal capacity

Although, the terminal improvement plan is primarily aimed at improving the efficiency of the terminal, the capacity is also improved. First, the capacity of the storage yard is recalculated. The capacity will increase to nearly 1 million TEU. This means that the storage is still the governing terminal component so the other components do not need capacity improvement. Also, the required berth length is calculated, here the new STS cranes are included because otherwise the waiting times for the vessels would become too high. The berth length is still sufficient.

Storage area

For the capacity calculation of the storage area equation D.3 is used. It is assumed that the ratio for empty to import to export containers, which is now 9:2:4, remains the same. Table D.10 shows the properties of the changed storage area. Also, the new capacity is added to the table. The capacity of the storage yard will increase to 973,000 TEU, which is a increase of 15%. $\frac{A}{A_{TEU}}$ represents the number of containers that can be stored inside the terminal. The RTG stacks for import and export are 22 TEU long, 6 TEU wide and 5 TEU high. For the empty storage the length depends on the available area.

	empty	**import**	**export**
$\frac{A}{A_{TEU}}$ [TEU]	18,000	2,640	5,280
t_d [days]	10	3	3
$r_{st} * m_c$ [−]	0.6	0.6	0.6
N_c [TEU/yr]	**394,000**	**193,000**	**386,000**

Table D.10: Capacity and properties of the storage area for the improved terminal (Empresa Portuaria Talcahuano San Vicente, 2018).

Quay length

To check if there is still enough quay length the calculation that is done in D.1.3 is repeated with some changed numbers. This is done for the year 2022 and for two different scenarios. In the first scenario the vessel growth is equal and in the second there is only growth of the large vessels. The crane capacity per berth is set to 85 $moves/hr$, which means the planned purchase of gantry cranes is incorporated. The STS are necessary to fulfil the requirement of a maximum 10% waiting time. The changed numbers and the required berth length are shown in table D.11. It can be observed that a 940 m quay is long enough. The capacity of the quay increases, as can be seen in table D.12, due to improved crane productivity.

	Equal vessel growth	**Only growth of large vessels**
$P \times N_{cb}$ [moves/hr]	85	85
C [TEU/yr]	973,200	973,200
N_{sy} [vessels/yr]	284	252
c_c [Containers/vessel]	1845	2076
u [−]	0.22	0.22
n [−]	2	2
L_s [TEU]	262	282
$Waiting time$ [%]	**3.8**	**3.8**
L_s [m]	**624**	**668**

Table D.11: Changed properties, maximum vessel waiting time and required berth length for the improved terminal (Empresa Portuaria Talcahuano San Vicente, 2018).

	Improved
$P \times N_{cb}$ [moves/hr]	85
m_b [%]	50
N_b [−]	2
f_{TEU} [−]	1.86
n_{hy} [hr]	8760
c_{ab} [TEU/yr]	1,385,000

Table D.12: Properties and capacity of the improved quay.

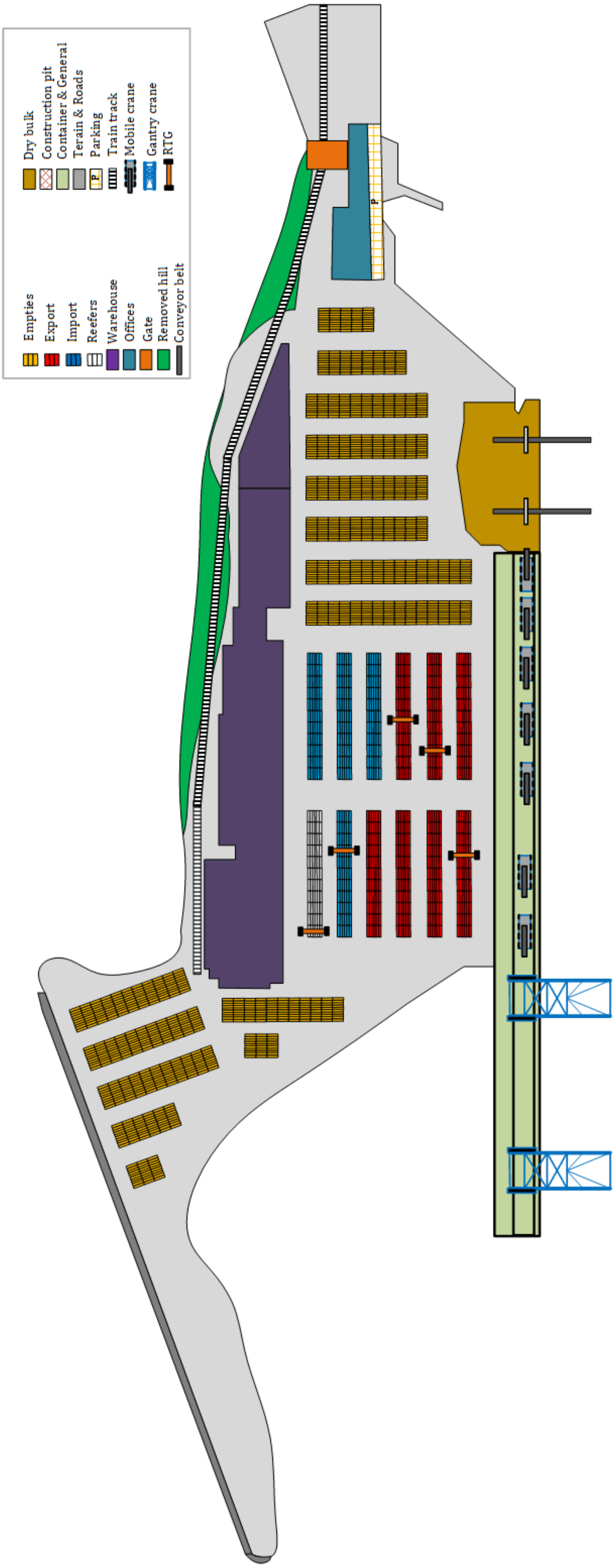

Figure D.15: New layout San Vicente Port

(This page is intentionally left blank)

E

Expansion options

Figure E.1: Possible site for terminal expansion. The water basin can be filled up to create extra land.

Source: Own photo (29 September 2018)

In this appendix, plans for future expansions are elaborated. Inland extensions are not possible, because San Vicente Port is surrounded by the Talcahuano city and the local fishery port. An offshore expansion is investigated. It should be flexible to anticipate on future changes: adaptive port design should be incorporated in the design procedure.

E.1. Scenarios

Figure E.2 shows the predicted container throughput in Twenty Foot Equivalent Units (TEUs) for San Vicente Port, according to two scenarios: (1) San Vicente Port preserves a market share of 40% of the total throughput of the Biobío region, and (2) San Vicente Port grows to a market share of 70% in the region. This is an optimistic scenario.

In addition, two scenarios regarding the distribution of vessels are defined: (1) the distribution of vessel lengths does not change for container vessels. All growth of San Vicente Port is equally distributed over container vessels of all lengths. And (2) there is a shift to larger vessels. All growth of San Vicente Port is the result of a growth in numbers of Panamax and New Panamax vessels.

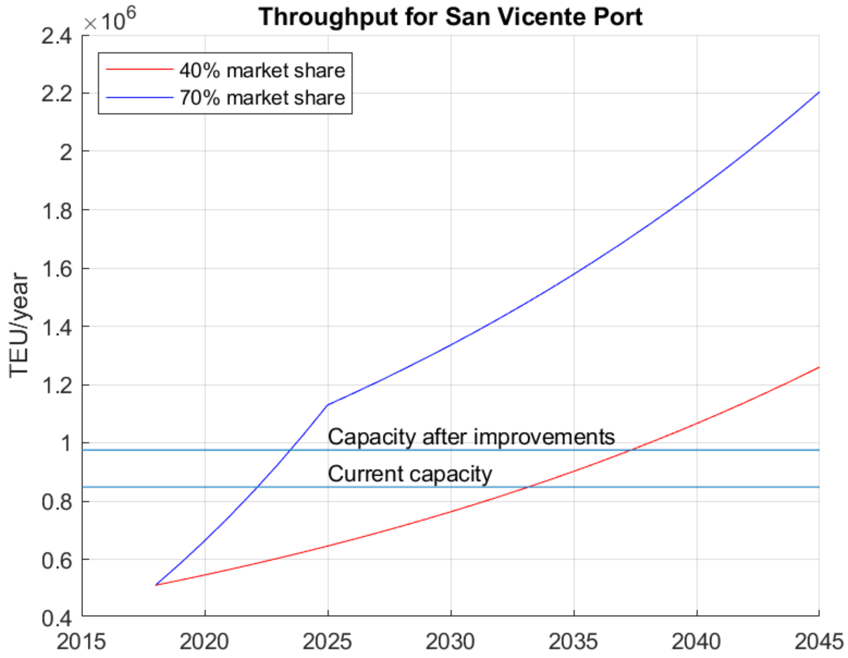

Figure E.2: Expected container throughput (in $TEU/year$) for the 40% and the 70% scenario.

E.2. The need of an expansion

The current capacity of the terminal is 848,000 TEU. The storage capacity is normative for the capacity, see table E.1. For the 40% scenario, this will be reached in 2035 and for the 70% scenario this will be in 2022. Then, measures to improve the capacity of the terminal are needed. With the improvements presented in appendix B.1.3 the capacity of the storage can be increased to 973,000 TEU. Quay capacity can be increased by installing Ship-to-Shore (STS) cranes. With these improvements the need for a port expansion can be postponed to the year 2040 for the 40% scenario and 2023 for the 70% scenario. If the throughput of the San Vicente Port develops according to the optimistic scenario, an expansion of the storage area is thus needed within 5 years. The terminal expansion for this scenario will be investigated in this appendix. The same expansion plans can be used for the 40% scenario, but the timeline and the cost calculations will be different.

	Capacity [TEU/yr]
Access road	6,083,000
Gate	1,477,000
Storage area	**848,000**
Quay	1,075,000

Table E.1: The capacity of the different terminal components.

E.3. Expansion options

Possible locations for an offshore expansion are (1) between the breakwater and the current terminal, and (2) on the outside of the breakwater. Only terminal expansions between the breakwater and the current terminal are investigated. This location seems most logical, for its proximity to the quay and the current storage yard.

Three expansion options are discussed in this report, see figure E.4. The proposed offshore expansion will create 13 ha of extra storage area. An option (C) would be to fill this area at once. In terms of flexibility and risk this is not a preferred option. Therefore, also more flexible options (A & B) are investigated with a phased development that can be adapted to changing market conditions.

Storage yard

Option A consists of two phases as shown in figure E.4a and E.4b. The first phase is to fill an area of 4 ha and in the second phase the remaining 9 ha is filled. Option B, which can be seen in figure E.4c and E.4d, also consists of two phases. Here the first phase is an expansion of 7 ha and in the second phase the remaining 6 ha is filled. The third option, option C, is to fill the water area at once, this can be seen in figure E.4e. Table E.2 gives an overview of the reclaimed land for the different options and phases.

	Phase 1	**Phase 2**
option A	4 ha	9 ha
option B	7 ha	6 ha
option C	13 ha	-

Table E.2: Reclaimed land area for the different options and phases

E.3.1. Berths

When the storage capacity increases, quay capacity might become normative. The different expansion options also provide space for a quay expansion. The possible quay locations for the different expansion interventions are discussed below. Also, the nautical conditions at the new quays are discussed according to the method discussed in appendix C.2.

Option A, phase 1

The first phase of option A is an expansion of 4 ha near the breakwater. Along this reclaimed land, parallel to the original quay, a 520 m long quay can be constructed. A 160 m margin between this quay and berth 5 is used. This is sufficient to moor vessels on both sides (PIANC, 2014a). The expansion is far from the original quay, which is bad for accessibility.

Between the new quay and berth 5 a basin is created, but because of the open structure of the quay no resonance will occur. Waves will be transmitted through the pile structure. As indicated in figure E.3 the waves will refract into the basin parallel to the new quay. In this situation, heave will be the governing vessel motion. Because the vessel is not attacked by perpendicular waves, rolling will be negligible. Its assumed that the wave conditions in front of berth 4 will not change. However no detailed simulations are preformed, to verify this assumption.

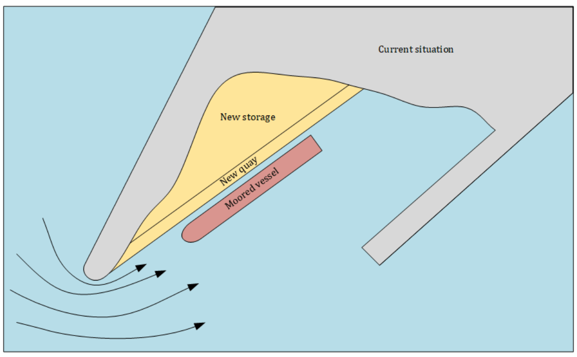

Figure E.3: Expansion option A, phase 1

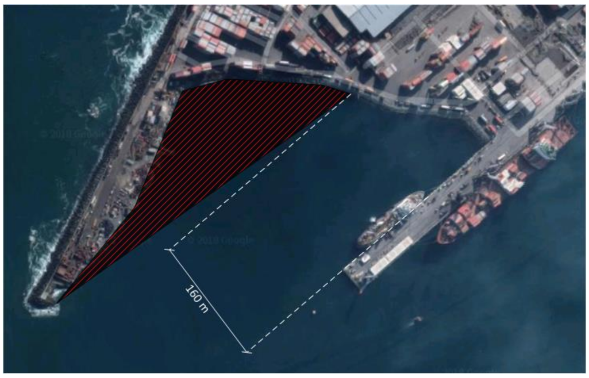

(a) option A, phase 1

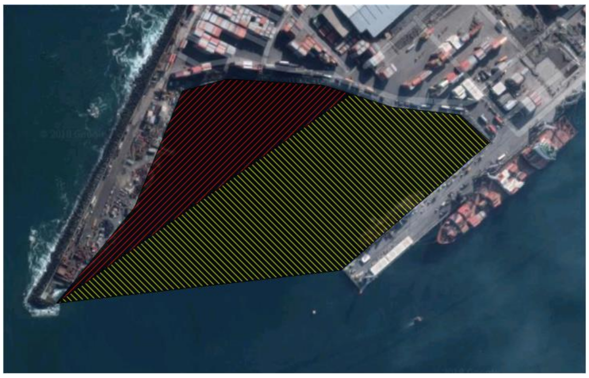

(b) option A, phase 2

(c) option B, phase 1

(d) option B, phase 2

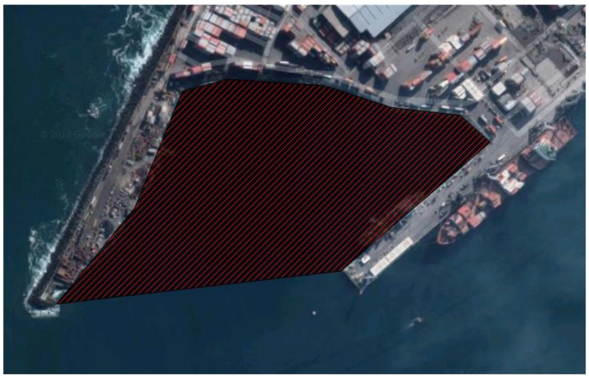

(e) option C

Figure E.4: Reclaimed land for different options and phases. Shaded red means phase 1, shaded yellow means phase 2.

Option B, phase 1

The first phase of option A is an expansion of 7 *ha* near the terminal, see figure E.5. Berth 5 is removed, but a new quay (300 *m*) can be constructed on the new water side, which is perpendicular to the original quay. This is ideal for terminal operations.

Figure E.5 shows that how waves will curve around the breakwater tip and arrive at the vessel perpendicularly. Therefore, the assumption that rolling can be neglected does not hold. It is expected that the conditions in front of berth 4 will change because of the land reclamation. However, no detailed simulations are preformed.

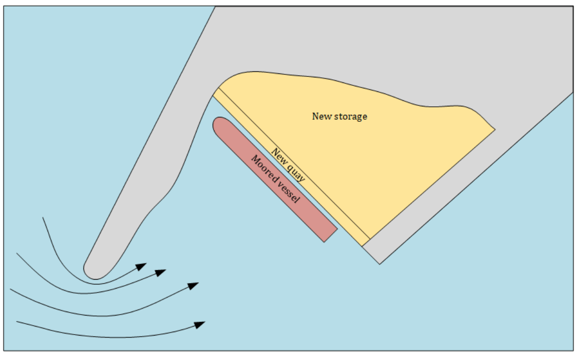

Figure E.5: Expansion option B, phase 1

For the first phases of option A and B, no simulations for vessel motions are preformed. This is because the vessel motion model that is used in appendix C is only applicable to heave motions. It is thus not possible to give an accurate comparison of the motions for these berth configurations. Based on the quay configurations, it is expected that the vessel motions in option A are smaller than in option B. For an exact understanding of vessel motions and (un)loading rates, the vessel motion model needs to be adapted in such a way that it can be applied to roll motions as well.

Option C; option A, phase 2; option B, phase 2

When the complete area between the breakwater and the terminal is reclaimed (13 ha), quay 5 is removed. A new quay can be constructed along the waterfront, with good accessibility to the storage (figure E.6).

The behaviour of the waves, refracting around the breakwater towards the new quay is shown in figure E.7. The waves refract around the breakwater tip and approach the quay with a slight angle. Because of this incident angle, both heave and roll are important. As mentioned earlier, the vessel motion model is only applicable to heave motions.

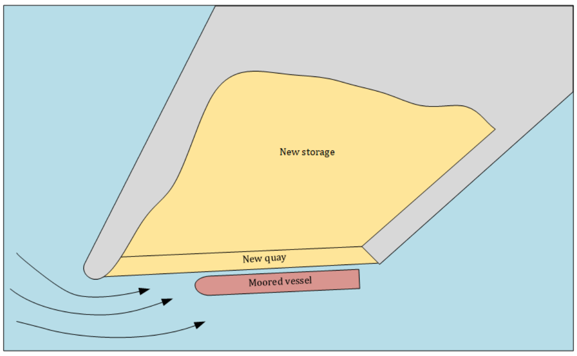

Figure E.6: Expansion option C; option A, phase 2 and option B, phase 2

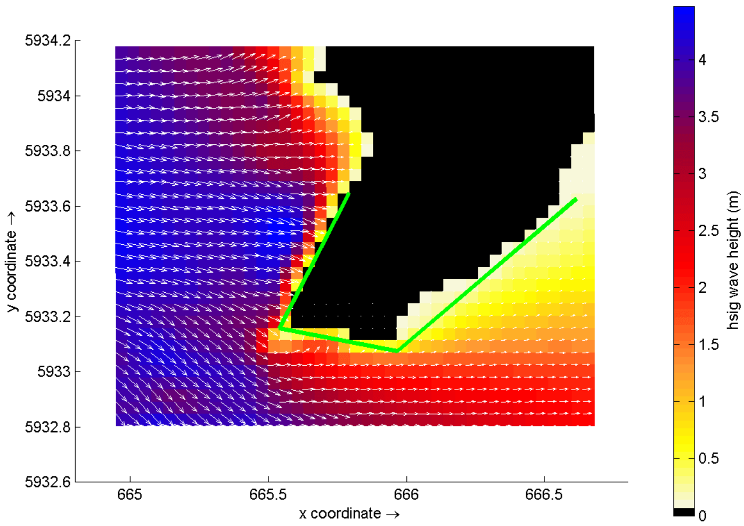

Figure E.7: Behaviour of waves around the breakwater tip for total land reclamation

The mooring conditions, based on **heave only**, are calculated to find the the (un)loading efficiency for each vessel class. These are presented in table E.3. For comparison, the heave motions the heave motions at berth 4 are given. It can be observed that the vessel motions at the new quay are much larger. Vessels here are much more exposed to the offshore waves, there is less sheltering from the breakwater. Please note that this calculation does not include the rolling motion, so the (un)loading efficiency will be lower than calculated. According to PIANC (2012), ports try to have efficient (un)loading 98% of the time. Based on table E.3 it can be concluded that the mooring criteria according to PIANC guidelines will not be reached.

Vessel type	**Heave criteria** [m]	**New quay** [%]	**Berth 4** [%]
I	0.4	99.36	99.97
II	0.4	95.71	99.68
III	0.4	86.58	98.78
IV	0.4	64.70	94.82
V	1.0	93.55	99.96
VI	0.4	39.03	83.37
VII_D	1.0	74.76	100.00
VII_G	1.0	74.76	100.00
VII_F	0.4	21.10	61.65

Table E.3: Percentage of time that there are optimal loading conditions (100% (un)loading efficiency), based on heave without a breakwater extension. Note: D = dry bulk, G = general cargo, F = Fishery

It can be concluded that the breakwater needs to be extended to have proper mooring conditions at a new quay in the year 2036 (if an extra berth is required). This is also the case for option A and B in phase 2. The breakwater extension research that is done in appendix C can be used for a first estimate of costs and effects on the wave climate.

E.4. Capacity

The capacity of the different terminal components is calculated with the new extensions. The capacity of the access road is not recalculated, because no interventions are done and the capacity was already sufficient, see table E.1. An overview of the results can be seen in table E.4. The capacity of the individual components is discussed below.

The capacity calculations are done using the equations from Ligteringen & Velsink (2012). These equations are used here, but for a detailed explanation reference is made to appendix D.

	Improved [TEU/yr]	**Option A** [TEU/yr]	**Option B** [TEU/yr]	**Option C** [TEU/yr]
Access road	6,083,000	6,083,000	6,083,000	6,083,000
Gate	1,477,000	1,477,000	1,477,000	1,847,000
Storage area	**973,000**	**1,152,000**	**1,284,000**	**1,552,000**
Quay	1,385,000	1,731,000	1,385,000	1,589,000

Table E.4: The capacity of the different terminal components for the starting points (improved layout) and the different expansion options.

Gate

Table E.4 shows that gate capacity is sufficient for expansion options A and B. For expansion option C, the capacity of the storage area has become larger than the gate capacity. The starting point is that gate capacity should never be normative for the capacity of the terminal. Increasing the gate capacity is thus essential.

Three solutions for increasing gate capacity are proposed: First, by changing the opening hours from 16 hr/day to 24 hr/day. This would increase gate capacity with 50%, but would imply that employees need to work at night. Second, by changing the maximum occupancy rate of the gate to 90% (currently 85%). This would have a negative impact on the waiting times for the gate. Last, by constructing an extra gate (five instead of four). This would increase the gate capacity with 25%.

The last solution (extra gate) is the preferred solution. There is already a fifth gate available, but it is not used at this moment. The gate capacity is calculated using equation (D.2) using the values in table E.5. The gate capacity is increased to 1,847,000 TEU/yr.

T_s [hr]	0.025
m_g [%]	85
n_{gate} [−]	5
f_{TEU} [−]	1.86
t_{hr} [hr]	16
N_g [TEU/yr]	**1,847,000**

Table E.5: Properties and capacity of the gate for expansion option C. Compared to the existing situation a fifth gate is used.

Storage

The reclaimed area is used for the storage of containers and warehouses. As an assumption, the division of space for roads, container storage and warehouses is kept the same.

The capacity of the storage yard is calculated with equation (D.3). Table E.6 shows the properties of the different expansion options and the capacities of the different types of containers. The storage capacity for each option is:

Option A:	1,152,000 TEU	(+18.4%)
Option B:	1,284,000 TEU	(+32.0%)
Option C:	1,552,000 TEU	(+59.5$)

	expansion option	**empty**	**import**	**export**
A [m^2]	A	14,400	3,200	6,400
A [m^2]	B	25,200	5,600	11,200
A [m^2]	C	46,800	10,400	20,800
$\overline{t_d}$ [days]	A,B,C	10	3	3
A_{TEU} [m^2/TEU]	A,B,C	4.11	6.9	6.9
$r_{st} * m_c$ [−]	A,B,C	0.6	0.6	0.6
N_c [TEU/yr]	A	**77,000**	**34,000**	**68,000**
N_c [TEU/yr]	B	**134,000**	**59,000**	**118,500**
N_c [TEU/yr]	C	**249,000**	**110,000**	**220,000**

Table E.6: Properties and capacity of the storage in the terminal depending on the expansion options. The density of empty containers depends on the location, there are two stackings with different density.

Quay

The quay capacity for the expansions is recalculated using equation (D.4). Expansion options A and B assume a crane capacity per berth of 85 $moves/hr$. For expansion option C, there are more STS cranes per berth to decrease the service time. This way long waiting times can be avoided. A crane capacity per berth of 97.5 $moves/hr$ is assumed.

According to PIANC (2014b) a maximum berth occupancy of 50% is acceptable. Berth 5 is no longer available in expansion options B and C, so the number of berths is reduced here. The values for the calculation and the results can be seen in table E.5.

	Option A	**Option B**	**Option C**
$P \times N_{cb}$ [moves/hr]	85	85	97.5
m_b [%]	50	50	50
N_b [−]	2.5	2	2
f_{TEU} [−]	1.86	1.86	1.86
n_{hy} [hr]	8760	8760	8760
c_{ab} [TEU/yr]	1,731,000	1,385,000	1,589,000

Table E.7: Properties and capacity of the quay in the terminal.

To check if the waiting times for the expansion options are still within limits, the calculation from section D.1.3 is repeated. The values for this calculation are shown in table E.8 for each vessel distribution scenario. The waiting times are calculated for the maximum capacity of the terminal. It can be observed that the waiting times (in units of service times) are below 10%, which is still considered acceptable (Ligteringen & Velsink, 2012). If the port authority wants to offer a higher service level, it is essential to decrease the waiting times. This means that an extra berth should be constructed. Section E.3.1 shows where extra berths can be located.

Table E.8 also gives the required length of the quay. The available length of the quay is 704 m (berth 5 is removed), so the available quay length is larger than the required quay length for all situations. Thee calculation is based on the average vessel length. Problems can occur for a situation two larger than average vessels will berth at the same time. However, this happens in the current layout as well. Now, these problems are solved with overlapping mooring lines and connecting some lines to a bouy. This can also be done for the expansion options.

	$\mathbf{A_I}$	$\mathbf{A_{II}}$	$\mathbf{B_I}$	$\mathbf{B_{II}}$	$\mathbf{C_I}$	$\mathbf{C_{II}}$
$P \times N_{cb}$ [moves/hr]	85	85	85	85	97.5	97.5
C [TEU/yr]	1,152,000	1,152,000	1,284,000	1,284,000	1,552,000	1,552,000
N_{sy} [vessels/yr]	336	287	374	312	453	365
c_c [Containers/vessel]	1845	2158	1845	2213	1845	2286
u [−]	0.26	0.26	0.292	0.29	0.31	0.30
n [−]	2	2	2	2	2	2
L_s [m]	262	288	262	291	262	295
Waiting time [%]	**5.6**	**5.6**	**7.4**	**7.4**	**8.6**	**8.0**
L_q [m]	**624**	**681**	**624**	**688**	**624**	**697**

Table E.8: The waiting time and required quay length for the expansion options. The waiting times are calculated when the terminal operates at full capacity: for option A (phase 1) this is in 2027, for option B (phase 1) this is in 2030 and for option C this is in 2036. The subscript I is used for the scenario of equal vessel growth. The subscript II is used for the scenario of only growth of large vessels.

E.5. Timeline

As described in E.2 a terminal expansion is needed in 2023 for the optimistic 70% market share scenario. This means that the first phase of expansion options A and B needs to be ready in 2023. The second phase of option A should be finished in 2027 and the second phase of option B in 2030. For the option C case, the entire area needs to be ready in 2023. An overview of the building timeline is shown in figure E.8. These years are based on the market development according to figure E.2.

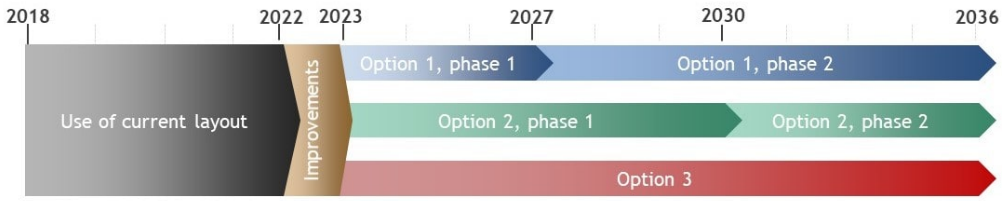

Figure E.8: Building time line for the 70% market share scenario

E.6. Costs of the expansion options

E.6.1. Unit costs

A list of basic cost for the terminal expansion can be founded in table E.9. The costs for land filling are mainly the filling material cost which are needed to fill the areas. The surface finishing costs are for concrete slabs as pavement for the terminal. **Please note, the costs of new equipment are not taken into account for the cost calculation.**

Activities	**Unit costs** [€]
Land filling	$5.00/m^3$
Mobilisation of equipment	$3.00M/times$
Surface finishing	$100/m^2$
Cost for improvements	$5.00M$

Table E.9: List of basic costs for terminal expansion

E.6.2. Quantities

The filling volume and surfaces per expansions option and phase are presented in table E.10. Moreover, the cost for the expansion options are shown in this table.

	option A		**option B**		**option C**
	Phase 1	Phase 2	Phase 1	Phase 2	
Quantities					
Filling volume $[m^3]$	1,200,000	850,000	1,400,000	650,000	2,050,000
Surface $[m^2]$	40,000	90,000	70,000	60,000	130,000
Costs					
Filling costs [M€]	6.00	4.25	7.00	3.25	10.25
Surface finishing costs [M€]	4.00	9.00	7.00	6.00	13.00
Mobilisations costs [M€]	3.00	3.00	3.00	3.00	3.00
Total costs [M€]	13.00	16.25	17.00	12.25	26.25

Table E.10: Quantities and cost for terminal expansions

E.6.3. Cash flow for expansion options

the discounted cash flow for the 3 expansions options is presented in figure E.9. The investment year for the expansions is one year before the required year mentioned in the building timeline of section E.5.

The yearly income presented in the cash flow is based on the throughput after execution of the improvement plan and the terminal expansions. The income can be calculated with:

$$INCOME = (TEU_{scenario.j} - TEU_{orignal}) \times f_{teu} \tag{E.1}$$

In which:

$INCOME$	=	Expected yearly income	[€]
$TEU_{scenario.j}$	=	Expected throughput according to scenario j	[TEU]
$TEU_{orignal}$	=	Capacity of the origal port layout	[TEU]
f_{teu}	=	income per TEU	[€/TEU]

For the discounted cash flow the following values are used:

- Interest rate: 4%
- Inflation rate: 2%
- Income per TEU: €10.- (Michou, 2017)
- Real costs for the improvement plan: €5,000,000.-

The Present Value of the expenditures, Net Present Value (NPV) and the Benifit Cost Ratio (BCR) of the cash flows are presented in table E.11:

	$\mathbf{PV_{exp}}$ [M€]	**NPV** [M€]	**BCR** [−]
option A	24.7	23.9	1.97
option B	24.1	24.5	2.02
option C	25.0	23.6	1.95

Table E.11: PV_{exp}, NPV and BCR of the terminal expansion options

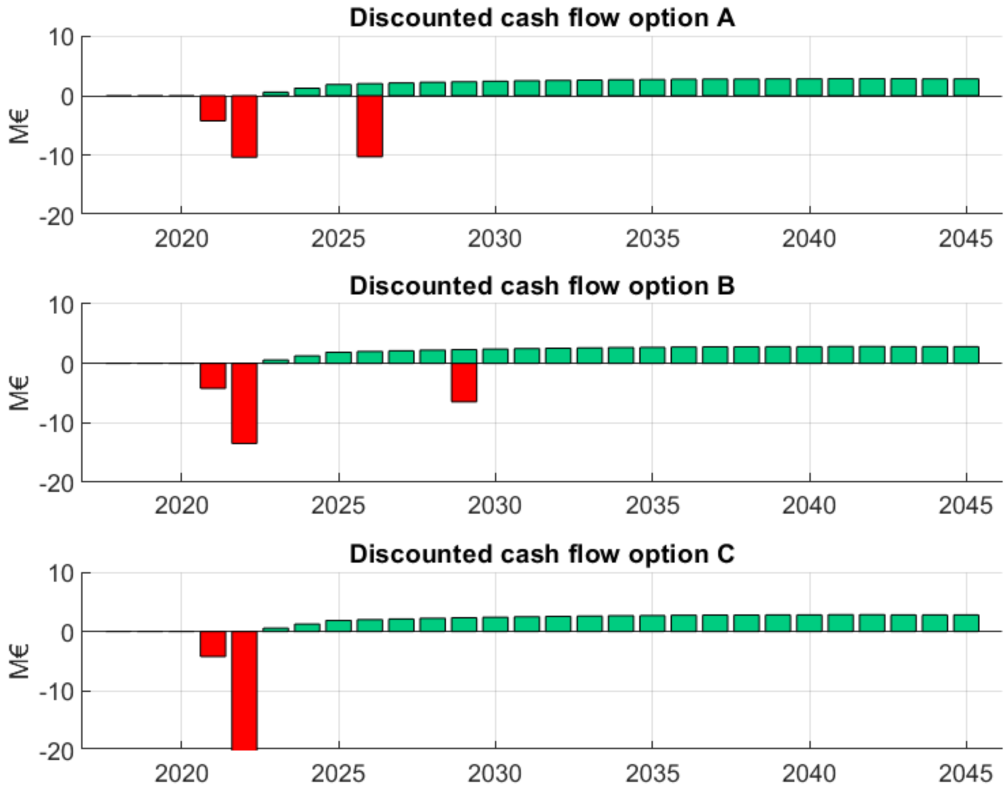

Figure E.9: Discounted cash flow for the 70% market share scenario for the three expansions options.

E.7. Multicriteria Analysis

A Multicriteria Analysis (MCA) is used to evaluate the three expansions options. First the criteria are determined. Then, the weight factor of the criteria is reasoned, followed by the determination of the value for each expansion option (Hertogh & Bosch-Rekveldt, 2015). A decision is made based on the MCA score and the costs.

E.7.1. Criteria

The following criteria are used in this MCA:

1. Berth changes:
   Berths are needed to (un)load vessels. The proposed expansion options (B and C) make usage of berth 5 impossible. Also, the expansion options offer the possibility to construct new berths.

2. Flexibility:
   It is not possible to predict the future and therefore it is important for terminals that they can implement adaption. Flexible port designs allow the port to adapt to changing conditions(Taneja, 2017).

3. Nautical conditions:
   Nautical conditions are important for the efficiency of the terminal. Offshore expansions can have an influence on the nautical conditions and therefore on the efficiency of the terminal.

4. Storage capacity (in phase 1):
   Although all studied expansions will ultimately have the same storage capacity, the storage capacity after phase 1 is different. A larger expansion in phase 1 mean more storage, but also more risk.

5. Traffic flow:
   Expansions change the location of container storage inside the port. This will change the traffic flow through the terminal. It is important that the quay are good reachable.

E.7.2. Weight factor

The criteria are compared in order to determine the weight factor. The results are summarised in table E.12. All criteria are compared in the following list:

- Berth changes vs Flexibility:
  Flexibility is more important than the berth changes. This is because berth changes will not have a large influence on the terminal operation. Flexibility makes it possible to have a large influence on the terminal operation depending on how the terminal is doing.
- Berth changes vs Nautical conditions:
  Berth changes is more important than the nautical conditions. Without the presents of berths it is impossible to (un)load vessels. Worse nautical conditions will make it difficult to moor and (un)load but this is still possible, it will only be slower.
- Berth changes vs Storage in phase 1:
  Storage in phase 1 is more important than the berth changes. This is because now already the storage is very dense which makes containers not good reachable and storage is running to the maximum capacity. Berths are no problem now and in the future.
- Berth changes vs Traffic flow:
  Traffic flow is more important than the berth changes. At this moment there are no problems with the berths, even if one berth would get lost this is not a big problem. On the other hand is traffic flow now already a problem in the port and it is possible that this problem will become bigger if the terminal gets even busier.
- Flexibility vs Nautical conditions:
  Flexibility is more important than the nautical conditions. The efficiency can be improved with better nautical conditions but it depends on the future if this is a requirement for the terminal. Flexibility is a powerful tool for a port to be sure of a bright future and so this is more important.
- Flexibility vs Storage in phase 1:
  Flexibility is more important than the storage in phase 1. Which scenario will come true is now unknown. Maybe it will be very good and a lot of storage is needed? But it is also possible that no extra storage is needed. Therefor flexibility is more important than storage in phase 1.
- Flexibility vs Traffic flow:
  Flexibility is more important than the traffic flow. Because the future is unknown it is important that a terminal can adapt. If thing go bad there will never be traffic problems. And if thing go good there will be extra money to spend to solve problems like bad traffic flow. Nevertheless the port must be flexible first.
- Nautical conditions vs Storage in phase 1:
  Storage in phase 1 is more important than the nautical conditions. If there is no storage for the containers it does not matter how good or bad the nautical conditions are. So first storage is needed and when this is present than one can think about efficiency.
- Nautical conditions vs Traffic flow:
  Traffic flow is more important than the nautical conditions. Both influence the efficiency of the terminal. If the nautical conditions are bad mooring will be difficult and (un)loading will take more time. But (un)loading of a container is only possible, even with bad nautical conditions, when a truck is present at the quay. Therefore it is more important that there are no traffic delays for the trucks inside the port than that the nautical conditions are perfect.
- Storage in phase 1 vs Traffic flow:
  Traffic flow is more important than the storage in phase 1. This is because a bad traffic flow influences the efficiency of the port and efficiency is important for the clients. Without clients extra storage is not needed at all.

The scores are entered in table E.12. The total score for criterion C Nautical conditions is 0. Because a 0 is not possible as a result, and every criteria has some value, all values are doubled and the 0 is changed to a 1. To get the weight factor of the criteria all number are divided by the total score for all criteria.

Criteria	**A**	**B**	**C**	**D**	**E**	**Total**	**Compensation**	**Weight factor** [%]
A Berth changes	x	0	1	0	0	1	2	9.5
B Flexibility	1	x	1	1	1	4	8	38.0
C Nautical conditions	0	0	x	0	0	0	1	4.8
D Storage in phase 1	1	0	1	x	0	2	4	19.0
E Traffic flow	1	0	1	1	x	3	6	28.5

Table E.12: Summary of the weight factor determination. X in the table means that the criteria cannot be compared. 1 means that the row criterion is more important then the column criterion. 0 means the opposite. The factors are summed to get the total score per criterion.

E.7.3. Grading

All options are evaluated for the given criteria and graded a score of 1-5. An explanation of the grading is given below:

1. Berth changes:
   (a) Option A: 5
   This option will generate extra berths possibilities. Besides all existing berths can stay.
   (b) Option B: 2
   With this option berth 5 will be removed. A new berth is possible but it will not be possible to store large ships because the quay length will be less than 320 m.
   (c) Option C: 3
   Just as for option B berth 5 will also be removed. Again it is possible to create a new berth but this time the length of the berth can be long enough, more than 400 m, for the largest ships that are mooring in San Vicente Port.
2. Flexibility:
   (a) Option A: 4
   The extension will be constructed in two phases if this option is chosen. This means the port is flexible to change plans if needed.
   (b) Option B: 3
   Two phases will construct the entire extension so it is possible to change plans halfway. The score is one point lower than option A because there are less options for berths and the area which is constructed in the first phase is larger, which means a larger investment in the beginning.
   (c) Option C: 1
   This option is absolutely not flexible because the expansion will be constructed at once.
3. Nautical conditions:
   (a) Option A: 4
   The new possible berth will be behind the breakwater. This means a good sheltered area for (un)loading of the vessels.
   (b) Option B: 3
   Also this option is behind the breakwater. The score is a point lower than option A because for a few wave directions it is possible to reach the back of the vessel.
   (c) Option C: 1
   The area behind the breakwater is completely filled so a moored vessel at the possible new berth location will be hit hard by waves.
4. Storage in phase 1:

   (a) Option A: 2
   The extension in the first phase is not so large but each ha means extra storage.
   (b) Option B: 3
   About half the extension will be constructed in phase 1. This means enough for the first years.
   (c) Option C: 5
   The full area in once means directly a lot of extra storage.

5. Traffic flow:
   (a) Option A: 1
   The existing quays are not good connected. There will be only one tight passage and it is pretty far from the quay.
   (b) Option B: 4
   Directly behind the most used berths means that the storage is good accessible. Also the existing area will be more squared which is good for an efficient traffic flow.
   (c) Option C: 4
   The same story hold as for option B, directly behind the most used berths and the possibility to use large square stacks. This extension creates possibilities for a nice traffic flow.

An overview of the grades is shown in table E.13. The score is multiplied with the weight factor. The sum gives the score per expansion option.

Criteria	**Weight factor**	***option A***		***option B***		***option C***	
	WF [%]	Score	WF × Score	Score	WF × Score	Score	WF × Score
A Berth changes	9.5	5	0.48	2	0.19	3	0.29
B Flexibility	38.0	4	1.52	3	1.14	1	0.38
C Nautical conditions	4.8	4	0.19	3	0.14	1	0.05
D Storage in phase 1	19.0	2	0.38	3	0.57	5	0.95
E Traffic flow	28.5	1	0.29	4	1.14	4	1.14
Total score	-	-	**2.86**	-	**3.18**	-	**2.81**

Table E.13: Determination of the value per criteria

E.7.4. Decision

The best option of the MCA is the option with the best score to cost ratio. The score is divided by the present value of the expenses, as can be seen in table E.14. Option B has the highest score and is therefore the best option for expansion. Option B wins because is is flexible, has a good extra storage in phase 1 and good possibilities for traffic flow. Also, the present value is the lowest for this option.

	Score	**Present value**	**Multicriteria score**
option A	2.86	24.7	0.116
option B	3.18	24.1	**0.132**
option C	2.81	25	0.112

Table E.14: The multicriteria score for the different expansion options

E.8. Terminal layout

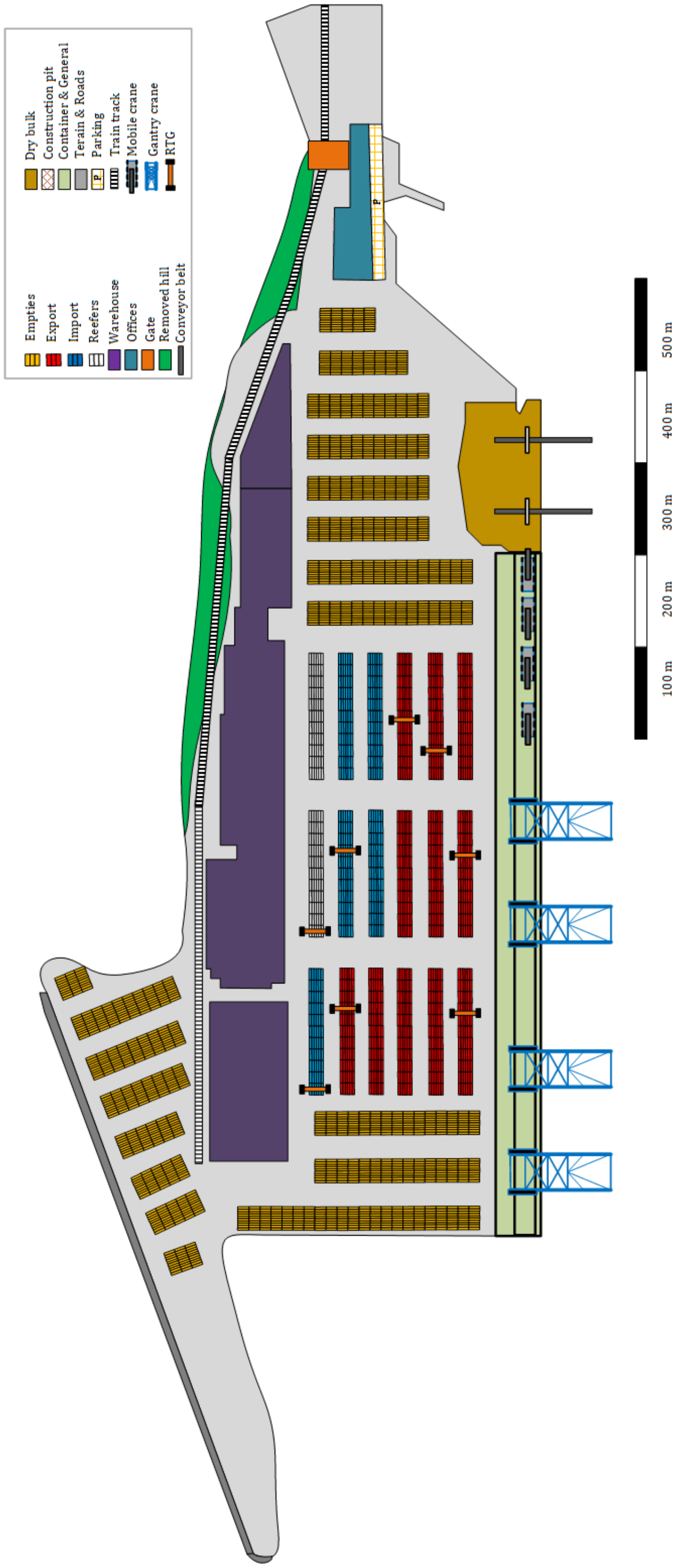

Figure E.10: Phase 1 of terminal expansion

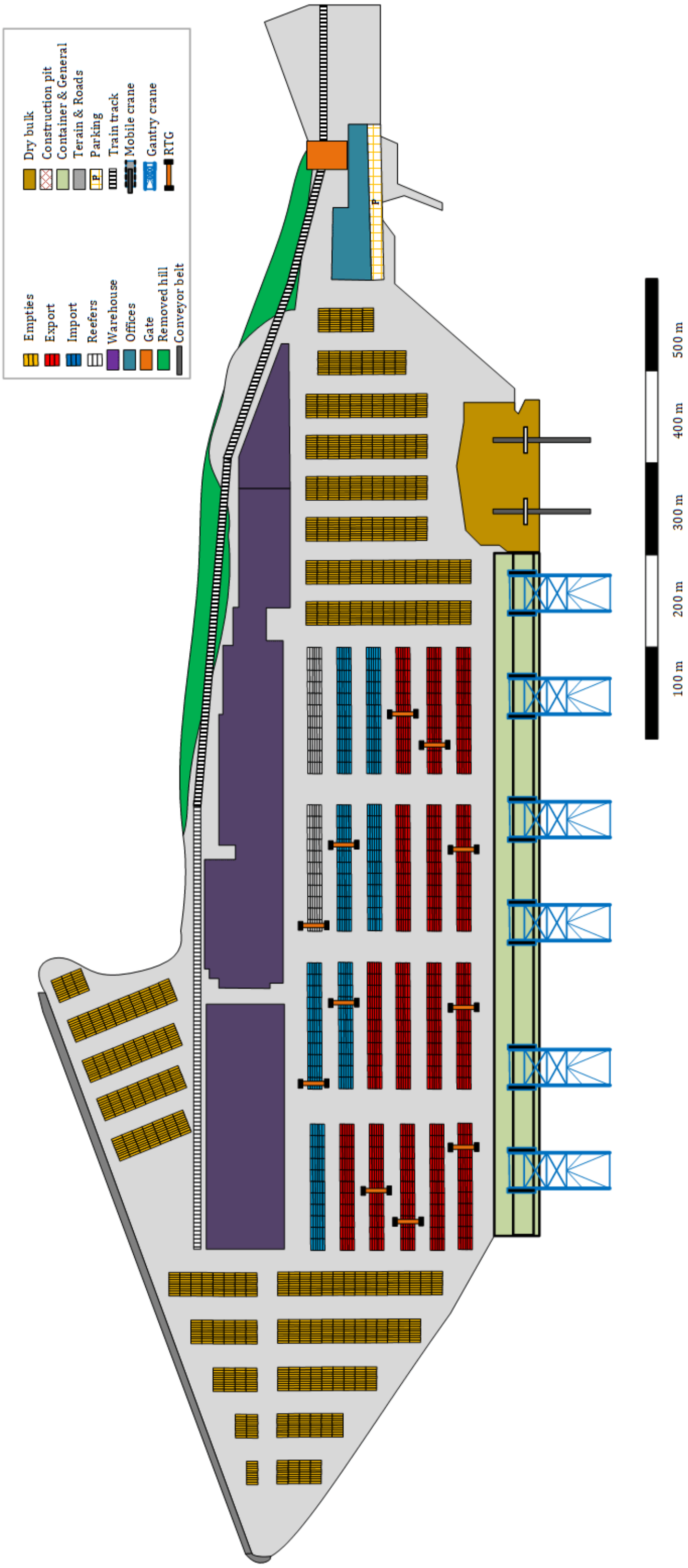

Figure E.11: Phase 2 of terminal expansion

(This page is intentionally left blank)

F

SIOP seminar 2018

Source: SIOP2018

The last three days of our stay in Chile, we were asked to present our results at the Seminario Internacional de Ingeniería y Operación Portuaria (SIOP) in Talcahuano. This symposium is a international three day port event (9 Nov. - 11 Nov. 2018) where researchers, port companies and the Dutch ambassador were present to share their knowledge and experience. After the SIOP, we had a meeting with the embassy of the Netherlands to have a small talk about our stay in Chile.

F.1. Seminario Internacional de Ingeniería y Operación Portuaria (SIOP)

We were present at the SIOP conference to present our research and to listen to other interesting speakers. Organisers of this seminar were among others: Empresa Portuaria Talcahuano San Vicente and Universidad Católica de la Santísima Concepción (UCSC). The following pictures give an overview of the seminar.

General introduction of the SIOP seminar.

Presentation by Jurgen Bartelink from the Regional Economy Envoy of the Embassy of the Kingdom of the Netherlands in Lima. This presentation was also given during the lectures of Ports and Waterways I by prof. em. Tiedo Vellinga.

Menno presenting our results at SIOP. Every speaker was given 15 minutes for their presentation.

General impression of the setting at SIOP. The main language at the seminar was Spanish. Even most international speakers gave their presentation in Spanish. Interpreters were present to translate everything to English.

Answering (Spanish) questions of the audience. The presentation was given in English.

F.2. Program of the SIOP

As mentioned before, the symposium took three days. During these three days, several topics where covered by different speakers. An overview of the schedule is given on the next pages.

PROGRAMA

MIÉRCOLES **7 NOVIEMBRE**

8.30 Horas Acreditación

9.00 Horas Apertura
•*Consuelo Raby*, Presidenta del Directorio de Puertos de Talcahuano
•*José Vargas*, Presidente SOCHID
•*Henry Campos*, Alcalde de Talcahuano
•*Harman Idema*, Embajador Países Bajos
•*Alexis Michea*, Coordinador General del Programa de Desarrollo Logístico, Ministerio de Transporte y Telecomunicaciones
•*Jorge Ulloa*, Intendente Región del Biobío

9.45 – 10.15 Horas
•Una experiencia de reconstrucción
Carlos Aránguiz, Gerente de Concesiones Puertos de Talcahuano

10.15 – 10.45 Horas CHARLA INTERNACIONAL
Maasvlakte 2: Hacia el puerto más sostenible del mundo
Jurgen Bartelink, enviado Regional para Asuntos Económicos de los Países Bajos.

10.45 – 11.15 Horas: Coffee break

11.15 Horas
•Desarrollo y Planificación Portuaria
Chairman: *José Vargas* (SOCHID)

11.20 – 11.40 Horas
•Auditoría de Capacidad del Sistema Portuario Nacional Mexicano
Pérez, G. (IDOM Consulting)

11.40 – 12.00 Horas
•Ventajas /.../ Puerto de Gran Escala central de Chile en la Bahía de San Antonio
Albornoz, J. F.

12.00 – 12.20 Horas
•Resumen Puerto de Bahía Blanca, Visión 2040
Gines, C., Weyland, F.

12.20 – 12.40 Horas
•Terminal Marítimo de Importación de Gas Natural Licuado Andes LNG
Rodríguez, C.

12.40 – 13.00 Horas
•San Vicente Terminal Internacional: Un socio estratégico que agrega valor
Junge, H.

13.00 – 14.30 Horas: Almuerzo

14.30 Horas
•LOGÍSTICAS PORTUARIAS
Chairman: *Rafael Aránguiz* (UCSC)

14.35 – 14.55 Horas
•Development of future expansion of San Vicente Harbour
Gribnau, K., Hemel, M., Kovoets, I., Onrust, M., (TU Delft)

14.55 – 15.15 Horas
•Política de asignación de espacio de almacenamiento para contenedores
Gaete, M., González, M., González, R., Astudillo, C.,

15.15 – 15.35 Horas
•Proyecto Sistema de Control Operativo Distribuido Integrado (DCS)
Monsalve, E., Navarro, M.

15.35 – 15.55 Horas
•Conectividad Portuaria de Chile en las Redes Logísticas Internacionales
Vega, A., Durán-San Martín, C.

15.55 – 16.30 Horas: Coffee break

16.30 Horas
•INGENIERÍA PORTURIA
Chairman: *Patricio Winckler* (UV)

16.35 – 16.55 Horas
•Solución Innovadora - Profundización de los Sitios 4 y 5 del Puerto de Arica
Repetto, A., Burgos, L.

16.55 – 17.15 Horas
•Implementación Sistema de Amarra Hidráulico: Shore Tensión
Allende, J., Dini, C.

17.15 – 17.35 Horas
•Desarrollo de un disipador de energía friccional /.../ defensa portuaria
Maureira , N., Villagrán, M., Sanzana, D., Friz, A., Arroyo, C.

17.35 – 17.55 Horas
•Análisis para la implementación de dispositivos shoreTensión
Rozas, C., García, R., Swiegers, P., Carrión B.

17.55 – 18.25 Horas CHARLA INTERNACIONAL
•Sistemas de predicción de variables oceanográficas para puertos en Nueva Zelanda
Peter McComb, Dr (MetOcean Solutions, Nueva Zelanda).

JUEVES **8 NOVIEMBRE**

SIOP Talcahuano 2018

9.00 Horas
•Ingeniería Portuaria
Chair: *Raúl Oberreuter* (ACHIPYC)
9.05 – 9.25 Horas
•Aplicación de un Análisis de Identificabilidad en un Modelo de Defensa Portuaria
Villagrán, M., Ramírez, R., Maureira, N., Muñoz E.

9.25 – 9.45 Horas
•Recomendaciones Prácticas para el Diseño de Muelles Flotantes
Troncoso, C., Salas, M., Cifuentes, C.

9.45 – 10.05 Horas
•Una Solución Innovadora para el Control de la Corrosión en Infraestructura Costera
Boré, G., Eliceiry, M.

10.05 – 10.25 Horas
•Ingeniería de tsunamis para aplicaciones portuarias, Algunos ejemplos
Winckler, P., Reyes, M., Sepúlveda, I., González, M.

10.25 – 10.55 Horas CHARLA INTERNACIONAL
•El rol del modelado físico en el desarrollo portuario
María Di Leo / HR Wallingford

10.55 – 11.30 Horas: Coffee Break

11.30 Horas
•Riesgos en zonas portuarias
Chairman: *Mauricio Villagrán* (UCSC)

11.35 – 11.55 Horas
•Detección de Tsunami a través del campo magnético local
Torres, C., Calisto, I., Figueroa, D.

11.55- 12.15 Horas
•Análisis de riesgo de daños en la maquinaria de un puerto frente a tsunami
Segovia, C.

12.15 – 12.35 Horas
•Simulación hidrodinámica de la deriva de contenedores en el puerto de Arica
Otárola, G., González, J., González, G., Zamorano, L.

12.35 – 12.55 Horas
•Propuesta Metodológica: Análisis de Riesgo en los puertos de Chile para la elaboración de estrategias de continuidad de negocios
Pedraza, P. A.

12.55 – 13.15 Horas
•Análisis y discusión del riesgo de tsunami en la zona urbana de las ciudades de Valparaíso y Viña del Mar
Reyes, M.

13.15 – 13.45 Horas CHARLA INTERNACIONAL
•Tsunamis por maremotos en Chile y el Pacífico, deslizamientos en Tierra Verde y volcanes submarinos en el laboratorio
Hermann Fritz / Georgia Tech

13.45 – 15.00 Horas: Almuerzo

15.00 Horas
•VISITAS TÉCNICAS*
•Puerto de Talcahuano y sector La Poza.
•Puerto de San Vicente

15.00 – 17.30 Horas
•TALLER INTERNACIONAL PORTS OF THE FUTURE*
El objetivo es generar conciencia y apoyo para el desarrollo portuario entre todos los grupos interesados. Abarca el desarrollo socioeconómico, los requisitos naturales y el impacto del diseño sostenible.
Jurgen Bartelink, enviado Regional para Asuntos Económicos de los Países Bajos.

* Taller y visitas técnicas, cupos limitados, con inscripción previa al correo: **organizadores@siop2018.cl**

SIOP Talcahuano 2018

VIERNES **9 NOVIEMBRE**

8.30 Horas
•Ingeniería Costera
Chairman: *Diego Moreno* (ACHIPYC)

8.35 – 8.55 Horas
•Desarrollo de un sistema de alerta de marejadas en la bahía de Valparaíso
Molina, M., Parra, C., Villalobos, D., Vargas, D. Y otros.

8.55 – 9.15 Horas
•Enfoque Bayesiano para la determinación de oleaje extremo
Carrión, B., Puelma A.

9.15 – 9.35 Horas
•Análisis y efecto de la atipicidad del evento de oleaje extremo de agosto 2015
Puelma, A., Carrión, B., Cuevas T.

9.35 – 9.55 Horas
•¿Es posible realizar pronóstico operacional de oleaje desde la escala global?
Lucero, F., Cienfuegos, R., Suárez, L. Y otros.

9.55 – 10.15 Horas
•Propuesta de una escala para categorizar el impacto de marejadas
Molina, M., Villalobos, D., Vargas, D. y otros

10.15 – 10.45 Horas CHARLA INTERNACIONAL
•Ondas largas y sus pronósticos para la actividad portuaria
Aitana Sánchez Forcén, Dr. /MetOcean Solutions, Nueva Zelanda

10.45 – 11.15 Horas Coffee Break

11.15 Horas
•Ciudades Puerto
Chairman: *Guacolda Vargas*, (Puertos de Talcahuano)
11.20 – 11.40 Horas
•Construcción Portuaria en San Antonio: Avanzando en comunicación con el entorno
Marcelo Guzmán, Gerente de Construcción (EPSA)

11.40 – 12.00 Horas
•Influencia del cambio climático en el diseño hipotético de una defensa costera
Mora, J., Winckler P.,

12.00 – 12.20 Horas
•Estudio integral del comportamiento de las playas de Viña del Mar
García, R., Carrión, B., Cuevas T.

12.20 – 12.40 Horas
•Metodología para la valorización multidimensional de la zona costera
Viveros, A., Reyes, M.,

12.40 – 13.10 Horas CHARLA INTERNACIONAL
•Desafíos para una industria portuario sostenible
Ricardo Sánchez (CEPAL)

13.10 Horas Clausura

Convoca:

Organizan:

Colaboran:

F.3. Presentation

The presentation that we gave on SIOP was focused on the improvement of nautical operations by a breakwater extension. The terminal operations and expansion plans where not discussed because they are based on confidential information given by the port authority of San Vicente Port. The presentation was executed by Menno Onrust. The presentation can be found on the next pages.

Nautical operations

Manoeuvring

- Downtime
- Limit: H_s= 1.5 m

Mooring

- (un)loading efficiency
- Limit: heave motion = 0.4 m

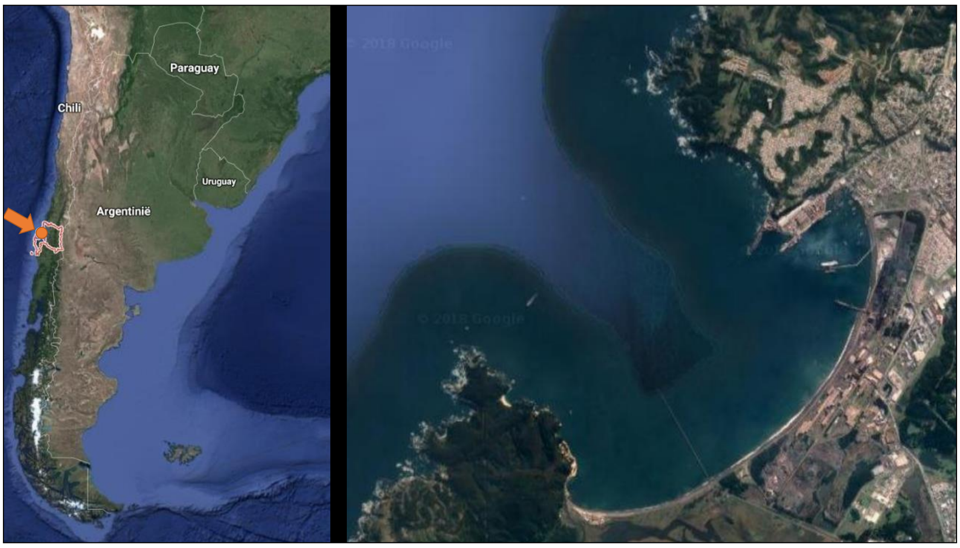

Methodology

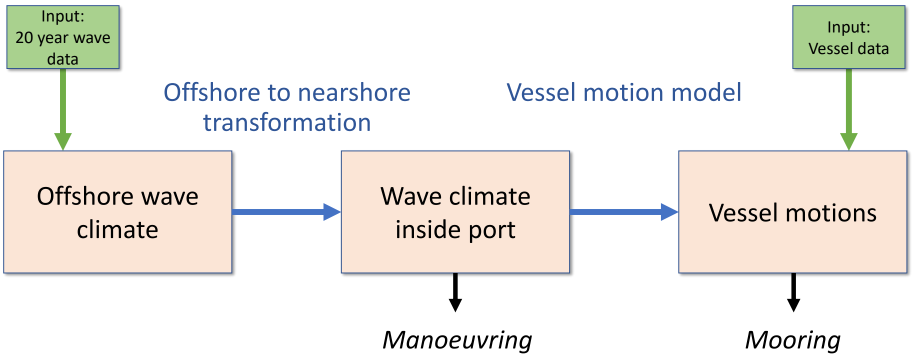

Offshore to nearshore transformation

- Numerical model: Delft3D
  - Quay and breakwater elements
  - Offshore bathymetry and bathymetry of San Vicente Bay
  - ‘Observation’-points for nearshore locations

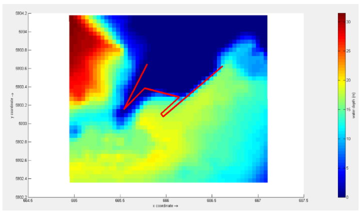

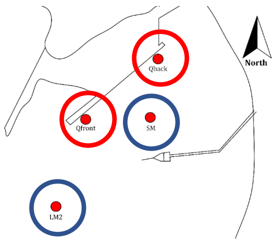

Offshore to nearshore transformation

1. **Wave grouping**
2. Delft3D simulations
3. Nearshore conditions
4. Interpolation
5. Nearshore wave climate

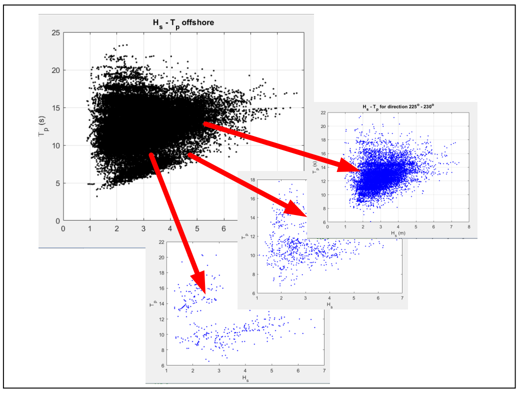

Offshore to nearshore transformation

1. Wave grouping
2. **Delft3D simulations**
3. Nearshore conditions
4. Interpolation
5. Nearshore wave climate

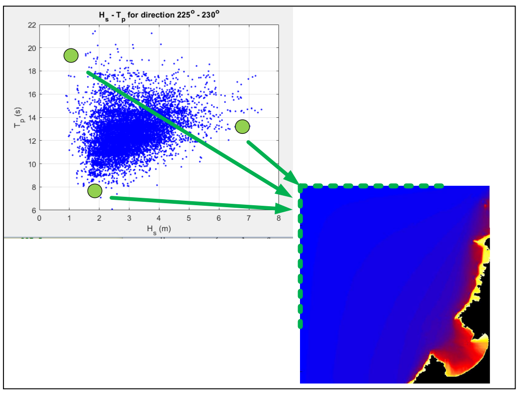

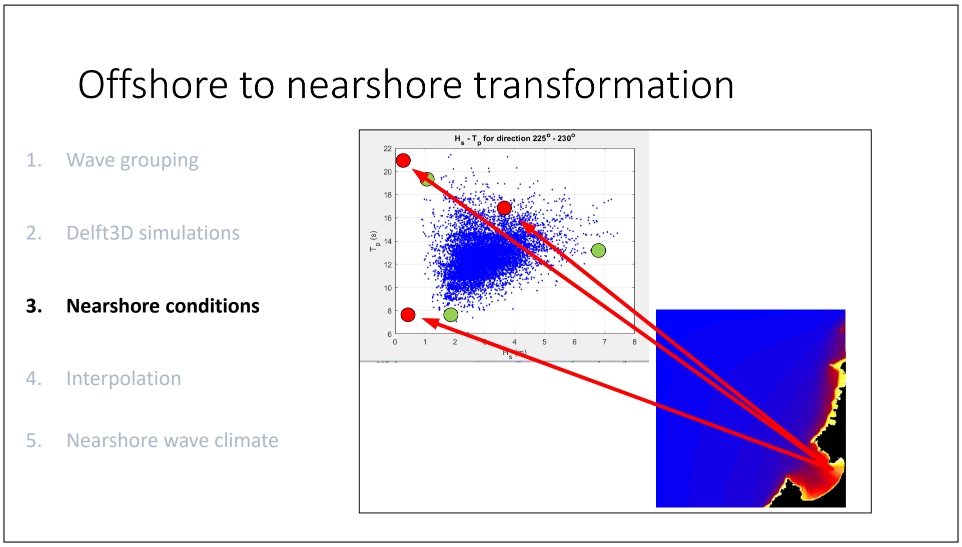
Offshore to nearshore transformation
1. Wave grouping
2. Delft3D simulations
3. Nearshore conditions
4. Interpolation
5. Nearshore wave climate
Hs - Tp for direction 225° - 230°

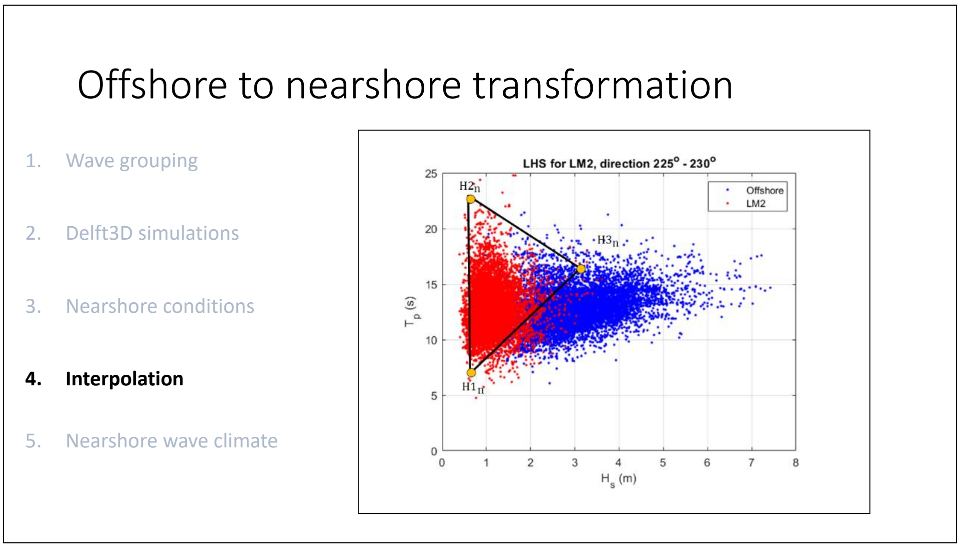
Offshore to nearshore transformation
1. Wave grouping
2. Delft3D simulations
3. Nearshore conditions
4. Interpolation
5. Nearshore wave climate
LHS for LM2, direction 225° - 230°
Offshore
LM2
H2n
H3n
H1n
Tp (s)
Hs (m)

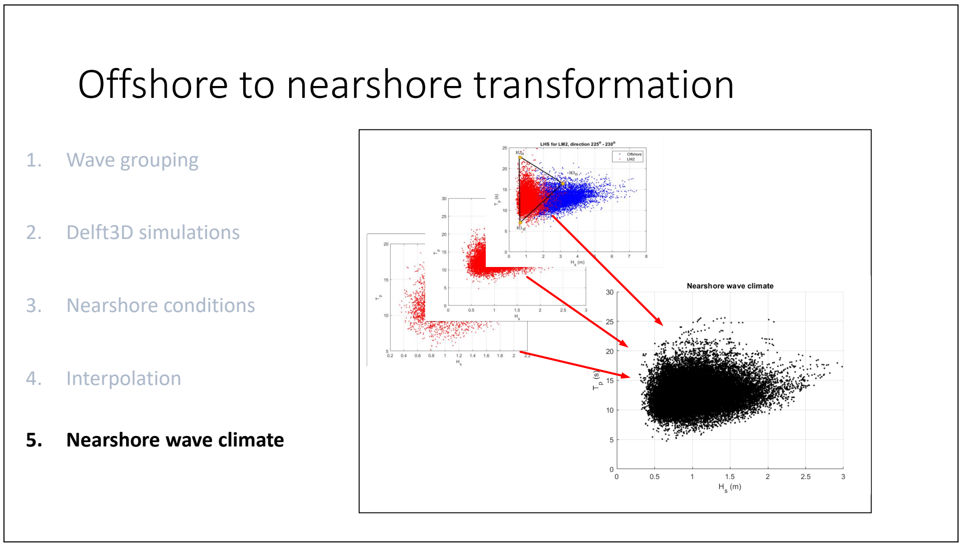
Offshore to nearshore transformation
1. Wave grouping
2. Delft3D simulations
3. Nearshore conditions
4. Interpolation
5. Nearshore wave climate
Nearshore wave climate
Hs (m)

Offshore to nearshore transformation

Result:
87% of the time possible manoeuvring conditions

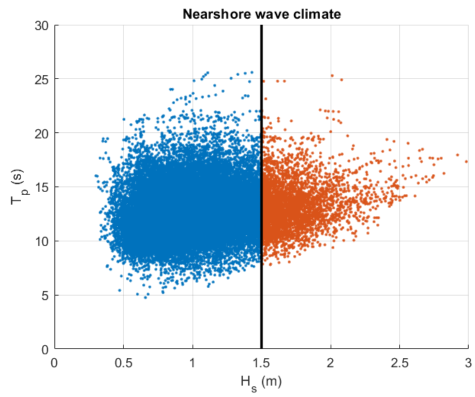

Vessel motion model

1. **Wave spectrum**
2. Response Amplitude Operator (RAO) and vessel grouping
3. Vessel motion spectrum
4. Heave oscilation

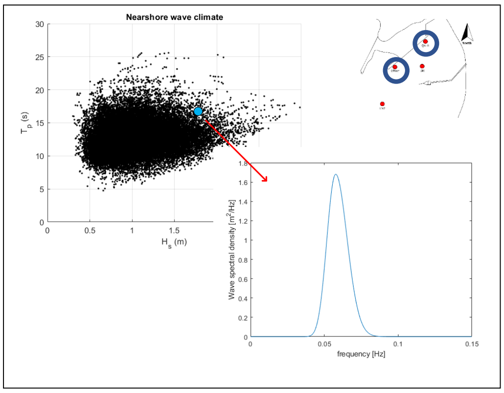

Vessel motion model

1. Wave spectrum
2. **Response Amplitude Operator (RAO) and vessel grouping**
3. Vessel motion spectrum
4. Heave oscilation

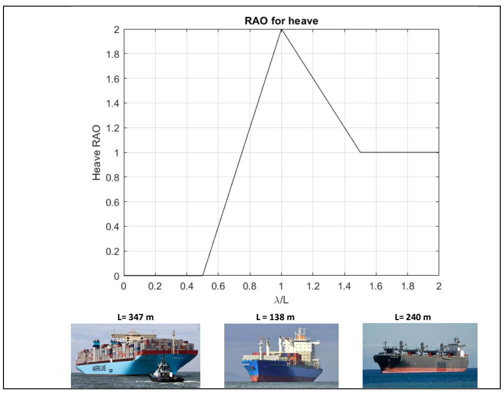

Vessel motion model

1. Wave spectrum
2. Response Amplitude Operator (RAO) and vessel grouping
3. **Vessel motion spectrum**
4. Heave oscilation

$$Wave\ spectrum\ \times RAO^2$$

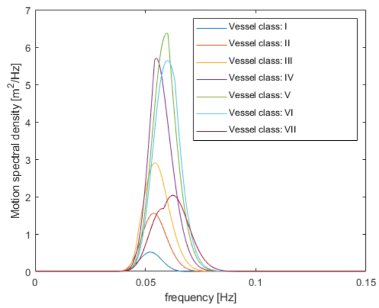

Vessel motion model

1. Wave spectrum
2. Response Amplitude Operator (RAO) and vessel grouping
3. Vessel motion spectrum
4. **Heave oscilation**

$$Heave\ = 4\,\sqrt{m_0}$$

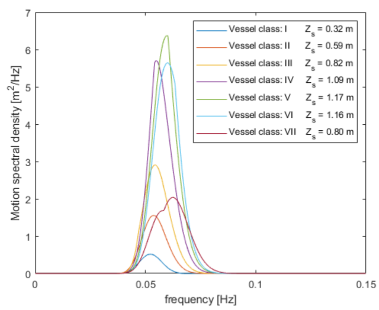

Vessel motion model

- Heave oscillation dataset per vessel (20 year)

Result:
95% of the time
optimal loading efficiency

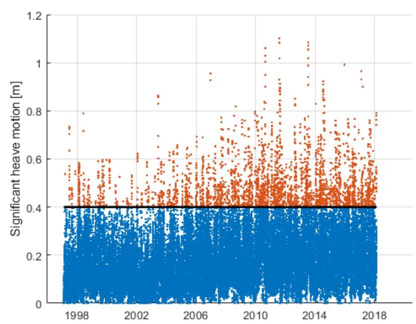

Breakwater extension

- Increase sheltered zone
- Decrease tug downtime
- Decrease vessel motion

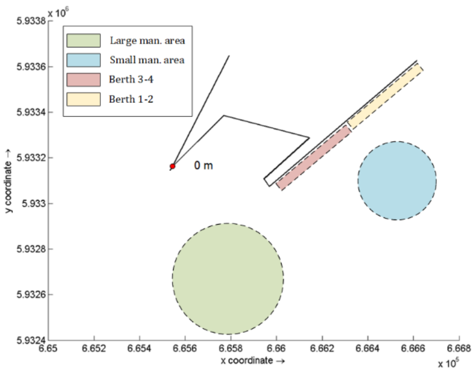

Breakwater extension

- Increase sheltered zone
- Decrease tug downtime
- Decrease vessel motion

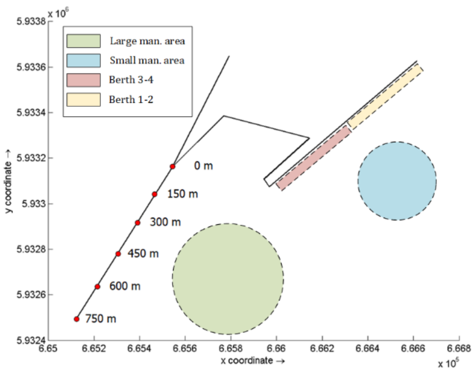

Influence of breakwater extension

Manoeuvring

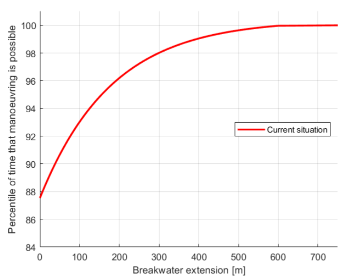

Mooring

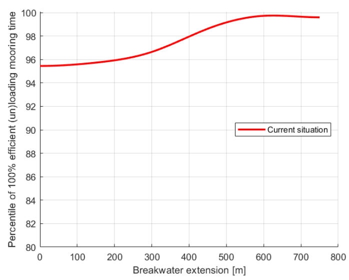

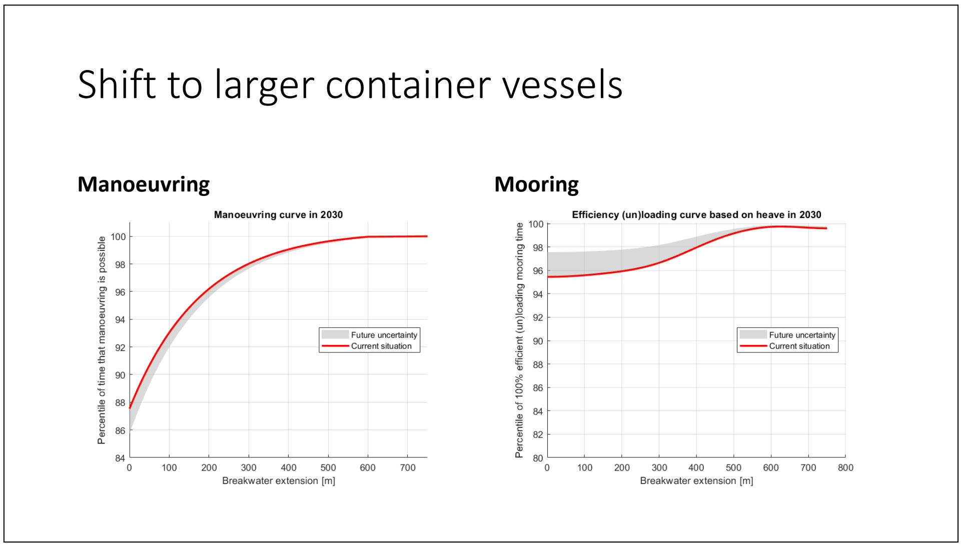
Shift to larger container vessels
Manoeuvring
Manoeuvring curve in 2030
Percentile of time that manoeuvring is possible
Breakwater extension [m]
Future uncertainty
Current situation
Mooring
Efficiency (un)loading curve based on heave in 2030
Percentile of 100% efficient (un)loading mooring time
Breakwater extension [m]
Future uncertainty
Current situation


Development of future expansion of San Vicente Harbour
Research on breakwater extension
Igor Koevoets
Koen Gribnau
Mart-Jan Hemel
Menno Onrust
San Vicente Port
Boskalis
TUDelft
Deltas, Infrastructures & Mobility Initiative
ARCADIS
UCSC

(This page is intentionally left blank)

G

Climate change

The first phase of our multidsciplinary project consisted of a climate impact analysis for the San Vicente Port.

We have written a separate report on the climate impact analysis for San Vicente Port. For convenience, this report is included in this report as an appendix.

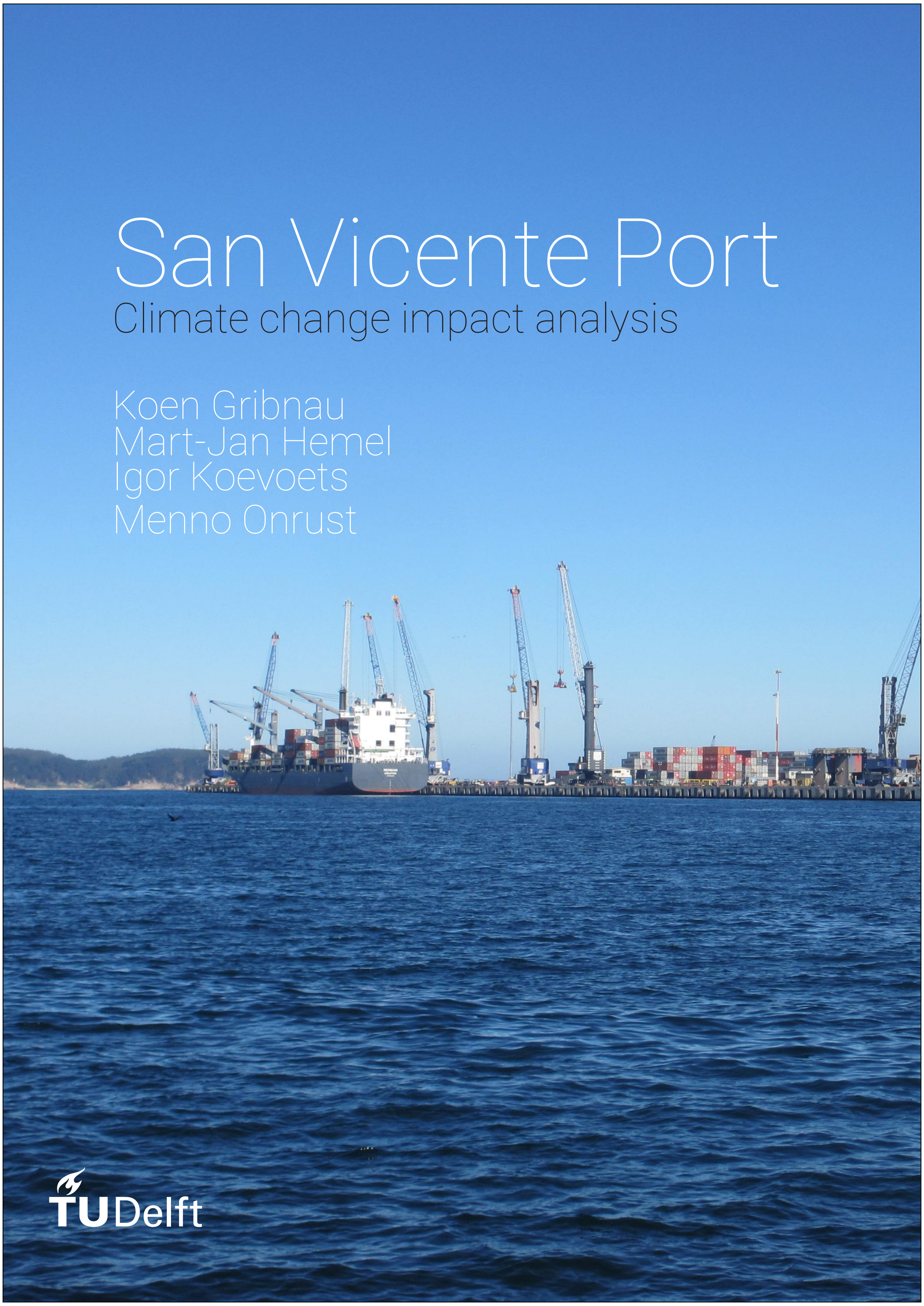
San Vicente Port
Climate change impact analysis
Koen Gribnau
Mart-Jan Hemel
Igor Koevoets
Menno Onrust
TU Delft

Cover: Container vessel at the San Vicente Port (Own photo, 12 Sept. 2018)

San Vicente Port

Climate change impact analysis

by

Koen Gribnau
Mart-Jan Hemel
Igor Koevoets
Menno Onrust

Project group logo

Date:	26 September 2018	
Project duration:	September 2018 – November 2018	
Supervisors:	Prof. dr. ir. Mark van Koningsveld,	TU Delft
	Dr. ir. drs. René Braam,	TU Delft
	Dr. ir. Rafaél Aranguiz	UCSC, daily supervisor

TU Delft

Preface

This report is the climate change impact report of the San Vicente Port. It presents the results of our research on climate change, which is the first phase of our multidisciplinary project. The multidisciplinary project (CIE4061) is a course in the master program of Civil Engineering at the Delft University of Technology. This means that the main purpose of this report is associated to educational ends. The project was realised from September 2018 to November 2018.

The project is carried out at the Universidad Católica de la Santísima Concepción (UCSC) in collaboration with the Delft University of Technology. The port authority of the San Vicente Port, Empresa Portuaria Talcahuano San Vicente, is the client in the project.

We would like to thank our supervisor Rafaél Aranguiz for finding the project, providing sufficient background and helping us when we got stuck. Also, we would like to thank Omar Salgado for receiving us at the port authority and providing sufficient information to carry out the project. We are very happy with Mark van Koningsveld and René Braam, who are our grading supervisors.

Last but not least, we would like to thank our sponsors for their financial support, Boskalis our main sponsor in particular; and our knowledge partners. Their logo's are given on the next page.

This report is intended for everybody with an interest in climate change for the Chilean coast. Sufficient background material is provided so that anyone with a basic knowledge about waves can understand the report.

Enjoy your reading!

Koen, Mart-Jan, Igor & Menno
Concepción, 26 September 2018

(This page is intentionally left blank)

Sponsors

Main sponsor

Boskalis (Main sponsor)

Sponsors

DIMI *Arcadis*

IV-Groep *DPI*

Knowledge partners

Client

(This page is intentionally left blank)

Contents

(This page is intentionally left blank)

Executive summary

Shipping is an efficient way to transport cargo around the world. A changing climate will influence ports. Ports use a long term planning for extensions, therefore climate change cannot be neglected when preparing a port masterplan. In this report a climate impact analysis has been executed for the San Vicente Port near Concepción, Chile.

The Intergovernmental Panel on Climate Change (IPCC) does a lot of research on climate change and has defined multiple climate change scenarios. The Representative Concentration Pathways (RCPs) are four scenarios based on greenhouse gas concentrations. This report assumes RCP 8.5, which is the worst case scenario.

Climate change has an influence on the sea level. Thermal expansion and land ice loss are the most important components of sea level rise, but vary regionally. The resulting sea level rise for San Vicente Port is 55 cm by 2100.

Due to climate change, the polar front shifts towards the poles, which effects the wave climate. On the Southern Hemisphere, this implies that the storm region moves southwards. Wave height, wave direction and wave period are directly influenced by this. For the San Vicente Port the wave direction will change 2.5° anticlockwise, the mean significant wave height will decrease with 0.1 m and the wave period will decrease with 0.05 s.

The sea level is expected to rise in the 21st century. The wave climate is not expected to change significantly. So, the impacts for the San Vicente Port are expected to be small. In some situations climate change can lead to more (un)favourable wave conditions.

(This page is intentionally left blank)

1 Introduction

This chapter outlines the importance of incorporating climate change in port planning. The project background is explained and the objective and scope are given.

1.1. Importance of climate change for port planning

Ships are currently moving 90% of the world's freight (International Chamber of Shipping (ICS), 2018). The forecasts show that the freight volumes and ship sizes are going to grow even further the coming years (SEA, 2017). Shipping of goods and seaports play an essential role in the global economy. Shipping is efficient and has a small carbon footprint relative to other modes of transport.

Climate change can affect ports. Possible changes due to climate change are among others temperature rise, sea level rise, more frequent extreme storms and changes in the wind and wave climate. More extreme storms and flooding can lead to a larger downtime of a port and more dredging activities due to an increase in sedimentation. Moreover, sea level rise can affect the required quay heights and melting ice can change sea routes and shift markets. The main components which influence the port's operations are according to a survey among port authorities are sea level rise, flooding, wave impact and sedimentation (Becker et al., 2011).

Port authorities have to anticipate to climate change to keep their ports efficient. Besides, proactive adaptions to reduce vulnerabilities are more cost effective than reactive strategies (Pielke, 2007). The earlier port authorities know that significant changes are needed, the easier they can prepare for these changes or incorporate these changes in other (infrastructural) projects. Given this, the moment for port authorities to start research if their ports will be affected by climate change is now.

1.2. Objective of this report

The objective of this report is a climate impact analysis for the San Vicente Port. The port authority of San Vicente Port, Empresa Portuaria Talcahuano San Vicente, is preparing a new masterplan and currently the port authority has insufficient insight into potential impact of climate change. The main objective of this report is to give the port authority insight in the (potential) weaknesses of the port with regards to climate change.

1.2.1. San Vicente Port

The climate impact analysis will be performed for the San Vicente Port. San Vicente Port is a mid-sized seaport (Forum, 2016) in the Bío Bío region in Chile. Its location is indicated in figure 1.1. The San Vicente Bay offers protection against severe wave impact. The port has a multipurpose terminal with four berths, but there is a shift towards more containerised cargo (Empresa Portuaria Talcahuano San Vicente, 2018).

1.2.2. Scope

This climate impact analysis will focus on two aspects:

1. Sea level rise
2. Changes of the offshore wave climate

The analysis is based on the RCP 8.5 scenario defined by the IPCC; background on this scenario is given in appendix A. The climate change impact is quantified for 2100. The results are based on previous scientific research. For the wave climate, only the changes of extratropical cyclone activity are taken into account.

1.3. Readers' guide

This research report starts with the effect of climate change on sea level rise which can be found in chapter 2. This chapter is followed by chapter 3 which focuses on the shift in tracks and intensity of extratropical storms due to climate change and how this influences the wave field at the coast of San Vicente port. After the influence of climate change on sea level rise and the wave field is known, conclusions and recommendations are given in chapter 4.

Figure 1.1: Map of South-America. San Vicente Port is a Chilean seaport, located near Concepción. [Google maps, 2018]

2
Sea level rise

The sea level strongly depends on the climate. When the climate changes, the sea level also changes. During the last century the global mean sea level has increased with 20 cm (IPCC, 2007). With the expected climate change the sea level will continue changing.

2.1. Sea level change components

Sea level change is not a global uniform phenomenom. It depends on several components which vary regionally (Goennert et al., 2009). Some components have a larger influence than others, therefore not all components were included in the research that is used for this report (Albrecht & Shaffer, 2016). The included components are the steric and dynamic sea level change, glacial isostatic adjustment (GIA) and sea level changes due to ice sheets and glaciers. Land water storage is not included for example, because this effect is relative small. Thermal expansion and land ice loss are the most important components of sea level change.

2.1.1. Steric and dynamic sea level change

Steric sea level changes refers to changes in sea level due to thermal expansion and salinity variations. A change in sea water temperature changes the density of the ocean water. A change in salinity leads to a change in ocean water density, as well. Both sea level temperature and salinity differ regionally. Especially the salinity can have a large effect on a local scale while it is small component on a global scale.

Dynamic sea level changes are associated with a change in sea level due to a change in ocean circulations. The ocean circulations are wind-driven. Climate change can affect these wind circulations (Hu & Bates, 2018).

2.1.2. Glacial isostatic adjustment

During the last glacial period, 20 000 years ago, large amounts of ice were dropped on the land. The weight of the ice pressed on the earth's crust which gave a deformation. The earth's crust started rebounding towards its original position when the ice melted. This process is called Glacial isostatic adjustment. The effect is location dependent.

2.1.3. Ice sheets and glaciers

Ice sheets and glaciers have a large effect on the sea level. Ice loss increases the volume of water in the ocean. The largest ice sheets on land are located in two regions, namely Greenland and West Antarctic. When land ice is melting at a certain location, the water is displaced and therefore the global mass distribution changes. The changes in global mass distribution result in local gravity changes.

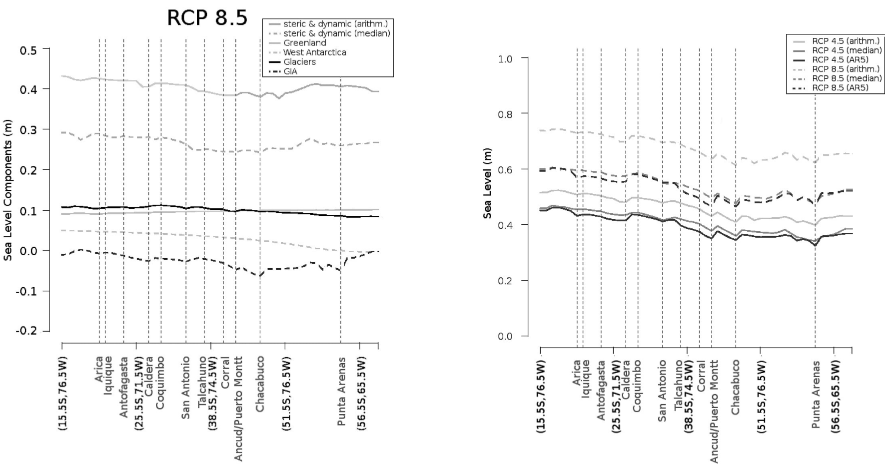

(a) Components of sea level rise (b) Total sea level rise

Figure 2.1: The different components of sea level change along the coast of Chile for climate scenarios RCP 8.5 (a) and the total sea level rise along the coast of Chile for climate scenario RCP 4.5 and RCP 8.5 (b) (Albrecht & Shaffer, 2016).

2.2. Sea level change

Climate scenario RCP 8.5 is used for the calculation of sea level change (Albrecht & Shaffer, 2016). The calculation is done for the year 2100. The results can be seen in figure 2.1a. The vertical axis represents the change in sea level and the horizontal axis represents the coast of Chile. San Vicente Port is situated close to Talcahuano. The different lines in the graph show the influence on the sea level for the different components that were discussed above. For the staric and dynamic component two lines are visible. The first is the arithmetic mean of the results and the second is the median. In the research it is suggested that the median is better than the mean, because the mean is largely influenced by a few models.

2.2.1. Sea level rise

When the different components are added together, the sea level rise in 2100 is visible according to RCP 8.5. Figure 2.1b shows the result of the components added together. Again, the horizontal axis represents the Chilean coast and the vertical axis shows the total sea level change. Both, the arithmetic mean and median are shown for the two climate scenarios. Also the AR5 is added, this is the sea level rise according to the fifth assessment report from the IPCC (IPCC, 2014). Besides climate scenario RCP 4.5, which is a less severe climate scenario, is shown for the three different calculation. The sea level rise near San Vicente Port differs per scenario between 40 and 70 cm. For the RCP 8.5 median scenario the sea level rise is 55 cm, almost similar to the RCP 8.5 AR5 scenario in which the sea level increases 50 cm.

2.2.2. Sea level rise according to other research

Similar research is done with SRES scenarios A1B, A2 and B2 (Slangen et al., 2011), RCP 4.5 and again RCP 8.5 (Slangen et al., 2014). Background about these scenarios can be found in appendix A. For those researches a global scale is used instead of the above presented regional scale (coast of Chile).

As can be seen in figure A.3 the SRES A2 scenario is the most comparable scenario to the RCP 8.5. As can be seen in figure 2.2a the sea level change near San Vicente Port for SRES A2 is about 50 cm. For the global RCP 8.5 research this is approximately equal to 60 cm as can be seen in 2.2b. The sea level rises according to all RCP 8.5 and SRES A2 scenarios mentioned in this chapter, have the same order of magnitude. The expectation of sea level rise are all between 50 and 60 cm.

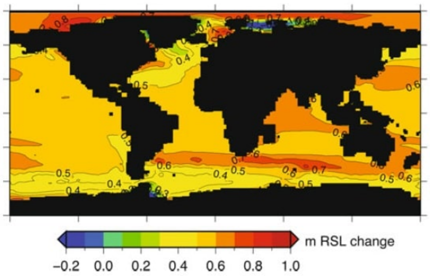

(a) Scenario SRES A2 (Slangen et al., 2011)

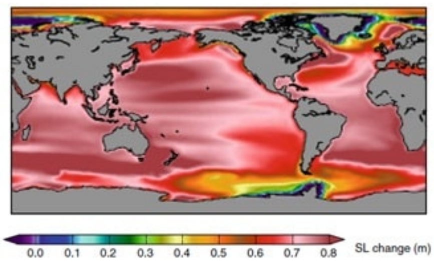

(b) Scenario RCP 8.5 (Slangen et al., 2014)

Figure 2.2: Sea level rise in 2100 for different climate scenarios

(This page is intentionally left blank)

3

Changes of the wave climate

Sea waves are generated by winds. Waves along the Chilean coast can be locally generated or swell waves from further offshore, as can be seen in figure 3.1. Near Chile, extratropical cyclones (ETCs) form an important generator of waves. Extratropical cyclones are characterised by strong winds, precipitation and temperature changes at the mid-latitudes. To understand the behaviour of these cyclones, background information is essential. A short introduction of the weather system is given in appendix B.

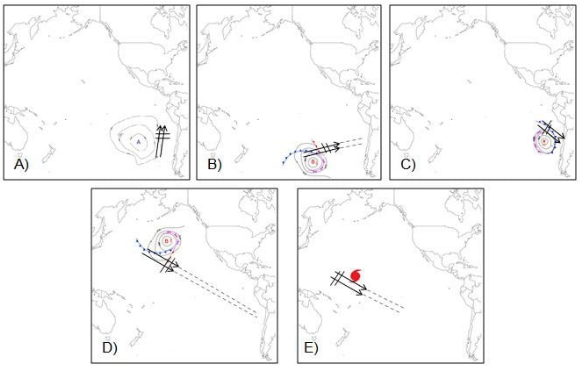

Figure 3.1: Waves reaching the Chilean coast can be generated locally or further away.

3.1. Extratropical cyclones in the present and future climate

Due to climate change, extratropical cyclones will change their tracks and intensity (Ulbrich et al., 2009), (Mizuta, 2012), (Graff & Lacasce, 2011). Before analysing the impact of climate change on the path, intensity, location and frequency of the extratropical cyclones, it is important to look at the present situation.

3.1.1. Present extratropical cyclone

In figure 3.2a the density of extratropical cyclones is shown for the Southern Hemisphere (SH) during the winter. A threshold depth for the SH of 960 hPa is used to filter the storms from the data. From these storms, the strongest 5% are plotted which can be observed in figure 3.2b.

From these figures, it can be observed that the largest cyclone densities are found close around the Antarctic continent. However, the cyclone region is spread out around the Antarctic continent to the South of Australia, Africa and South America. The storms in this area create a wide spectrum of waves travelling towards the northern continents. The location and magnitude of a storm in the extratropical cyclone region determines the properties the generated waves.

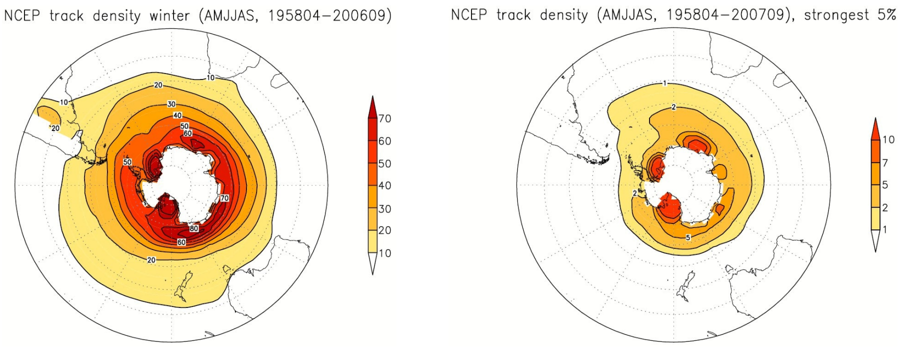

(a) SH extratropical cyclone density

(b) SH extratropical cyclone density strongest 5%

Figure 3.2: SH: NCEP-NCAR reanalysis track density, winter (AMJJAS) 1958-2006. Figure is a cone projection of the South Pole. (Ulbrich et al., 2009)

3.1.2. Future extratropical cyclone

The region around the equator is getting warmer and as a result, the atmospheric circulation cells get squeezed towards the poles (Reichler, 2009). This is called tropical widening. The widening will move the polar fronts towards the poles.

Research is done about the influence of this shift on the extratropical cyclone region. All had the same qualitative outcome: the SH cyclone area will move further south towards Antarctica. Moreover, storms will be more intense and less frequent (Ulbrich et al., 2009), (Mizuta, 2012), (Graff & Lacasce, 2011). The shift in cyclone area can be seen in figure 3.3 which describes the extratropical cyclone density difference between 2071–2100 and 1961–1990. The southwards shift of the cyclone band is more or less meridional equally distributed. This shift lead to less cyclonic activity around 50°S and increased activity around 60°S (Ulbrich et al., 2009). The frequency of activity of cyclones at the SH will decrease (Graff & Lacasce, 2011)(Mizuta, 2012).

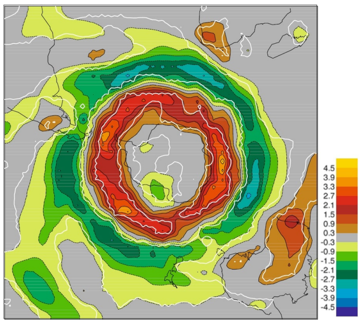

Figure 3.3: Predicted future (2071-2100) density of ETCs relative to the current density (1961-1990). Red indicates that the ETC density will increase; green that the ETC density will decrease. Please do note that the total number of cyclones is not presented. The figure is a cone projection of the South Pole. (Ulbrich et al., 2009)

3.2. Effects on the wave climate at San Vicente Port

The shift of the extratropical cyclone region will cause three major changes: (1) the wave height, (2) the wave period and (3) the approach angle of incoming waves will change along the coastline of Chile depending on the location. As stated before, the intensity of extratropical cyclones will become larger, which causes higher waves and longer wave periods that will travel towards the South of Chile. Because less cyclonic activity is expected around 50°S and above, the wave height will decrease in the middle of Chile in the future. The decline in storm region towards Antarctica, as described in section 3.1, will lead to a shift in wave tracks towards the north. A change in the wave angle is expected towards the Chilean coast. An example of a wave track shift is presented in figure 3.4. In this figure it can be observed that a storm closer to the South Pole will create a smaller approach angle towards the coast of San Vicente.

The expected changes of wave heights and incoming wave angles can be verified according to Camus et al. (2017). For the RCP 8.5 scenario the expected wave statistics are projected with a regional model (Western South America) for the period 2071-2099. Changes in the wave statistics with respect to the period 1979-2005 are presented in figure 3.5. The figure shows that the mean H_s and H_{p95} will increase in the Northern and Southern part of Chile, but the wave heights in the middle part will decrease. This result is equal to the expected result, except the increased wave heights in the Northern part of Chile. This increase is due to an increase in the intensity of the tropical storms. However, this phenomenon is not discussed in this report and not relevant for the San Vicente Port.

The wave the peak periods increase as expected in the Southern part of Chile. The changes are relative small, smaller than 0.25 s for all locations. An anticlockwise change of 2°-3° is expected for the wave directions.

For the San Vicente Port, the offshore wave conditions near Talcahuano are important. The following changes in wave climate can be observed for this location in figure 3.5:

- The mean H_s decreases with 0.1 m
- The mean H_{p95} decreases with 0.2 m
- T_p decreases with 0.05 s
- The mean wave direction changes anticlockwise with 2.5°

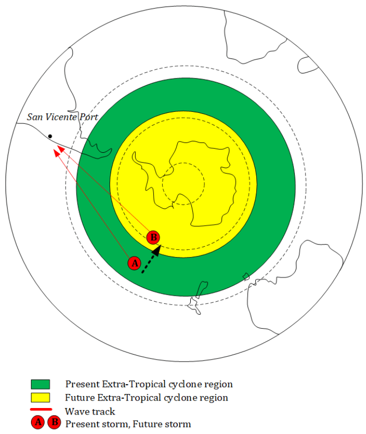

Figure 3.4: Climate change effects the wave properties. The shift of the storm region further towards the poles results in a change in wave generation area (example: from A to B). This means that the approach angles of incoming waves in the San Vicente Port changes. The figure is a cone projection of the South Pole.

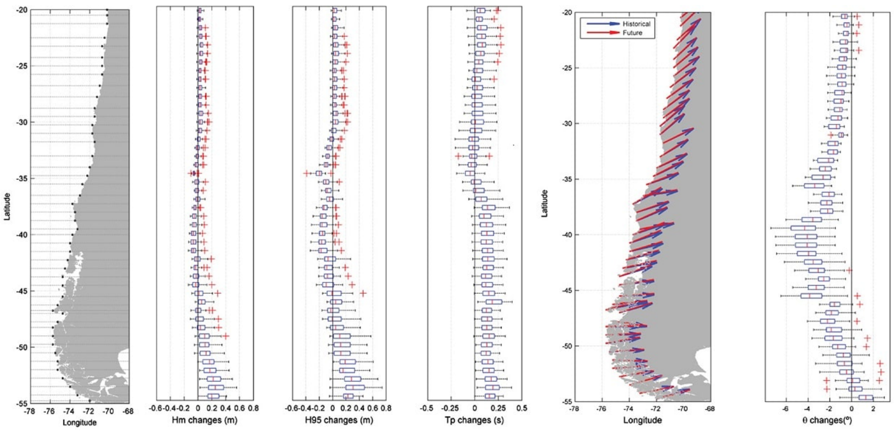

Figure 3.5: Change in wave statistics projected along the Chilean coastline for 2071-2099 with respect to 1979-2005. The locations, intermodel changes of H_s, H_{p95}, T_p, θ and the present and future values of θ are given for climate scenario RCP 8.5. (Camus et al., 2017)

(This page is intentionally left blank)

4

Conclusions and recommendations

Conclusions

A climate change impact analysis is executed for the San Vicente Port for the period until 2100. Corresponding to this climate impact analysis, the following results are obtained for the location of San Vicente Port:

- The sea level will rise 55 cm.
- The mean significant wave height will decrease 0.1 m.
- The mean 95% wave height will decrease 0.2 m.
- The wave period will decrease 0.05 s.
- The wave direction will change 2.5° anticlockwise.

The change of the wave climate is not expected to have large implications for the San Vicente Port.

Recommendations

The following is recommended with regards to the improvement of this climate impact analysis:

- Surge has not been part of this research on the climate change analysis at San Vicente Port. Although surge is not as important as in for example the Netherlands (due to the steep coastline), we recommend that it is included in future research. The changing winds suggest that surge levels will change in the future, but we do not have insight in the exact trends.
- Tropical storms have not been the focus of this research, but can be important for waves from the northwest. The influence and processes of climate change on these northwestern storms are unknown to us, but Camus et al. (2017) have included this in their results (which are used in this report).
- This study assumes RCP 8.5 which is the worst case scenario. If countries are committed to the Paris agreement, this is unlikely to happen. Then, the values given in this report are an exaggeration.

The following is recommended with regards to the application of this climate impact analysis:

- Sea level rise, due to climate change, should be taken into account. However, it should be noted that earthquakes have a larger effect on relative sea level rise. For example, after the 2010 earthquake a land rise of nearly 1.6 meter was recorded.
- The RCP 8.5 scenario will give a decrease in wave height and period which can lead to more favourable conditions. When studying stability of vessels, higher and longer waves will be more detrimental. In this case, climate change should **not** be taken into account.
- A decrease in wave angle towards the port of San Vicente could result in more wave action in the port basins. This would cause difficulties with vessel operations. In this case, climate change effects should be taken into account.

- The wave angle should **not** be adapted when designing breakwater structures. The design of the breakwater is based on extreme waves coming from the northwest and the climate change effects discussed in this report do not have impact on this.

References

Albrecht, F. & Shaffer, G. (2016). Regional sea-level change along the chilean coast in the 21st century. *Journal of Coastal Research*.

Becker, A., Inoue, S., Fischer, M. & Schwegler, B. (2011). Climate change impacts on international seaports: knowledge, perceptions, and planning efforts among port administrators. *Springer*.

Camus, P., Losada, I. J., Izaguirre, C., Espejo, A., M.Menéndez & J.Pérez. (2017). Statistical wave climate projections for coastal impact assessments. *Earth's Future*.

Chandler, D. (2010). *Explained: Radiative forcing*. Retrieved 20-09-2018, from `http://news.mit.edu/2010/explained-radforce-0309`

Empresa Portuaria Talcahuano San Vicente. (2018, September). *Interview with port authority*.

Forum, I. T. (2016). Ports policy review of chile. *International Transport Forum*.

Goennert, G., Jensen, J., von Storch, H., Thumm, S., Wahl, T. & Weisse, R. (2009). Der meeresspiegelanstieg ursachen, tendenzen und risikobewertung. *Die Küste*.

Graff, L. S. & Lacasce, J. H. (2011). Changes in the extratropical storm tracks in response to changes in sst in an agcm. *Journal of Climate*.

Hu, A. & Bates, S. C. (2018). Internal climate variability and projected future regional steric and dynamic sea level rise. *Nature communications*.

International Chamber of Shipping (ICS). (2018). *Shipping and world trade*. Retrieved 18-09-2018, from `http://www.ics-shipping.org/shipping-facts/shipping-and-world-trade`

IPCC. (2000). *Emissions scenarios*. Cambridge, United Kingdom: Cambridge University Press. (N. Nakicenovic and R. Swart)

IPCC. (2007). *Observations: Oceanic climate change and sea level*. Cambridge, United Kingdom: Cambridge University Press. (N. Bindoff and J. Willebrand and V. Artale and A. Cazenave and J. Gregory and S. Gulev and K. Hanawa and C. Le Quere and S. Levitus and Y. Nojiri and C. Shum and L. Talley)

IPCC. (2014). *Climate change 2014: Synthesis report*. Geneva, Switzerland. (R.K. Pachauri and L.A. Meye)

Mizuta, R. (2012). Intensification of extratropical cyclones associated with the polar jet change in the cmip5 global warming projections. *Geophysical Research Letters*.

Nations, U. (2015). Paris agreement. *United Nations*.

Pielke, R. (2007). Future economic damage from tropical cyclones: sensitivities to societal and climate changes. *Philosophical transactions of the royal society a*.

Reichler, T. (2009). Changes in the atmospheric circulation as indicator of climate change. *Elsevier*.

SEA. (2017). *Market forecast report 2017*. SEA Market Forecast WSG.

Slangen, A., Carson, M., Katsman, C., van de Wal, R., Köhl, A., Vermeersen, L. & Stammer, D. (2014). Projecting twenty-first century regional sea-level changes. *Springer*.

Slangen, A., Katsman, C., van de Wal, R., Vermeersen, L. & Riva, R. (2011). Towards regional projections of twenty-first century sea-level change based on ipcc sres scenarios. *Springer*.

Ulbrich, U., Leckebusch, G. C. & Pinto, J. G. (2009). Extra-tropical cyclones in the present and future climate:a review. *springerlink*.

USGCRP. (2017). *Climate science special report: Fourth national climate assessment* (Vol. I). Washington, DC, USA: U.S. Global Change Research Program. (Wuebbles, D.J. and D.W. Fahey and K.A. Hibbard and D.J. Dokken and B.C. Stewart and T.K. Maycock)

A
IPCC's climate scenarios

This appendix provides background on the IPCC's climate scenarios.

A.1. Climate scenarios

To predict how the emission will evolve scenarios are created by several international institutions. There are different scenarios possible. Simple scenarios use a target as a starting point. An example of a simple scenario with a target is the Paris Agreement of 2015. The target of this scenario is to keep the global average temperature well below 2 °C above the pre-industrial level (Nations, 2015). Other type of scenarios are time dependent and include the development of for example the population, energy sources and technology.

A.2. SRES scenarios

The Intergovernmental Panel for Climate Change (IPCC) uses a global climate model to get time dependent scenarios. The SA90 was the first presented series of scenarios by the IPCC in 1990. These scenarios were a few year later replaced by the IS92. In 2000 the IPCC presented the Special Report on Emission Scenarios (SRES) which is a more complex version of IS92. These three series of scenarios are all emission based scenarios. For the SRES the IPCC used 40 emission scenarios which are divided into four families. These four families can be seen in table A.1. These families depend on an environmental or economical focus and a global or a regional orientation. Figure A.1 shows the 40 different emission scenarios due to fossil fuel and industry (IPCC, 2000). The CO_2-emission due to land-use is not inserted in this graph. On the horizontal axis is the timeline visible and on the vertical axis the global carbon emission. The red lines are scenarios from the A1 family, the A2 family scenarios are brown, the B1 family scenarios are green and the B2 family scenarios are blue.

	More economical focus	More environmental focus
Globalisation	**A1** *17 scenarios*	**B1** *9 scenarios*
Regionalisation	**A2** *6 scenarios*	**B2** *8 scenarios*

Table A.1: Families of scenarios used in the SRES

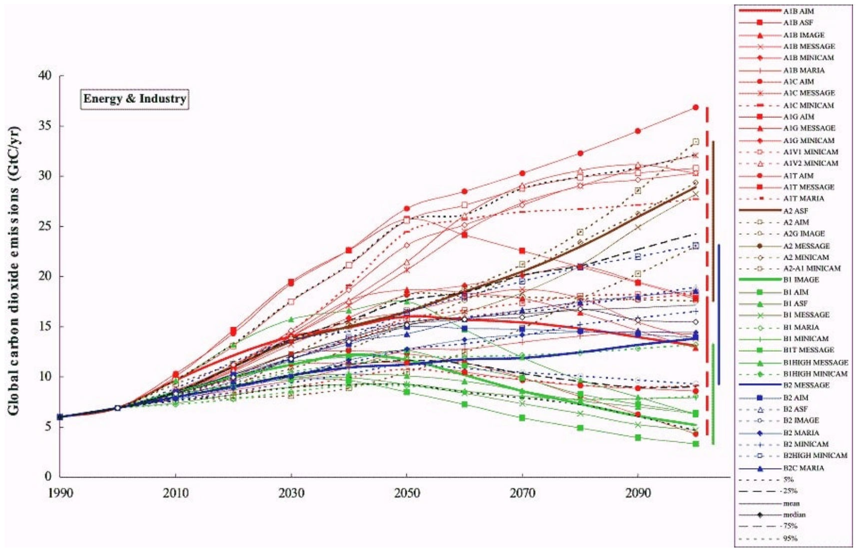

Figure A.1: The 40 SRES climate scenarios (IPCC, 2000)

A.3. RCP scenarios

The most recent scenarios presented by the IPCC are the Representative Concentration Pathways (RCPs) in 2014. The IPCC introduced four RCPs; RCP 2.6, RCP 4.6, RCP 6 and RCP 8.5. The largest difference between the SRES and the RCPs is that RCPs are radiative forcing scenarios and not emission scenarios. Radiative forcing is a direct measure of the amount that the Earth's energy budget is out of balance (Chandler, 2010) and correlated with greenhouse gas concentration. Each of the four scenario is tied to one value, which represents change in radiative forcing in W/m^2 at the tropopause by 2100 with respect to the pre-industrial level. For example, the change in radiative forcing in RCP 2.6 is +2.6 W/m^2. The pathways of the four scenarios are presented in figure A.2. As a result of the change from emission to radiative forcing there is no longer a connection between RCPs and emission scenarios. The RCP scenarios are calculated backwards, starting with radiative forcing values to derive the emissions trajectories.

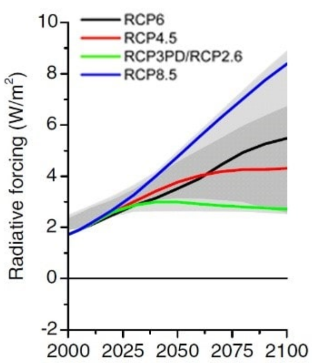

Figure A.2: The 4 RCP climate scenarios (IPCC, 2014)

A.4. Comparing SRES and RCP

The SRES scenarios can be compared with RCP scenarios when both scenarios are transposed to the same dimensions. Comparable dimensions are for example carbon emission per year and the atmospheric carbon dioxide concentration. The SRES scenarios are compared with the RCP scenarios in figure A.3. The top figures give a comparison in carbon emission per year, the middle figures show the atmospheric carbon dioxide and the lower figures compare the global mean temperature change. Some SRES scenarios have a similar layout compared with a RCP scenario, for example SRES A1FI has a similar layout like RCP 8.5.

A.4. Comparing SRES and RCP 17

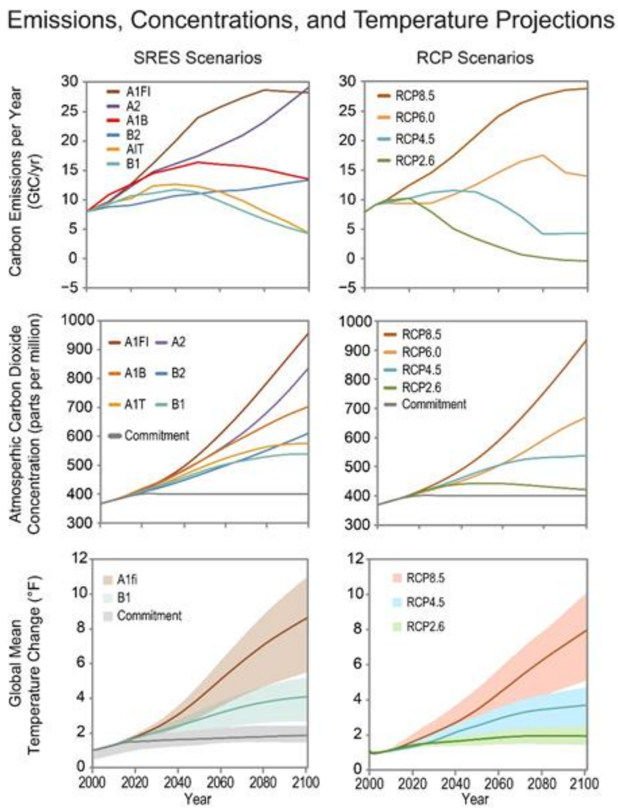

Figure A.3: SRES scenarios compared with RCP scenarios according to carbon emission per year (top), atmospheric carbon dioxide concentration (middle) and global mean temperature change (bottom) (IPCC, 2014)

A.5. Comparing actual emission with RCP scenarios

The CO_2-emission of the past years is observed and compared with the RCP scenarios in figure A.4. From 2005 until 2013 the total emission was higher than the prediction of the RCP 8.5, which is the most extreme scenario. After 2013 the actual emission has flattened, while according to the RCP 8.5 the emission growth continues. Comparing the actual emission status with the RCP scenarios, the actual status is between the RCP 8.5 and the RCP 4.5 scenario.

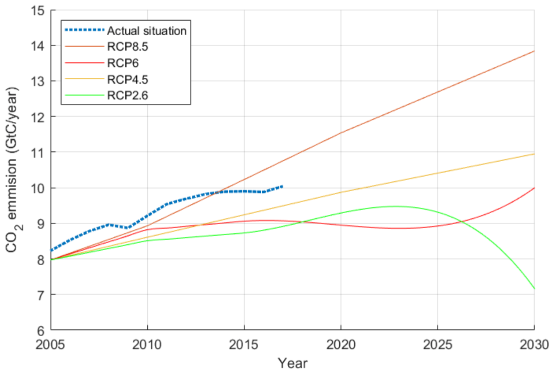

Figure A.4: SRES scenarios compared with actual emission (USGCRP, 2017)

A.6. RCP scenarios for climate analysis

For the climate change impact analysis the RCP 8.5 scenario will used. As described in section A.5, the RCP 8.5 is the most extreme scenario defined by the IPCC. Moreover, the actual emission is less than the prediction in the RCP 8.5. Using this RCP 8.5 gives the most extreme results, which are maybe even overestimated.

B

Global weather system

This appendix gives a general overview of the global weather system and introduces the term extrotropical cyclones. First the atmospheric circulation is explained and the world's jet streams are studied. Then, background on the emergence and importance of cyclones is given.

B.1. Introduction

Our planet maintains a temperature gradient derived from the differential solar heating of the spherical surface of the planet. The highest temperatures are found at the equator and the lowest temperatures at the North and South Poles, this is shown in Figure B.1. The tropics receive more heat from the Sun than they radiate back into outer space. The poles, on the other hand, have less influx of heat then outflux. This results in a thermal imbalance. Tropical heat is dispersed to higher latitudes through atmospheric circulation and ocean currents. Although the ocean currents are important for the global weather system, this report focuses on the atmospheric circulation and the processes in the atmosphere.

Weather phenomenon, like wind, precipitation and clouds, are related to the presence of high and low pressure systems in the troposphere (lower atmosphere). Weather systems in the mid-latitudes, such as extratropical cyclones, are caused by instabilities in the upper troposphere (more in section B.3). Tropical cyclones are caused by strong temperature gradients in the tropics.

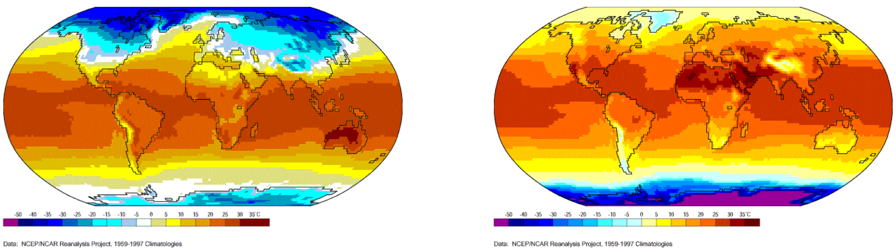

(a) Air temperature in January

(b) Air temperature in July

Figure B.1: Global air temperatures in January (a) and in July (b). The Sun's radiation heats the Earth, but this is not evenly distributed. This results in a temperature gradient with the highest temperatures occurring at the equator and the lowest temperatures at the North and South Poles.

Source: Climate Lab Section, Department of Geography, University of Oregon

B.2. Atmospheric circulation

Atmospheric circulation is the large-scale movement of air. The major driving force is the uneven distribution of solar heating, and it is effective in transporting energy to the pole regions. The global scale atmospheric circulation pattern was described by George Hadley in the early 18th century. In each hemisphere, he distinguished a primary circulation cell known as Hadley cell and two secondary circulation cells at higher latitudes. The mid-latitude cell is located between 30° and 60° latitude; the Polar cell beyond 60°. Figure B.2 shows the location of these cells.

Coriolis effect The Coriolis effect is the apparent deflection of moving objects in a rotating frame of reference. Due to the earth's rotation, moving objects on the Norther Hemisphere are deflected to the right and on the Southern Hemisphere to the left.

B.2.1. Hadley cell

The Hadley cell is a meridional circulation cell that transports heat from the equator to about 30° latitude on either side of the equator.

- Moist air at the equator is warmed by the Earth's surface, thus decreasing in density.
- As it rises, it causes heavy precipitation and creates a low pressure zone. The air mass rises to the tropopause, about 10-15 kilometers above sea level, where it is forced poleward by the continual rise of air below.
- As the air moves poleward, it cools, becomes denser and gains a strong eastward component due to the Coriolis effect. The resulting winds form the subtropical jets.
- At this latitude, the air masses descend, a high-pressure zone is formed.
- Near the surface, a frictional return flow completes the loop, absorbing moisture along the way. The Coriolis effect gives this flow a westward component, creating the trade winds (These are the prevailing easterly winds found at the tropics).

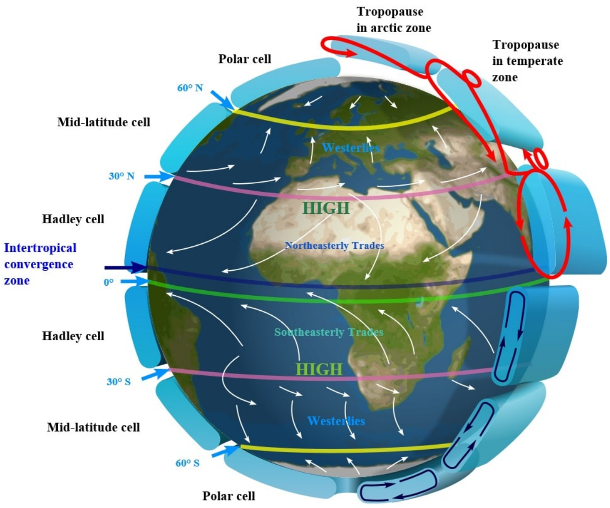

Figure B.2: Global atmospheric circulation: the locations of the circulation cells are indicated, as well as the direction of the main winds. High pressure zones are present at the Poles and at about 30° latitude; low pressure zones are present at the equator and at about 60° latitude. The location of these zones shift northwards in Northern Hemisphere summer and southwards in Northern Hemisphere winter.

B.2.2. Mid-latitude cell

The Mid-latitude cell, also known as the Ferrel cell, is a secondary circulation cell that is mainly driven by the Hadley and Polar cell.

- As the air masses at 30° latitude descend, a part flows poleward at the surface level.
- At the 60th parallel this flow of air collides with the cold polar air masses from the arctic and is forced to rise.
- At high altitude the rising air diverges towards the poles; the rest moves towards the equator, where it collides with the high-level air of the Hadley cell.

B.2.3. Polar cell

The polar cell is the convection cell in the arctic region.

- Although relatively cool compared to equatorial air, the air masses at the 60th parallel are still sufficiently warm to undergo convection and drive a thermal loop. The air rises to the tropopause (about 8 km at this latitude) and moves poleward.
- When it reaches the polar areas, the air masses have cooled considerably and are more dense than the underlying air.
- The air descends, creating a cold, high-pressure zone at the poles.
- It is then forced towards the 60th parallel, completing the polar cell. The Coriolis effect gives this flow an eastward component, creating the polar easterlies.

The Hadley cell and the polar cell are determinant for the weather in their domain. Their thermal characteristics ensure that the effects of transient weather phenomena are rare and have a negligible effect. The high- and low pressure systems that are found every day in the mid-latitudes, rarely appear above the 60th and below the 30th parallels.

B.2.4. The Polar jet stream

At the boundary between the polar cell and the mid-latitude cell, cold air from the arctic and warm air from the subtropics meet. The polar front between these air masses is characterised by a strong temperature gradient.

The temperature gradient signifies that the flow is subjected to baroclinic forcing. Air masses with different temperatures have different densities causing a pressure difference that drives a flow. Rather than flowing directly from the warm to the cold area, the flow is deflected by Coriolis and flows along the boundary of the two air masses. This is described by the thermal wind balance:

$$-f\frac{\partial v}{\partial z} = g\frac{\partial \rho}{\partial x} \tag{B.1}$$

Where f is the Coriolis parameter, $\frac{\partial v}{\partial z}$ the longitudinal wind shear, g the gravitational acceleration and $\frac{\partial \rho}{\partial x}$ the density gradient. At the polar front, the sub-tropical air mass is undercut by the more dense polar air mass. As a consequence the surface pressures are relatively low and the pressures at high-altitude are relatively high. The lack of friction at high altitude leads to the formation of the planetary wind circulation that is organised into tight jets.

Figure B.3 shows the jet stream at the interface between the warm and cold air masses. The jet stream typically has a width of a few hundred kilometers and a height of several kilometers. The meandering shape is often referred to as Rossby waves. The presence of the jet stream is extremely important for aviation, where the high wind speeds are used to save fuel and flight time.

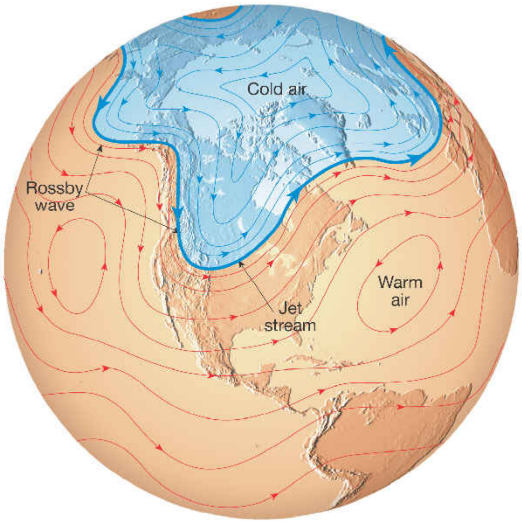

Figure B.3: Polar jet stream in the Northern Hemisphere. The polar front forms the boundary between the cold arctic and the warm tropical air masses.

B.3. Extratropical cyclones

The jet stream is forced and steered by the thermal gradient. Where temperature differences between the air masses air greatest, the largest wind speeds are observed. Baroclinic instabilities lead to the formation of extratropical cyclones through a process called cyclogenesis.

Extratropical cyclones (ETCs) are large scale low pressure systems that occur in the mid-latitudes. For that reason, they are also called mid-latitude cyclones; weather forecasters often describe them as depressions. ETCs and anticyclones (high pressure systems) drive the weather over much of the Earth.

Figure B.4 shows how the process of cyclogenesis works:

A Initially, there is a stable polar front.

B Due to instabilities so called Rossby waves form in the position of the polar front.

C Divergence in the jet stream causes a reduction of the atmospheric pressure at surface level. The lowered pressure attracts air, creating convergence. The inflow of air is diverted by Coriolis: the cold front progresses towards the equator; the warm front progresses more slowly.

D As the poleward portion of the cold front overtakes a section of the warm front, an occluded front is formed. The warm air is pushed to the upper atmosphere.

E Eventually, the cyclone becomes barotropically cold and slowly weakens.

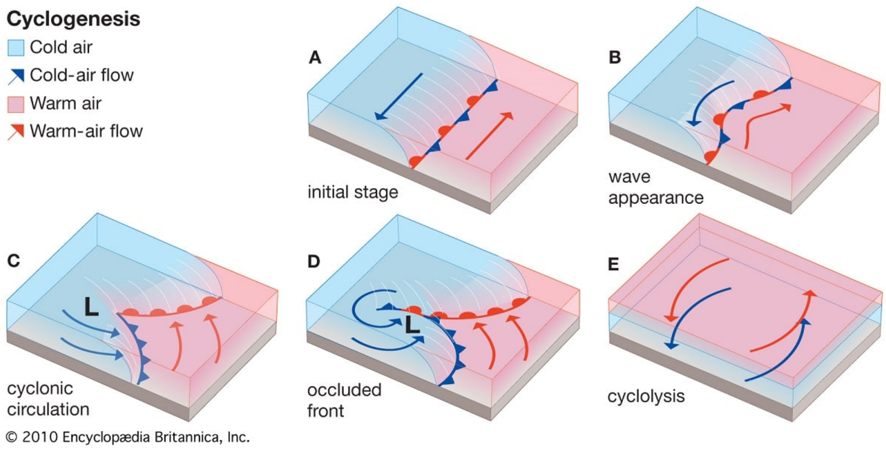

Figure B.4: Cyclogenesis is the process of extratropical cyclone formation. 5 stages can be identified.